The Thesis Committee for Ivan Enrique Garcia Delgado
Certifies that this is the approved version of the following thesis:

Use of Geotextiles with Enhanced Lateral Drainage in roads over expansive clays

APPROVED BY
SUPERVISING COMMITTEE:

Supervisor:

Jorge G. Zornberg

Amit Bhasin

Use of Geotextiles with Enhanced Lateral Drainage in roads over expansive clays

by

Ivan Enrique Garcia Delgado, B.S.C.E.

Thesis

Presented to the Faculty of the Graduate School of

The University of Texas at Austin

in Partial Fulfillment

of the Requirements

for the Degree of

Master of Science in Engineering

The University of Texas at Austin

May 2015

Dedication

I dedicate my thesis work to my parents, Ivan Garcia and Flor Delgado, for always providing me the most they can and making it possible for me to get my Masters from one of the best universities in the nation. I thank them as well as the rest of my family, Flor and Frank Garcia, for always been there whenever I had to vent. I dedicate it as well to my girlfriend which suffered through many nights of me trying to explain my research to her and seeing if she agreed with me. I dedicate my work as well to all my friends at UT who helped me in many ways.

Acknowledgements

I would like to first thank Dr. Jorge Zornberg for all his support and guidance with this study. I would also like to thank Tencate Geosynthetics for their support from the very beginning of this project. I would like to thank as well the Texas Department of Transportation which helped make this study possible and have provided much appreciated support. I would also like to thank all the students from Dr. Zornberg's research group that helped me many times, including Marcelo Azevedo, Hossein Roodi, Chris Armstrong, and Larson Snyder. Marcelo provided much guidance in the area of the moisture data as well as helped out during all the installations in SH-21. Hossein provided much insight and recommendations in the analysis of the visual condition surveys and helped in conducting many of the actual surveys and assisted in all installations done in SH-21. Chris helped as well with his experience with Cook Mountain formation and assisted as well in all installations. Larson was a big help with all installation done in SH-21, especially during the installation of the vertical arrays where he was the Bobcat operator. I would like to acknowledge as well Dr. Amit Bhasin who helped me as well in the understanding of the distresses in the pavements and took time from his schedule to review my work. Finally, I would like to acknowledge my family and friend that have helped me through this whole process and reach my goals.

Abstract

Use of Geotextiles with Enhanced Lateral Drainage in roads over expansive clays

Ivan Enrique Garcia Delgado, M.S.E.

The University of Texas at Austin, 2015

Supervisor: Jorge G. Zornberg

Expansive clays are very abundant across the central United States in general and in the state of Texas in particular damages induced by expansive clays have been reported to reach several billions of dollars per year. Volume changes in expansive soils due to change in their moisture content varies has caused significant cracking in roads and has resulted in costly maintenance projects over the lifetime of these roads.

In Texas, expansive soils have been often treated with lime stabilization, which is not always possible, and in some cases by removing and replacing them with non-expansive soils, which can be very costly. Recently, geosynthetic reinforcements have been incorporated in roads founded on expansive clays to make the structure stiffer and less prone to cracking. A new geotextile, which is capable of providing enhanced lateral drainage through capillarity has been recently develop. Facilitating moisture redistribution would be a feasible approach for roads on expansive clays as they may lead uniform vertical displacements resulting in minimized cracking in the asphalt layer.

Eight test sections with different geotextiles were constructed on State Highway 21 in Bastrop, Texas. The road is founded on expansive clays. A number of geotextiles, including one with enhanced lateral drainage capabilities, were incorporated to 500 feet long test sections. All sections were equipped with sensors to monitor moisture beneath the

geotextiles and were periodically surveyed to document pavement distresses. Results showed that the geotextile with enhanced lateral drainage was able to maintain a uniform moisture content along the length of the soil in contact with this geosynthetic. Condition surveys showed that the geotextile with enhanced lateral drainage prevented cracking in the portion of the pavement above it. As expected, cracks often developed in areas of the pavement section beyond the extent of the geotextile. This suggested that the geotextile was capable of providing enhanced lateral drainage, although placement of the geotextile over the full width of the road (and not only under the shoulder) would be necessary to minimize the development of longitudinal cracks.

In conclusion, the geotextile with enhanced lateral drainage can deal with pavements on expansive clays by improving the pavements long-term performance.

Table of Contents

List of Tables

List of Figures

Chapter 1 : Introduction

1.1 RESEARCH MOTIVATION

Expansive clays cover around one-fourth of the United States and have been blamed for billions of dollars in damages (Zhang & Belmont, 2011). Figure 1.1 shows the presence of expansive clays in United States. There is a large presence of expansive clays in the state of Texas, with many roads founded on these soils. Texas's climate with prolonged dry periods and sudden intense rain events puts roads under distress due to the volume changes in the foundation soils. These volume changes in the pavements result in cracks which are costly to fix.

During the drought of 2011 Texas roads were put to the test and performed badly with roads like SH-21, which is the focus of this study, ending up with significant damage. Figure 1.2 shows photos of SH-21 located in Bastrop, Texas. Typically in Texas, expansive clays are dealt with lime stabilization, removal and replacement of expansive clays, and in recent times with geosynthetic reinforcements in the base layer.

Lime stabilization is not possible when there is a high sulfate concentration in the soil, this can result in major problems. Removal and replacement of the expansive clays can be extremely costly since in some areas the active zone define as the area susceptible to volume changes can be reasonably deep. The disposal of the soils is expensive as well as the costs of bringing in better fill which in some cases may not be located close by. When the length of the roads is taken into consideration, costs can be extremely high. The use of geosynthetic reinforcements in the base layer cost effective but does not deal with the expansive clays as the alternative like lime treatment or removal and replacement do. The reinforcement stiffens the whole pavement structure to make it flex less with volume changes in the subgrade and thus crack less.

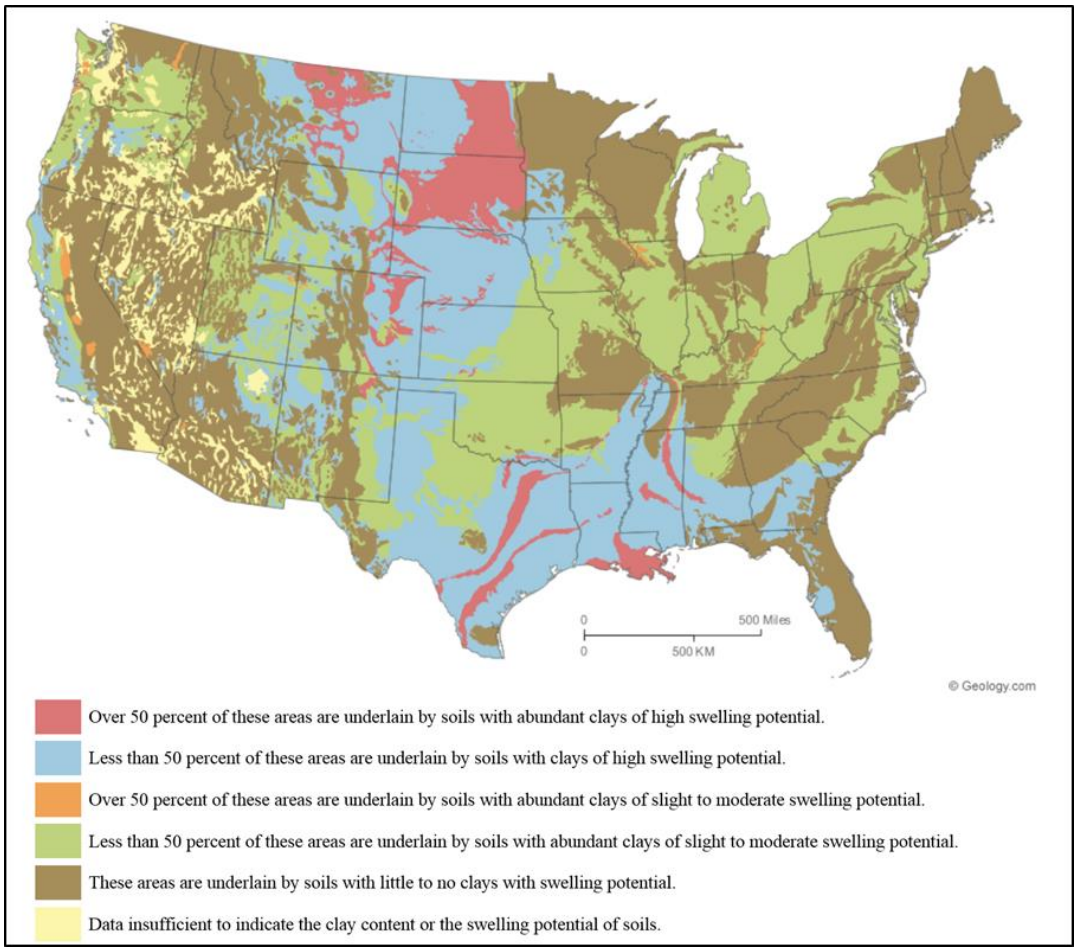

Figure 1.1: Map of expansive clays in the Continental United States (Olive, 1989)


Figure 1.2: Photos from SH-21 before rehabilitation

The possibility of using a geotextile that is able to provide reinforcement and help deal with the expansive subgrades would be a feasible approach. The geosynthetic industry has recently produced a geotextile which contains "wicking fibers" which are able to provide enhanced lateral drainage within the textile through capillarity. Such properties in a geotextile placed between the base layer of a road and its expansive subgrade could have major benefits.

The geotextile, if able to redistribute moisture beneath it through its enhanced lateral drainage, could possibly equilibrate the moisture beneath it. In expansive soils this could result in the soils expanding or contracting equally beneath the geotextile. This could have important benefits for roads in Texas, which could perform much better and crack significantly less during seasonal cycles. The road if constructed above a geotextile as described above, would move up and down as the soils beneath it expand and contract as a single mass, thus not generating tensile stresses in the asphalt resulting in cracks. The use of this geotextile under roads in Texas such as SH-21 in Bastrop, Texas, could result in important monetary savings due to less reparations of the surface asphalt.

1.2 RESEARCH OBJECTIVES AND SCOPE

This study's main objective was to compare the hydraulic performance of a geotextile with enhanced lateral drainage to that of other geotextiles in expansive clays in the field. The second objective of this study was to compare how the geotextile with enhanced lateral drainage compares to other geotextiles at dealing with the reduction of cracking in roads founded on expansive clays.

In order to achieve both objectives, construction of field test sections was conducted. This involved 8 test sections that were constructed during the rehabilitation of a state highway in Bastrop, Texas, called SH-21. Four geotextiles were used which were

called for this study GT1, GT2, GT3, and GT4. The test sections were equipped with moisture sensors placed underneath the geotextiles to monitor moisture variations below. The second objective of this research is achieved through evaluation of the performance of periodic visual condition surveys where the test sections were walked while documenting distresses.

Using the data from moisture sensors, the hydraulic performance of the 4 geotextiles was evaluated by investigating the patterns of moisture content over time under the geotextile and how it varied from one sensor to another. The performance of each geotextile at dealing with cracking was evaluated by evaluating the data from the surveys and quantifying the magnitude and frequency of cracks during the different periods.

1.3 OVERVIEW OF THE THESIS

This thesis has been organized into a total of 6 chapter. Chapter 1, which is the introduction, presents the motivation for this study as well as the objectives and scope of the study. Chapter 2 provides the background information relevant to complications related to the presence of water in pavements and how this water has been removed in the past. It includes 4 case histories of projects were GT4 was used and how it performed. It includes as well explanation on the setup used to measure moisture content below the geotextiles works. Chapter 3 focuses on describing the location of the test sections regarding past performance of the road as well as soils present at the site. Information on recommendations provided to TxDOT on how to fix the road provided by the Texas Transportation Institute from a study done previously at the site is covered, as well the alternatives ultimately adopted by TxDOT. The involvement of The University of Texas at Austin in modifying the design in order to perform this study is covered as well as all the process that took place to construct the test sections. Chapter 4 covers the process of

the installation of the moisture sensors and dealing with certain complications that arose in more detail as well as the installation of additional sensors. It also covers the results obtained after more than 2 years of readings and the discussion of the data. Chapter 5 describes the procedures and results of the visual condition surveys. Finally, Chapter 6 presents the conclusions for this study as well as recommendations for future work on this project.

Chapter 2 : Literature Review

"Past and current research has clearly established the detrimental effects of inadequate subsurface drainage within a road environment" (Lebeau, 2009). The presence of water within a pavement structure can lead to many problems like reduction of subgrade and base/sub-base strength, differential swelling in expansive subgrade soils, frost heave, and migration of fine particles into the base or sub-base (Rokade, 2012). "Water related problems are thus responsible for decreased pavement life, increased cost for maintenance, and increased pavement roughness, and occur throughout all regions and climates of the US" (Stormont, 2001). Proper drainage in pavements is thus very influential on a roads performance over time.

2.1 IMPORTANCE OF SUBSURFACE DRAINAGE

2.1.1 Sources of water

Water infiltration into pavements has been extensively studied as documented in the report by Hare et al. (1990) on their report regarding drainage in airport pavements. The water within the pavement structure has been found to be originated mainly from infiltration through existing cracks in the pavement as well as infiltration from the shoulders. Rokade et al. (2012) also mentions that possible sources of water in pavements can be "melting of ice during freezing/thawing cycles, capillary action, and seasonal changes in the water table". Figure 2.1 shows multiple points of entry for water to penetrate pavement structures.

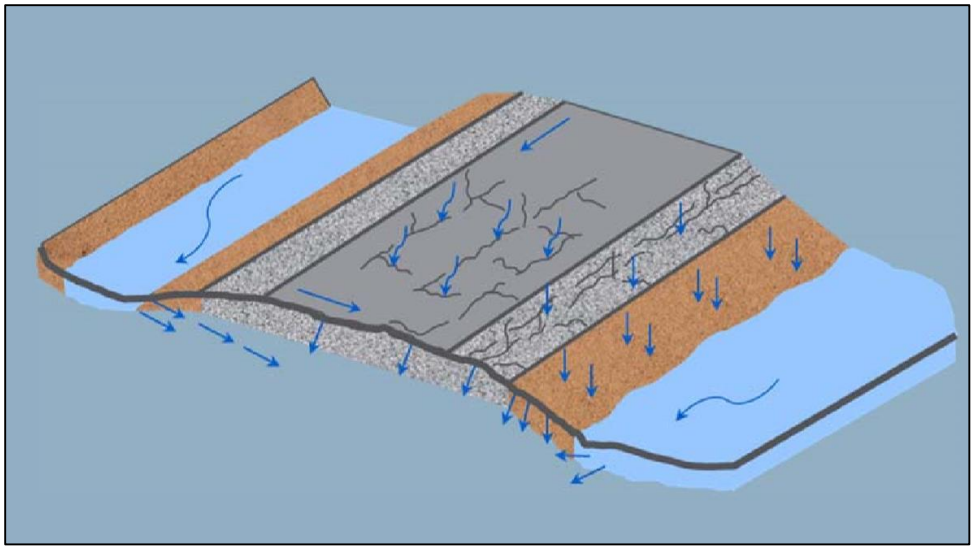

Figure 2.1: Source of water in a pavement (Tencate Mirafi, 2015)

2.1.2 Effects of water in pavements

The presence of water in pavement systems is one of the main reasons leading to premature failure. One of the main detrimental effects of increases in water content within a pavement structure is the water effect on the resilient modulus of unbound layers. The resilient modulus of soils can be affected by moisture content, dry density, and degree of saturation. The one variable that is out of a designers control and thus more important is moisture content. Figure 2.2 shows the decrease in resilient modulus with increasing moisture content. Possible reasons for this effect are that the moisture content affects the state of stress of the soil through suction and pore water pressures and that it affects the soil structure (ARA, Inc., ERES Division, 2000). As a resultant of a decrease in the resilient modulus, permanent deformation will increase in the pavement layers leading to pavement deterioration like increase rutting as well as fatigue cracking.

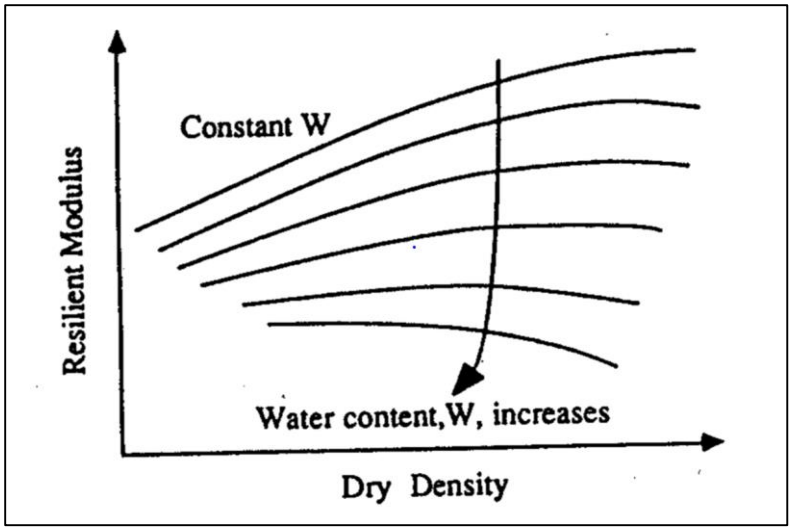

Figure 2.2: Effect of water content on Resilient Modulus (ARA, Inc., ERE Division, 2000)

The effect of water content on the resilient modulus has been well known for fine-grained soils but it has been found that it also affects base materials (Stormont, 2001). Figure 2.3 shows how the level of saturation reflects in the amount of permanent deformation experience in 2 different types of base material. Stormont and Zhou (2001) reference various studies that found that increase in fines worsened the effect of saturation in base materials.

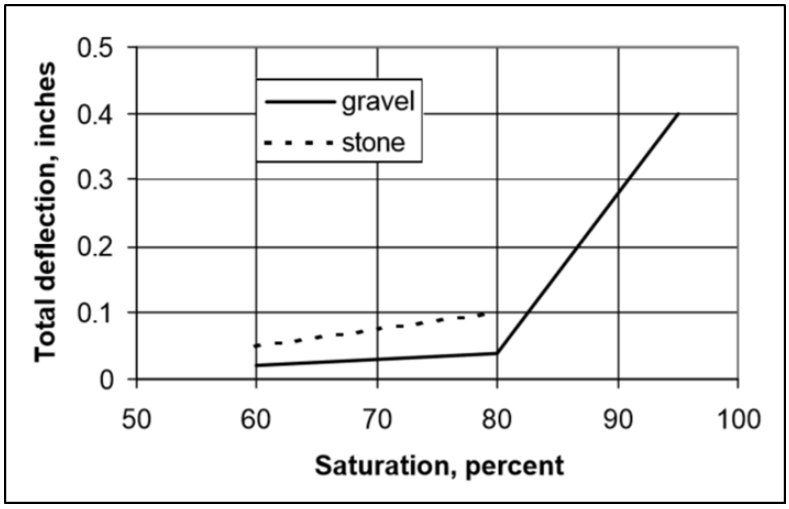

Figure 2.3: Total deflection measured after 1,000 load cycles (Stormont, 2001)

Water can also have detrimental effect on base materials which have been asphalt treated as well as cement treated. The water can cause stripping where the asphalt coating is separated from the base material, thus causing a decrease in resilient modulus and strength (Stormont, 2001). Similar results were reported by Stormont and Zhou (2001) regarding cement treated base materials.

Pavement structures with inadequate drainage may lead to water reaching the subgrade, which is often a fine-grained soil. Fine-grained soils are especially susceptible to experiencing a reduction in the resilient modulus with an increase in water content. The presence of excess water in the subgrade can result in large hydrostatic pressures under the pressure of a wheel on the pavement, this in turn can lead to load bearing deficiencies (Lebeau, 2009).

In the particular case of expansive clays, which cover one-fourth of the United, States and have been to blame for billions of dollars in damages (Zhang, 2011), drainage is particular important.

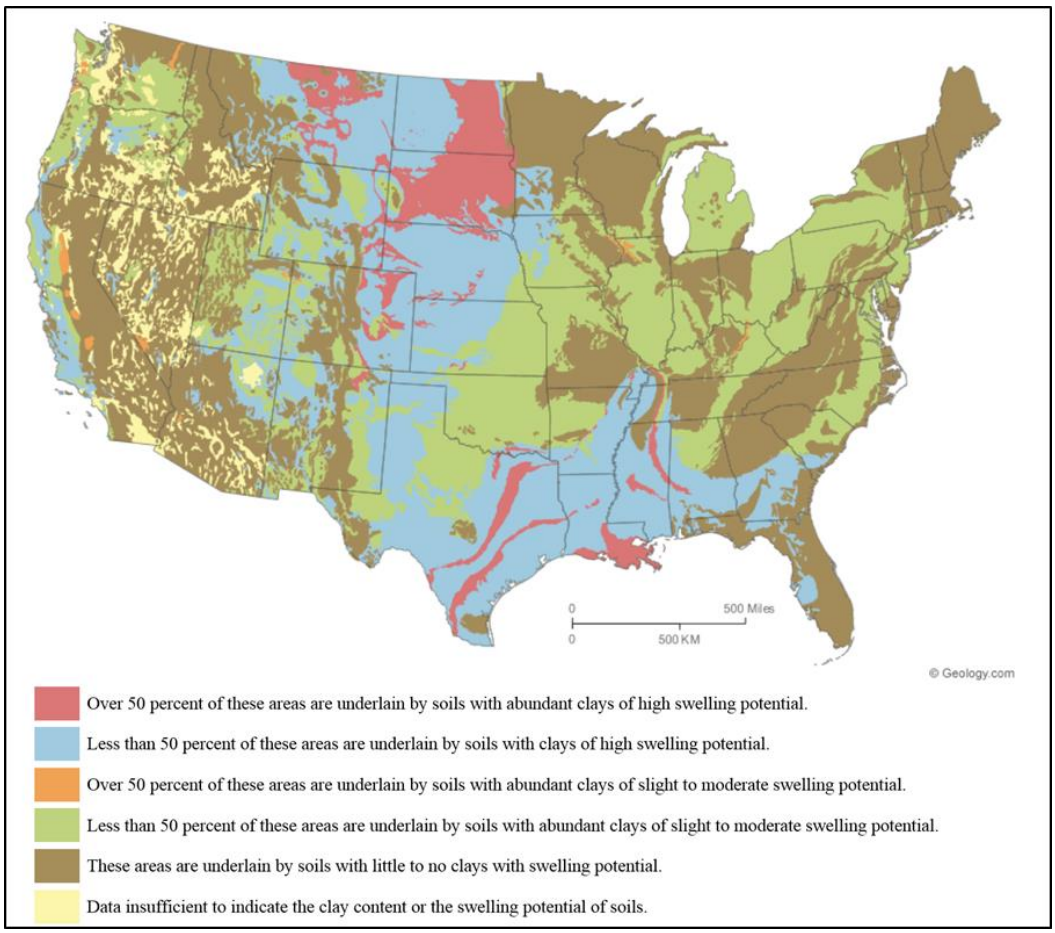

Figure 2.4: Map of expansive clays in the Continental United States (Olive, 1989)

Expansive clays are soils that change volume due to changes in water content. These soils experience swelling when they increase water content and shrinking when they decrease water content. The expansive soils cause problems with seasonal fluctuations in climatic and environmental factors in a zone identified the active zone (Jones, 2012). Figure 2.5 below shows a sketch taken from Chapter C5 on Expansive Soils from the ICE manual which shows the active zone and how the moisture content can vary seasonally with water content reducing during the hot season or summer. In the case of Texas, these variations can be very significant with summers reaching temperatures in excess of 100°

F. These seasonal fluctuations and their effect on water content in the soil can cause "pavement heave during wet season and shrinkage during dry season" (Zornberg, 2009). These vertical movements cause tensile stresses in the road which can lead to longitudinal cracks appearing as shown in Figure 2.6.

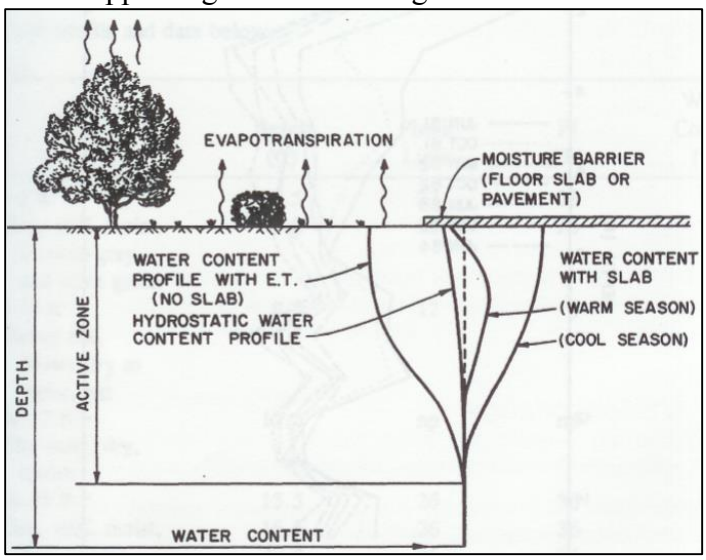

Figure 2.5: Active zone (Jones, 2012)

Figure 2.6: Longitudinal cracks in SH-21, Bastrop, Texas

2.2 TYPES OF PAVEMENT DRAINAGE

Excess water within pavement structures is known to be detrimental to its performance. There are multiple ways this excess water can exit the pavement structure, including surface evaporation, lateral seepage, subgrade percolation, through cracks and joints, and with a subsurface drainage system (Hare, 1990). "Studies of pavements showed sections of pavements containing a drainage layer drained more rapidly after a rain event than did sections without a drainage layer; thus, the pavement spent less time in a saturated condition" (Rokade, 2012). Thus the use of an appropriate drainage layer can aid in reducing or eliminating the damaging effects excess water can have on a pavement structure.

Pavement subsurface drainage systems have been incorporated in design since the 1700s (Lebeau, 2009). The most typical drainage systems are described in detail in "Airport Pavement Drainage" (1990). The typical example shown in this report consists of an opened grade base drainage layer which has a filter fabric to prevent fines from entering the base layer and edge drains and intercept drains with outlet pipes to drain the structure. Figure 2.7 shows the details of the example of a typical subsurface drainage system as shown by Hare et al. (1990). The water in this figure is described as entering through point A which is a crack or joint in the pavement surface which then flows to B which is the interface between the surface material and base material. From B the water flows to C, which is a point in the base drainage layer from which it then flows to D which represent the edge drain. Finally, from D the water flows to E which is the entrance of the outlet pipe and from there it ends at F from which the water is disposed of.

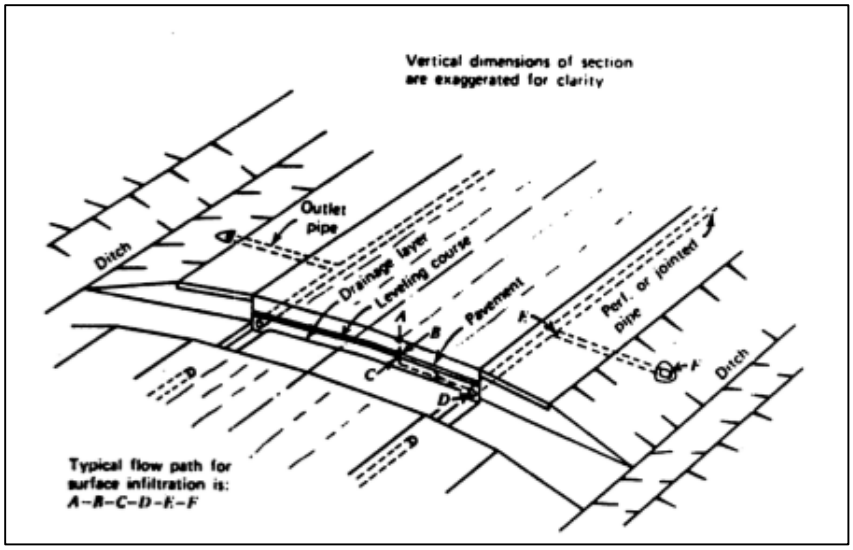

Figure 2.7: Typical Pavement Subsurface System (Hare, 1990)

The "Airport Pavement Drainage" report includes a few paragraphs that describe each component of their typical subsurface drainage system. The longitudinal edge drains are described as consisting of a "perforated collector pipe surrounded by a protection filter". Figure 2.8 shows examples of typical edge drains for rehabilitated projects.

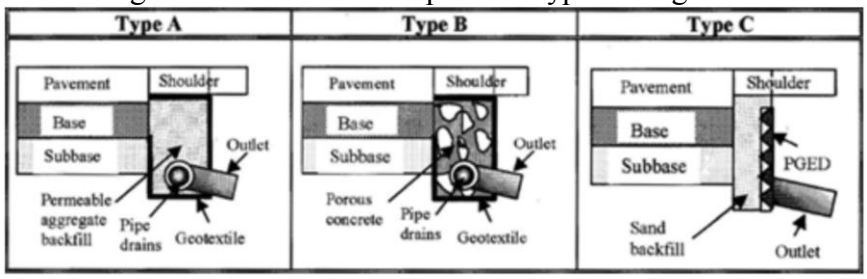

Figure 2.8: Typical Edge Drains (Christopher, 2006)

Other components of the typical pavement subsurface drainage system are the transverse and horizontal drains, which capture the water under the pavement. This type of drainage (Hare, 1990) usually consists of a trench and collector pipe covered by a protector filter. The horizontal drains can then guide the excess water into the edge drains in order for it to be disposed.

As alternates to transverse drains, permeable bases can also be used. Permeable bases are designed to move water quickly from within the pavement structure to the edge drains in order to dispose of it in the side ditch or they can be day lighted directly to the side ditch (Christopher, 2006). These permeable bases typically cannot contain fines in order to have adequate permeability values. The issue with permeable bases is that in order for them to conform to the permeability values they must be a coarse uniform gravel. In order to construct the base course with such a material, it must be treated with asphalt or cement in order to stabilize the material for construction. Figure 2.9 shows an example of a permeable base which is day lighted directly into the side ditch.

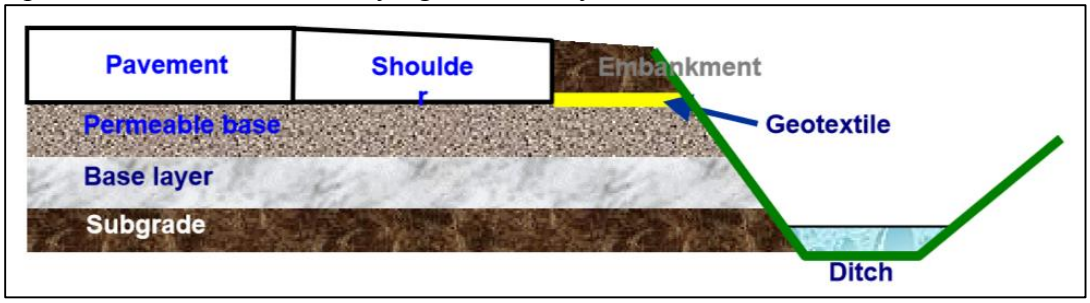

Figure 2.9: Day lighted Permeable Base (Christopher, 2006)

Another version of the example of the pavement structure with the permeable base is the dense graded stabilized base with a permeable shoulder. This example is included in Chapter 7 of "Geotechnical Aspects of Pavements" (2006). The system is described as consisting of a non-erodible dense graded base underneath the traffic lanes which will provide the structural capacity where it is most needed and a permeable base underneath the shoulder which will provide an exit for the excess water in the pavement. Figure 2.10 below shows a sketch of an example of a pavement structure with the non-erodible base layer beneath the traffic lane and the permeable base underneath the shoulder with an edge drain to dispose of the water.

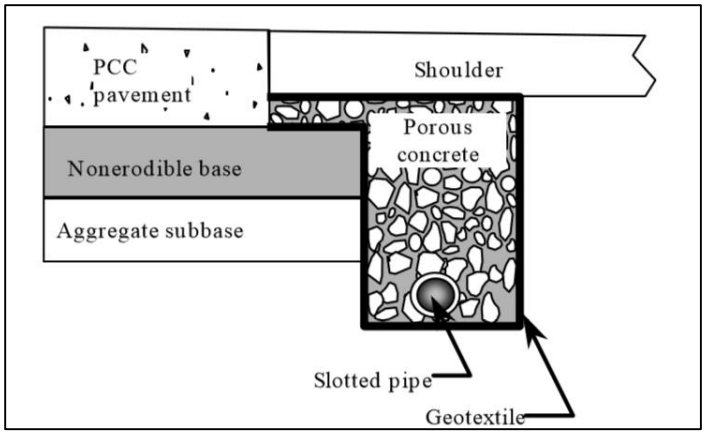

Figure 2.10: Example of pavement structure with non-erodible base and permeable shoulder (Christopher, 2006)

There is also the case where a subbase is incorporated in the pavement structure and is used to help in the subsurface drainage. A subbase is often added in order to decrease stresses in the subgrade and provide a stronger structure. The subbase can also assist in drainage by "enhancing vertical water movement by combining the effects of gravity, seepage distance, and discharge area" (Lebeau, 2009). Lebeau (2009) performed a parametric study using numerical modeling together with an "extended form of the time to drain problem" and "subbase material characteristics under saturated and unsaturated conditions". They found that with the use of adequate subbase material the time to drain could be changed from days to minutes. Their study evaluated different subbase materials consisting of fine sand, medium sand, and gravelly sand. The numerical results showed that the key material for the subbase should be a fine grained material with "large air entry value and high saturated hydraulic conductivity". In the study the medium and gravelly sand subbase materials showed larger times to drain due to the generation of capillary barriers with water ponding in the upper portion of the subbase layer.

Alternative subsurface drainage systems have recently incorporated the use of geosynthetics. The drainage blanket or geocomposite drain, is an example and consists of

a highly permeable layer which is described by Hare et al. (1990) as a "layer whose width and length in the direction of flow is large relative to its thickness". They can be placed below the pavement surface to intercept and infiltration water or can be placed under the base aggregate to shorten the drainage path and drain the structure quicker (Christopher, 2006). Geocomposite drains typically have permeability values that range from 10 ft/day to 100 ft/day (Hare, 1990). This type of drainage systems have been shown to perform very well in pavements.

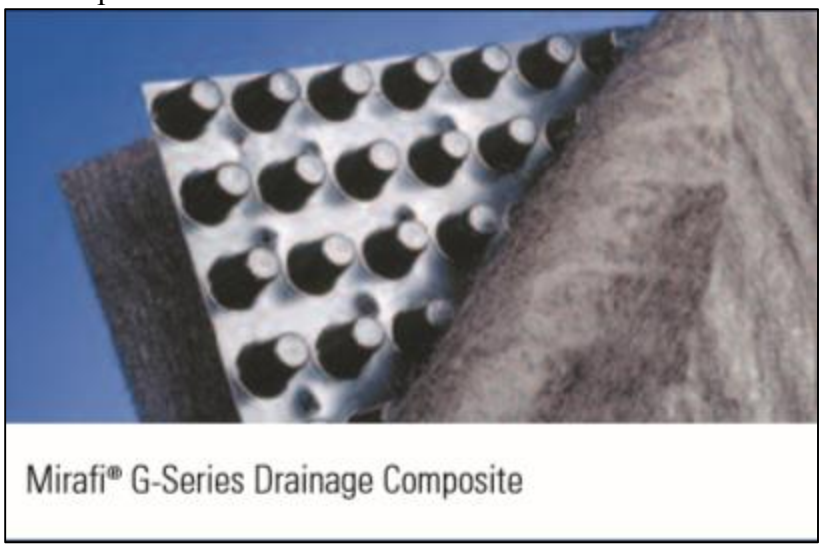

Figure 2.11: Example of a Geocomposite Drain (Tencate Mirafi, 2015)

A comparatively new type of geocomposite drain systems is the geocomposite capillary barrier drain (GCBD). The GCBD consists of transport layer on the top, a geonet in the middle, and a geotextile at the bottom. Figure 2.12**Error! Reference source not found.** shows a sketch of the components of the GCBD and how it drains water out of the pavement structure. The GCBD works by creating a capillary barrier caused by the geonet which causes water to accumulate above it until there is enough water at which capillary breackthrough occurs. The water that accumulates ideally is carried by a transport layer typically consisting of a geotextile in order to prevent breakthrough and water infiltrating

into the subgrade or underlying layers. The third and bottom layer is another geotextile whose function is primarily separation. Additional benefits to using geosynthetics in drainage systems is the possibility of adding properties like reinforcement, control of desired properties, system is thinner than traditional ones constructed with soil layers and the geosynthetics are easily accessible (Henry, 2015).

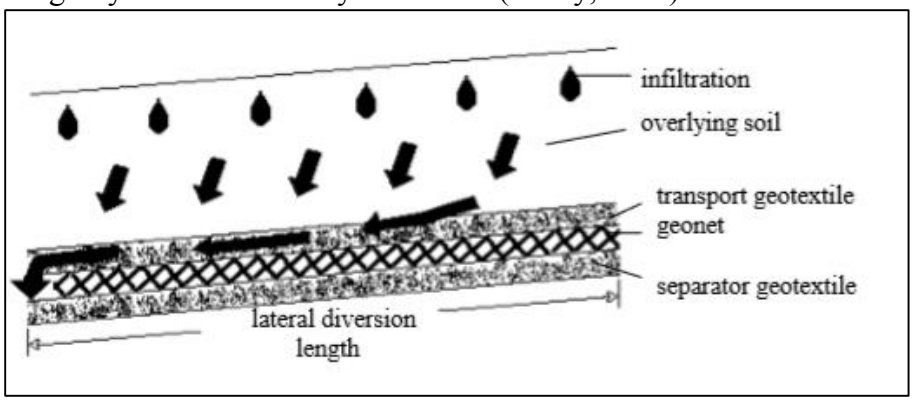

Figure 2.12: Example of Geocomposite Capillary Barrier Drain (Henry, 2015)

New technology has been developed where wicking fibers are incorporated into geotextiles in order to prevent capillary barriers when they are not intended. As previously mentioned the capillary barrier will prevent water from flowing and thus cause it to accumulate at the layer interface which has detrimental effects on the pavement structure. The use of wicking fibers are able to reduce the effects of the capillary barrier in geotextiles through mechanisms like enhanced lateral drainage (Azevedo, 2013). An example of such a geotextile is Mirafi's H2Ri which contains hydroscopic and hydrophilic blue nylon yarns which provide wicking action in order to move water through the plane of the geotextile. Figure 2.13 shows a cross section of the wicking fibers and Figure 2.14 shows a picture of the geotextile itself. This geotextile is able to provide improve lateral drainage through the wicking fiber and provide soil reinforcement, separation, confinement and filtration as well (Tencate Mirafi, 2011).

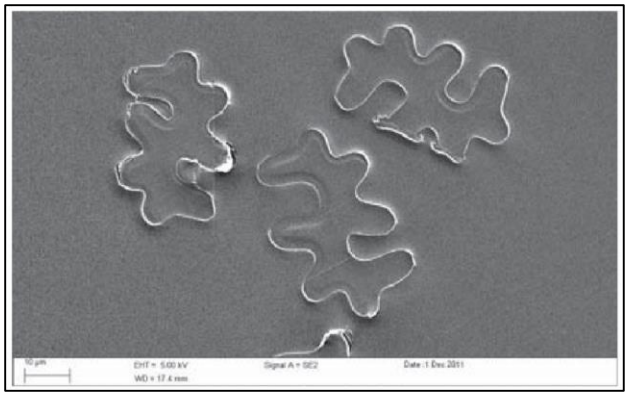

Figure 2.13: H2Ri wicking fiber cross section, Scale: 50µm (Azevedo, 2013)

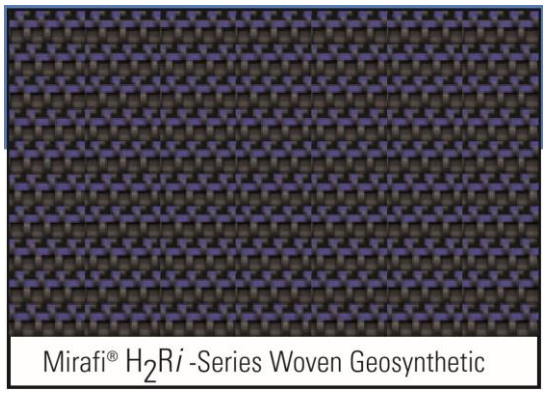

Figure 2.14: Picture of H2Ri geotextile (Tencate Mirafi, 2011)

2.3 GEOTEXTILE WITH ENHANCED LATERAL DRAINAGE

A woven geotextile composed of standard PP and nylon wicking fibers where the PP fibers are hydrophobic while the nylon fibers are hydrophilic has been developed. The pattern of weave and PP fibers guide the water along the nylon wicking fibers (Azevedo, 2013). The wicking fibers are composed of approximately 200 fibers that are bundled together as shown in Figure 2.15 which demonstrates the fibers' capability of wicking moisture vertically using water with a phosphorescent die and black lights. The combination of the PP fibers and the nylon wicking fibers results in a geotextile able to provide reinforcement as well as improved lateral drainage, separation, confinement and filtration.

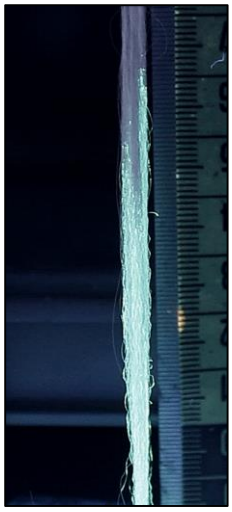

Figure 2.15: Picture of the wicking fibers with glow in the dark water

This geotextile has been studied in order to assess its effectiveness in projects with different situations related to excess water. Some testing was done as well by GeoTesting Express where they built a section of road inside a large box which consisted of 12" of base material, a geoynthetic, and a layer of material resembling a subgrade as shown below in Figure 2.16. Four different geotextiles were tested and the results showed that the section with GT4 performed best by requiring the biggest number of cycles necessary to reach rutting depths of 1", 3" and 4". The results are included in the webinar on "Enhanced lateral drainage in pavement systems" in Tencate's website (Tencate Mirafi, 2015). Figure 2.16 contains the results from GeoTexting Express's experiments and shows that the section with the GT4 required the most cycles in order to reach rutting depths desired. They suggested the reason for this was GT4's ability to remove excess water from the subgrade and base material which resulted in a stronger material.

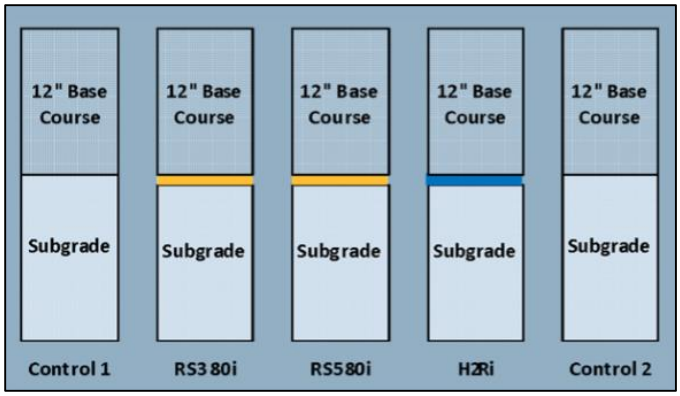

Figure 2.16: Test setup run by GeoTesting Express (Tencate Mirafi, 2015)

Table 2.1: Results from GeoTesting Express's testing (Tencate Mirafi, 2015)

	Number of Cycles		
Section	1" (25 mm) Rut Depth	3" (75 mm) Rut Depth	4" (100 mm) Rut Depth
Average Control	11	54	65
Mirafi® RS380*i*	24	282	647
Mirafi® RS580*i*	24	406	1320
Mirafi® H_2R*i*	30	426	1506

Case histories have been reported where GT4 was used in order to try and deal with particular problems. The first case history is located in the area of The Retreat at Corona County of Riverside in California (Tencate Mirafi, 2012). This area is a luxury golf course community which had difficulties with a large section of roadway built on the side of a hillside. Natural groundwater continuously percolated into the roadway causing it to be very saturated and leading to very poor performance. The engineer on the project was Geosoils, Inc., and they recommended that the road section be excavated as deep as possible and place GT4 on top of the subgrade. The section of this roadway consisted of the subgrade, GT4, 6" of base material, a geogrid, 6" of base material, and 4" of asphalt concrete. Figure 2.17 shows two pictures during the process of installation of GT4 as well

as placement of base material. The use of H2Ri allowed the excess water to be expelled which resulted in good performance of the roadway.

Figure 2.17: Roadway in Corona, CA, in construction with H2Ri (Tencate Mirafi, 2012)

The second case history is located in Jefferson County, Wisconsin (Tencate Mirafi, 2013). In this case STH-106 was reconstructed in a marshy area and experienced differential settlements very quickly after completion. The Jefferson County Highway Department needed a solution that would require as little excavation of the wet, organic soils at the site and contacted Ero-Tex who distribute TenCate products in that area. The case history described the site profile as "wet and saturated silt and peat deposits to depths exceeding 30 feet below the existing pavement". It was important to maintain excavation of the natural material to a minimum so TenCate Geosynthetics designed a structure composed of GT4 at the bottom, 15" crushed stone layer, single layer of Mirafi BXG110 geogrid, 15" layer of crushed stone and then the pavement aggregate base course and asphalt flexible pavement. Figure 2.18 shows the GT4 geotextile with the crushed stone layer being placed above it. The structure described above was described in the case history as a "raft" like structure on which the roadway would be built. The results from the use of this structure was that the excavation was kept to a minimum with only 30" excavated. The GT4 together with the rest of the structure provided a rigid platform on which to build the

roadway and support it. The GT4 geotextile helped by reinforcing the structure and distributing the load more efficiently onto the weak subgrade as well as draining the excess water to strengthen the natural material. Unfortunately for this case history no more information was provided other that the road was successfully built.

Figure 2.18: Raft like platform with H2Ri for roadway construction (Tencate Mirafi, 2013)

The third case history is located in St. Louis County, Missouri (Tencate Mirafi, 2012). For this case a new bridge was to be built over the Missouri River on top of saturated soils. The excess water had to be removed from where the bridge abutments where going to be located to TenCate was contacted with regards to the possible use of the GT4 geotextile. There had already been a design developed which consisted of prepared subgrade, drainable aggregate layer 4" thick, road base aggregate layer 4" thick and a concrete section surface layer. The idea of using the GT4 geotextile was to be able to replace the permeable layer for purposes of cost savings. The use of the GT4 geotextile allowed for a reduction in the drainable base of 2" thanks to the wicking property of the geotextile. The design had the GT4 day lighted or ending into a french drain. The efficacy of the GT4 geotextile was proved the next day after it was installed, ¼" of rain fell and on the next day evidence of GT4's drainage capabilities was evident at the side of the roadway as shown in Figure 2.19.

Figure 2.19: Evidence of H2Ri's drainage capabilities (Tencate Mirafi, 2012)

The fourth case history is about a section of the Dalton Highway called Beaver Slide in Alaska (Tencate Mirafi, 2010). The Dalton Highway connects the oil fields of Prudhoe Bay and the city of Fairbanks thus resulting in a large amount of truck traffic. The highway on top of this is exposed to a very harsh environment which results in poor performance. One of the problems is frost heave, during spring melt water accumulates in the road embankments and when temperature drop frost boils form. It was found during the excavation of the old roadway that there was an organic tundra layer 4 to 5 feet below the road surface and there was frozen soils present as well as water due to the presence of a high water table. The structure to support the new road was built by placing a layer of GT4 over the subgrade followed by 18" of an unspecified material and another layer of GT4. The University of Alaska Fairbanks got involved in this project and installed sensors below and above the first layer of GT4 as well as above the second layer of GT4 in order to measure moisture and temperature (Zhang X. P., 2014). The site was monitored for a year and data from the sensors showed the GT4 moving water through the pavement section without letting it accumulate. As a result the section with GT4 installed was

observed to be in very good shape after a year as shown in Figure 2.20 while the section without it was almost impassable.

Figure 2.20: Image of section in Dalton Highway, AK, with H2Ri (Tencate Mirafi, 2010)

2.4 MOISTURE SENSORS

Two different types of moisture sensors where used in this study to evaluate the moisture underneath pavement sections. The sensors are manufactured by Decagon Devices and are commercialized under the names of EC-5 and ECH20-TE/EC-TM or 5TE. Figure 2.21 and Figure 2.22 shows pictures of both sensors.

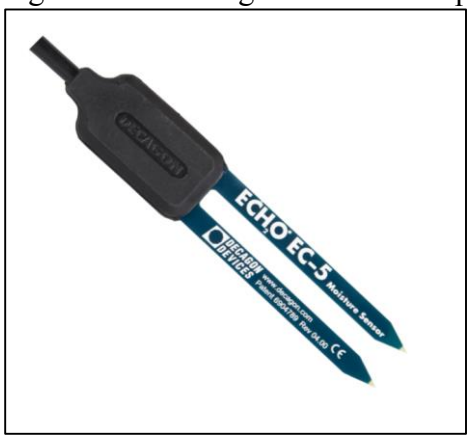

Figure 2.21: EC-5 moisture sensor by Decagon Devices (Decagon Devices, Inc., 2015)

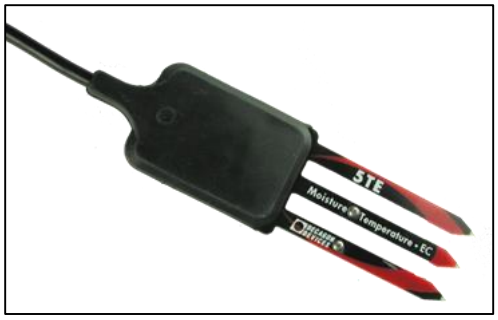

Figure 2.22: 5TE moisture/temperature/electric conductivity sensor

Both sensors are able to measure volumetric water content using capacitance techniques. The sensors determine the permittivity of a medium by measuring the time needed to charge a capacitor using the medium around the sensor as a dielectric. The time can be predicted using Equation (2.1).

$t = -RC \ln[\frac{V - Vf}{Vf - Vi}]$	(2.1)

In Equation (2.1), R is the series resistance for the prongs, C is the capacitance, Vf is the applied voltage, Vi is the starting voltage, V is the voltage to which the capacitor was charged and t is the time to charge the capacitor. Equation (2.2) can be used to calculate capacitance where k is the dielectric permittivity, A is the area of the plates and S is the separation of the plates. This equation is solved for k and then substituted into equation (2.1).

$C = \frac{kA}{S}$	(2.2)

The result is Equation (2.3) used to calculate the dielectric permittivity of the medium where the sensor is installed and used to determine the volumetric water content of the medium.

$\frac{1}{k} = \frac{1}{t}\left[\frac{RA}{S} \ln\left(\frac{V - Vf}{Vi - Vf}\right)\right]$	(2.3)

The sensors come calibrated with a calibration equation determined by the manufacturer. The equation is one that was determined by the manufacturer to work for all soils providing an accuracy within ±3% and resolution of 0.1% of VWC (Decagon Devices, Inc., 2015). The calibration equations for both sensors used in the field are included below, (2.4) is for the 5TE sensor and (2.5) is for the EC-5 sensors.

$\theta = 1.087 * 10^{-3} * Raw - 0.629$	(2.4)

$\theta = 8.5 * 10^{-4} * Raw - 0.48$	(2.5)

The 5TE sensor, unlike the EC-5, is able to measure temperature and electric conductivity is addition to volumetric water content. The electric conductivity is measured using a 4-probe array as shown in Figure 2.23. The temperature is measured using a surface mounted thermistor. The way the thermistor is installed on the sensor the reading is an average temperature along the prong surface.

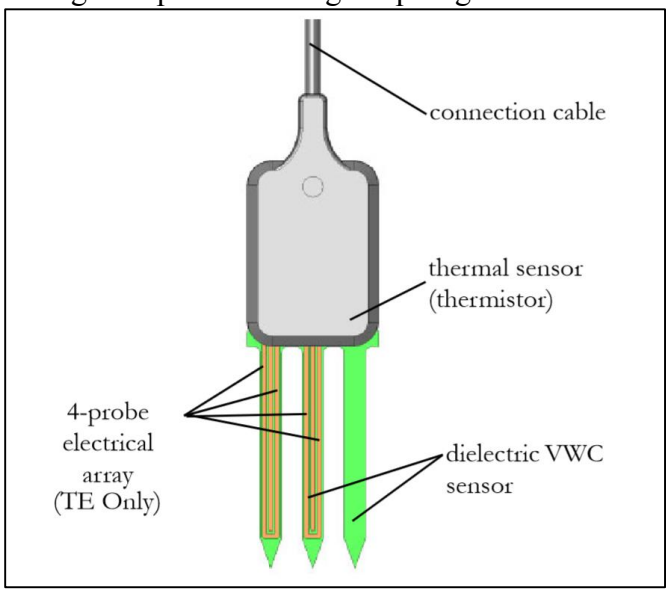

Figure 2.23: 5TE sensor and its components (Decagon Devices, Inc., Version 7)

Decagon Devices manufactures data loggers, which are compatible with these sensors, in the case of this project the Em50 were utilized and are shown in Figure 2.24. This data logger connects to the sensors through 3.5 mm stereo jacks and has 5 ports.

Figure 2.24: Decagon Em50 data logger (www.decagon.com)

The data logger is setup using Decagon's software called ECH2O Utility. Figure 2.25 shows how the program looks when it is first opened up. The program allows for the data logger to be named as well as put any information related to the location of the data logger. The program allows as well for the date and time to be set and tell the data logger what type of sensors are connected to it and how often to sample them. An important feature that it has is the ability to connect the sensor and data logger and leave without having to do any calibrations unless they are desired.

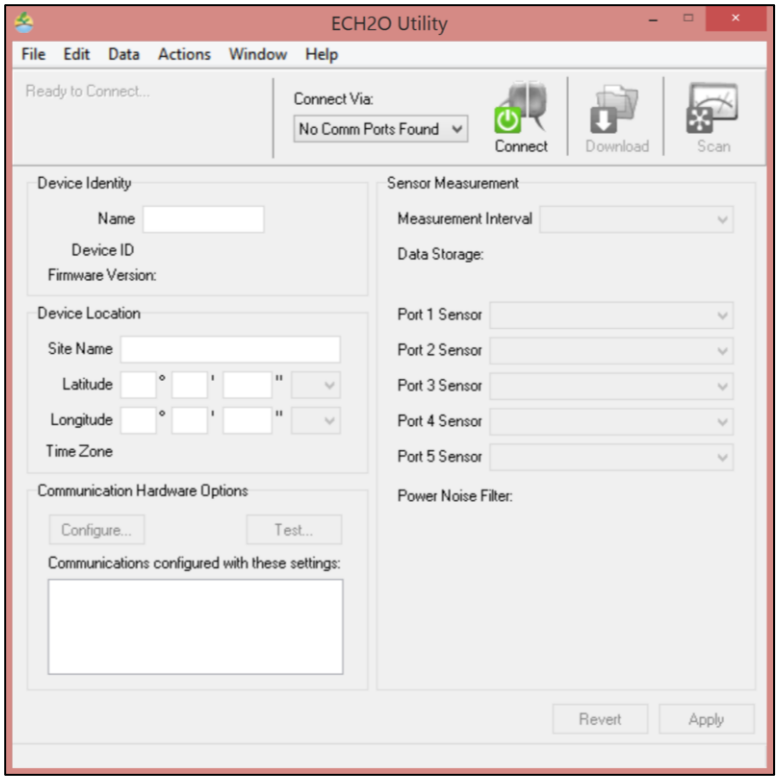

Figure 2.25: ECH2O Utility interface

The program allows for the data logger to scan the sensors and see what they are reading which is very useful to check quality of installation and functionality of the sensors. Figure 2.26 shows the screen that comes up when the button for Scan is pressed. The example below is for the scan of a data logger connected to 4 EC-5 sensors and one 5TE sensor.

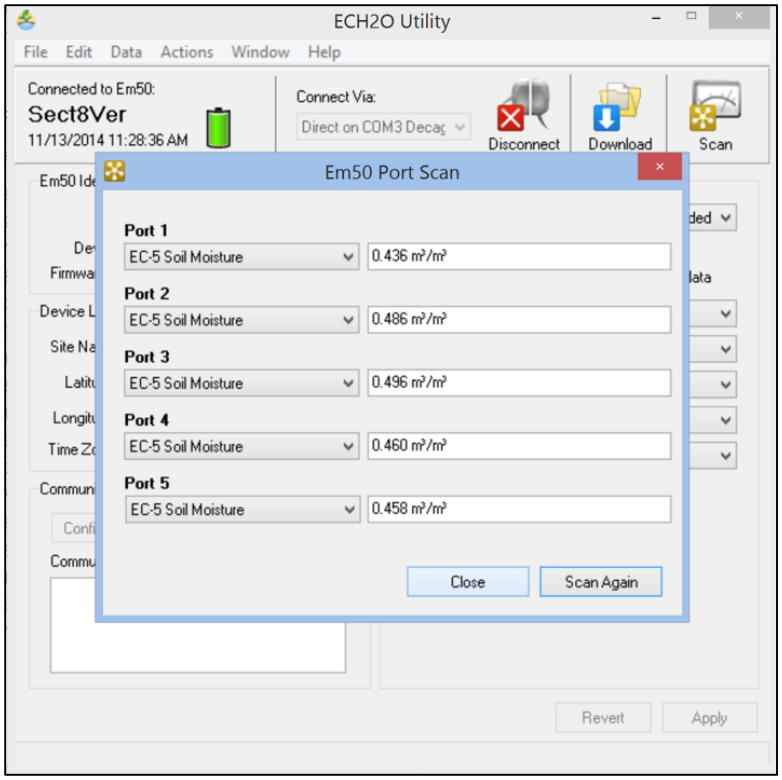

Figure 2.26: Data logger scan

The program creates Excel or text files with the raw and processed data which can then be downloaded to the computer via a stereo-USB cable (Decagon Devices, Inc., Version 8).

Chapter 3 : Description of SH-21

3.1 SITE LOCATION

Texas State Highway 21 (SH-21) runs from approximately San Marcos, Texas, to the border with Louisiana. The field monitoring conducted as part of this study was done at a section of SH-21 located approximately 44 miles east of Austin in an area of Bastrop, Texas, as shown in Figure 3.1.

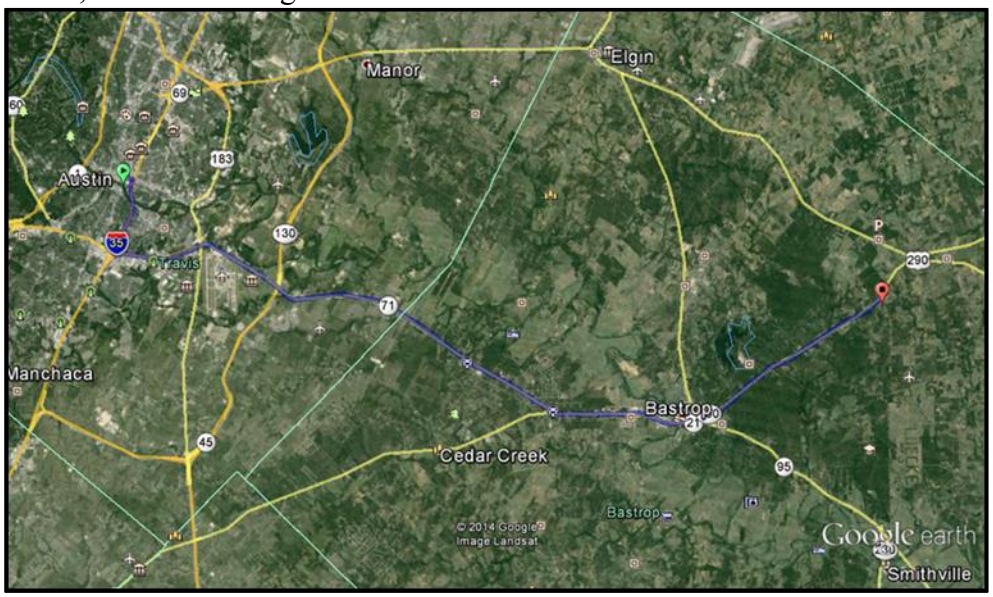

Figure 3.1: Site Location

The area of SH-21 being studied is located approximately 1.6 miles southwest from the intersection of SH-21 with SH-290. This portion of SH-21 lies on the geologic formation defined as Cook Mountain Formation, which is characterized by high plasticity soils. Figure 3.2 shows a view taken during construction in the site of the soils pertaining to the Cook Mountain Formation. Figure 3.3 shows the various geologic formations in the area of study as well as surrounding areas.

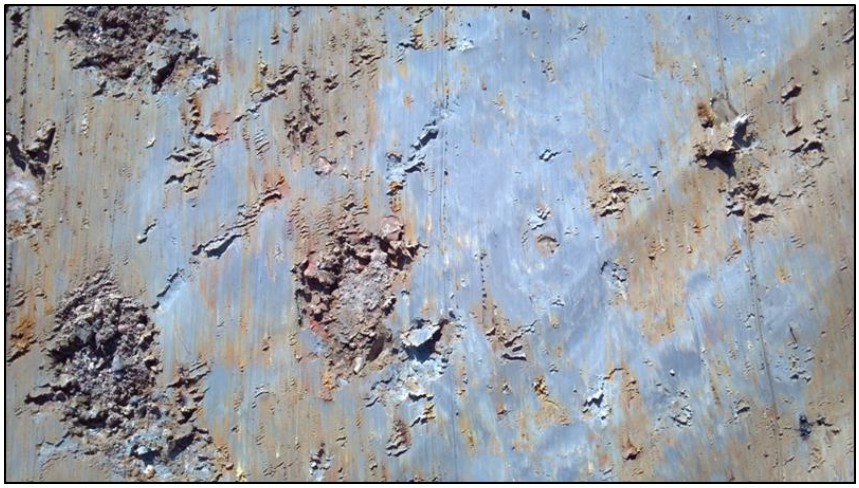

Figure 3.2: Photo of Cook Mountain Formation in SH-21

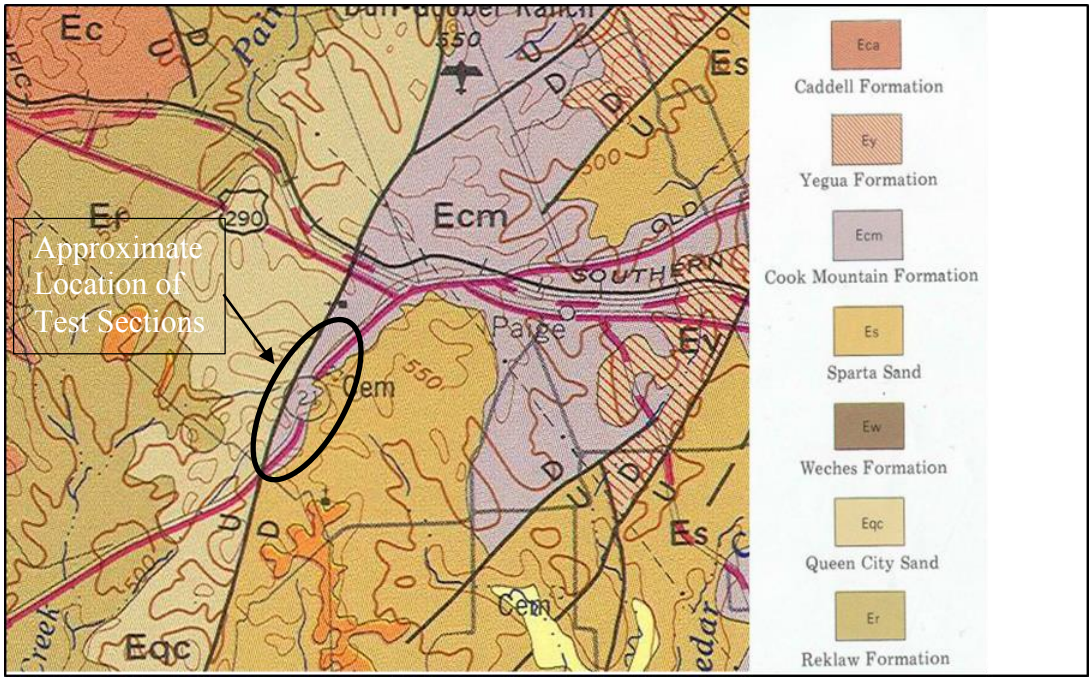

Figure 3.3: Geologic formations near SH-21 area of study (Barnes, 1981)

3.2 HISTORY OF SH-21 AREA OF STUDY

The pavement section of SH-21 under study has historically shown poor performance. It lies in the Cook Mountain Formations, as shown in Figure 3.3, which has been known to consist of expansive clays. The pavement has shown distresses ranging from rutting, vertical deformations, edge cracks and longitudinal cracks. The edge of the road

had noticeable longitudinal cracks which were deep and wide (Zornberg, Roodi, & Azevedo, August 2013). Multiple times the road had received maintenance with level ups and sealing of cracks. However the results had not been adequate. Photos of SH-21 prior to reparations are included in Appendix A, where the previously mentioned distresses can be observed. Due to the poor performance of SH-21, the Texas Transportation Institute (TTI) did an assessment in order to find possible solutions to the problem.

3.3 RESULTS OF PRE-CONSTRUCTION STUDY

TTI compiled a "Pavement Design Report" in which it investigated possible reasons why the section in question in SH-21 had been performing so poorly and suggested ways to correct this (Texas Transportation Institute, 2010). The section they investigated is shown in Figure 3.4. The section of SH-21 evaluated in this report started southwest of the intersection of SH-21 and SH-290 and extended approximately 2.85 miles southwest on SH-21. The current conditions on SH-21 were evaluated using Ground Penetration Radar (GPR) in order to develop a profile of the pavement structure and estimate the amount of level ups made as well as to identify and measure the lengths of cracks. Table 3.1 summarizes the findings from the TTI investigation regarding distresses present on the road and areas of level ups.

Figure 3.4: Section of SH-21 studied by TTI (Texas Department of Transportation, 2010)

Table 3.1: Distresses measured on SH-21 (Texas Department of Transportation, 2010)

Distress	Total length Northbound (feet)	Total length Southbound (feet)	Total length Combined (feet)	Total length as percent of total project length
Minor edge cracking	4161	5311	9472	32
Level ups	5925	5510	11435	38
Longitudinal cracking in inside wheel path of outside lane	324	312	636	2
Longitudinal cracking in inside lane	161	442	603	2

Results from the GPR showed that the typical structure in SH-21 consisted of around 10” of hot mix asphalt, 10” of base layer, and an old hot mix asphalt (HMA) layer below, and then the subgrade at the bottom. Multiple places were found where level up thickness was significant suggesting these areas might have been performing worse than others. Figure 3.5 shows the thickness of the top layer of SH-21 going north bound as measured using the GPR.

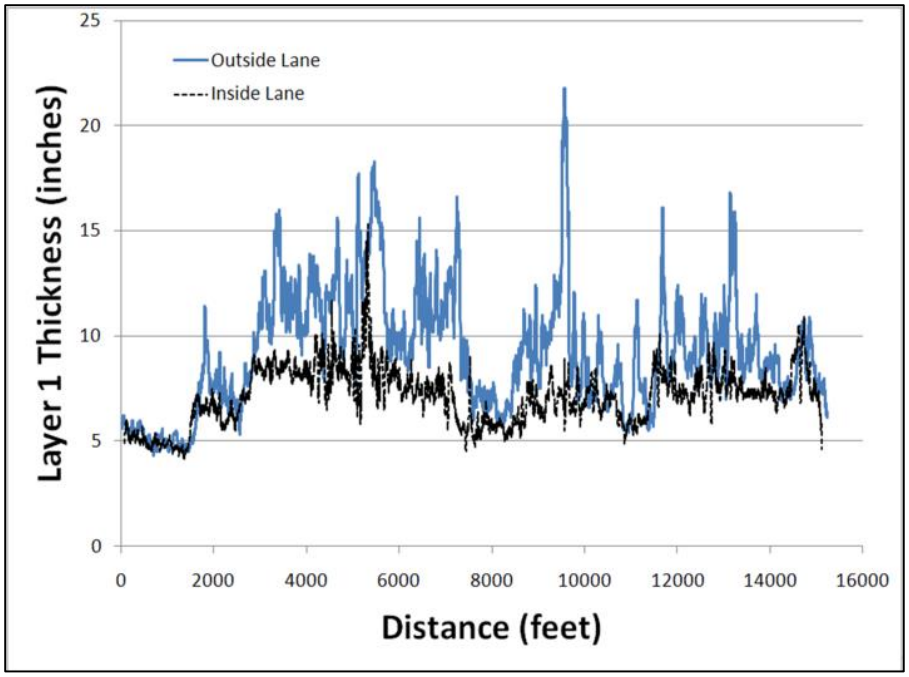

Figure 3.5: Thickness of Asphalt on SH-21 Northbound (Texas Department of Transportation, 2010)

As part of the investigation, TTI also performed 9 borings, 3 of which were performed on the road through the asphalt and the remanding 6 were done on the side slope. Figure 3.6 below shows the profile obtained from the three borings done through the road. The presence of the old HMA pavement structure was only found in SB2.

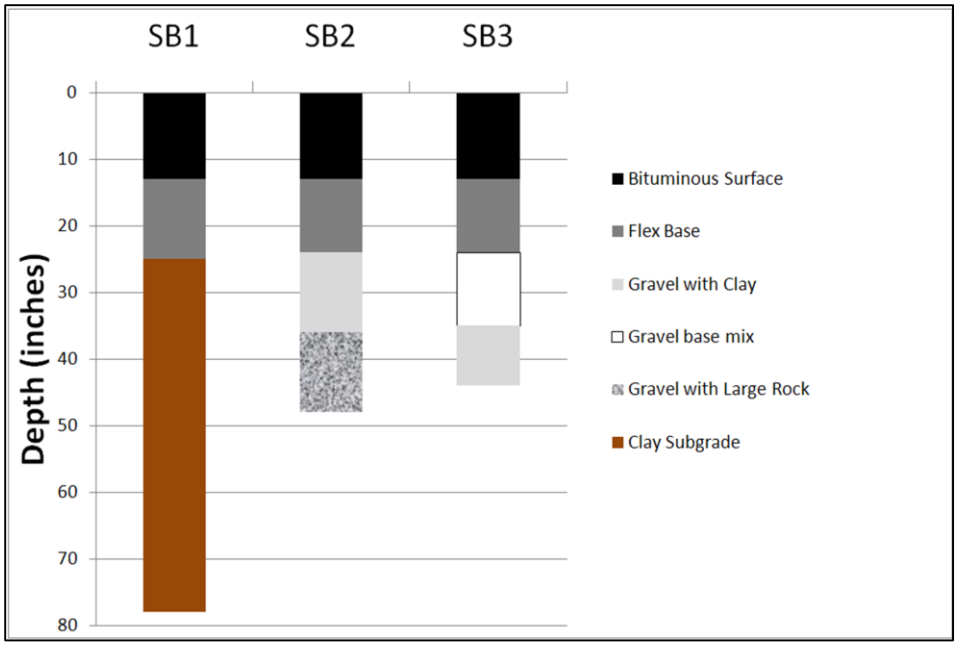

Figure 3.6: Profiles obtained from borings (Texas Department of Transportation, 2010)

As part of the soil exploration phase, dynamic cone penetration (DCP) tests were conducted in order to detect weak zones where possible shear failures could occur. The TTI report indicates that prior to starting the work, it was thought that one reason for the extensive longitudinal cracking could be due to issues with steep shoulders observed at the side. Due to these steep shoulders, it was a possible that the cracks were due to shear failures on the side of the road. The report included graphs such as the one shown in Figure 3.7, where the horizontal axis is for soil strength and the vertical axis is for depth in inches. From the DCP results, TTI found that there was a weak zone between 24 and 36 inches that they found to coincide with the old HMA pavement layer. The results for the DCP tests performed at the different borings are included in Appendix A.

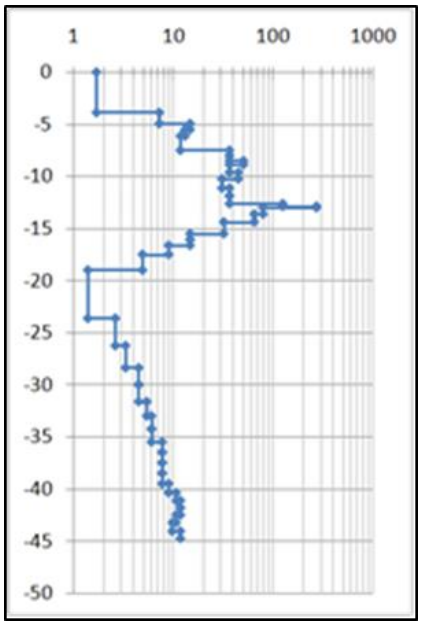

Figure 3.7: DCP results for SB5 done 4 ft from the edge of the road (Texas Department of Transportation, 2010)

In addition to the DCP tests, TTI also obtained soil samples, which were used to conduct geotechnical tests. Table 3.2 summarizes the results from the laboratory tests done on the soils samples from the borings done in SH-21. From the table below it was observed that the soils in the area showed a high plasticity index, which is typical of expansive soils.

Table 3.2: Laboratory test results from SH-21 soil samples (Texas Department of Transportation, 2010)

Boring No.	Depth Top	Depth Bottom	Moisture Content %	Passing No. 200 %	LL %	PI %	Sulfate Content %	Organics (SOC) %
SB-1	20	25	27.6	52.6	61	42	120	
	25	29	27.4	48	59	41	120	
	29	37	16.1	66.9	33	16	100	
	37	42	141.7	63.2	59	33	106	
	42	53	29.8	60.7	54	30	100	
	53	78	29.6	59.3	61	34	106	
SB-2	24	32	27.8				NA	NA
	32	48	18.2				NA	NA
SB-3	NO	SOIL						
SB-4	0	12	18.4	68.9	35	13	100	
	12	36	23.8	50.5	61	42	480	0.23
	36	44	22.3	54.6	48	29	<100	1.29
	44	58	18.6	48.8	36	21	120	1.05
	58	72	12.8	43.5	38	23	140	0.72
SB-5	20	24	22.3	61.5	65	47	106	0.21
	24	39	27.6	68	81	59	2220	0.21
	39	55	20.1	64.7	65	45	2180	3.21
SB-6	12	24	22.6	65.1	67	47	114	0.2
	36	54	20.9	55.6	60	33	280	1.9
SB-7	18	28	21.3	53.1	42	25	120	0.18
	28	38	29.2	60.9	54	32	120	2.97
	38	52	32.3	60.2	71	45	120	2.36
	52	62	33.7	66.1	72	42	180	1.74
	62	75	24.8	49.9	81	51	1660	0.3
Boring No.	Depth Top	Depth Bottom	Moisture Content %	Passing No. 200 %	LL %	PI %	Sulfate Content %	Organics (SOC) %
NB-1	14	22	25.5	41.3	50	33	120	0.54
	32	36	33.9	40.9	62	40	106	0.58
	36	54	40.9	43.3	59	33	134	3.06
	54	72	30.2	49.7	64	41	146	1.76
NB-2	17	22	24.5	68.9	45	16	29	0.31
	22	36	30.3	92.7	51	19	32	2.41
	36	60	29.5	77.9	54	23	31	2.78

From these results, the report provides recommendations that included the addition of a shoulder with a minimum with of 4 feet. From the findings from the DCP tests, it was concluded that the cut would have to be at least 36 inches deep to eliminate the weak layers found and from there start the shoulder in order to provide adequate lateral support. It was also recommended that the shoulder be daylighted in order for it to drain adequately. In addition to the construction of a new shoulder, different recommendations were also given for different parts of SH-21 depending on the distresses present. The recommended cross sections are included in Appendix A.

For the majority of the length of SH-21 investigated in the TTI report, the recommendation was to add shoulder with a minimum width of 4 feet and a full depth reclamation of the outer lane as shown in Figure 3.8.

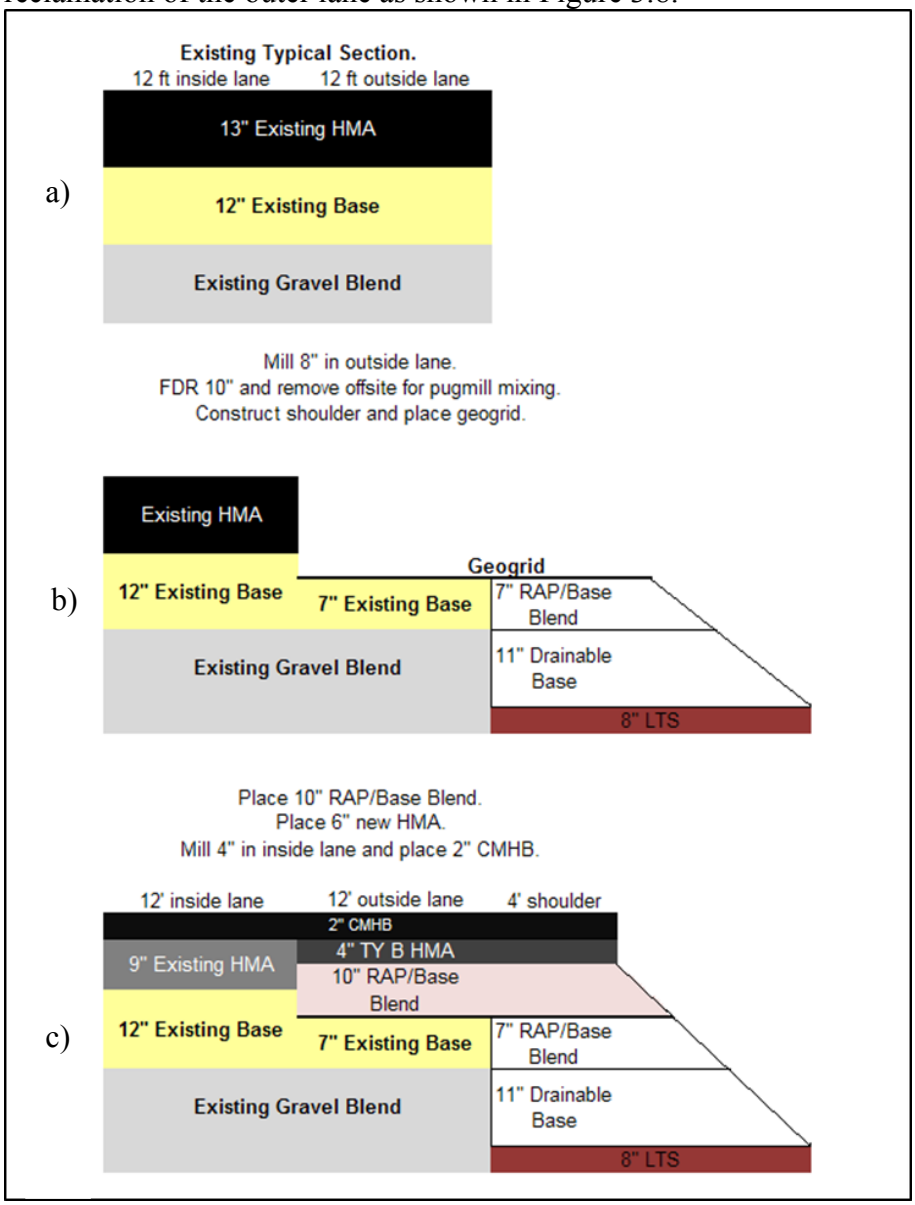

Figure 3.8: Recommendation for majority of evaluated area of SH-21 (Texas Department of Transportation, 2010): a) Pre-existing pavement structure, b) Suggested milling of asphalt and addition of Shoulder, and c) New recommended pavement structure

3.4 FINAL TXDOT DESIGN

After the recommendations to TxDOT provided in TTI (2010), TxDOT decided on a slightly different design based on what the study's recommendation. The final design for the area where the test sections for this study are located is shown in Figure 3.9 and Figure 3.10.

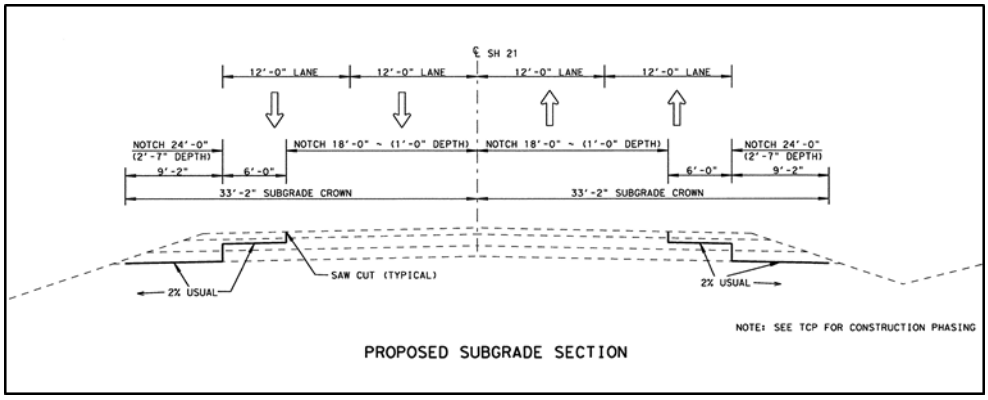

Figure 3.9: Excavation portion of rehabilitation (design plans for SH-21 from TxDOT)

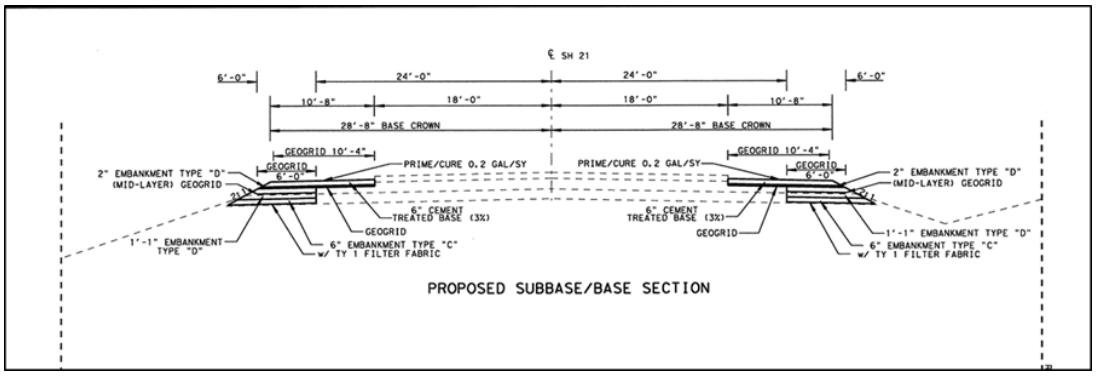

Figure 3.10: Construction of new shoulder (design plans for SH-21 from TxDOT)

The reparation involved initial milling of 3" of the asphalt layer from the inner lane and excavation of 12" in the outer lane. A 36" excavation in the shoulder area was planned which required reaching the subgrade. After the excavation process was completed, TxDOT planned to place a generic geotextile filter fabric above the subgrade in the shoulder area (geotextile commercialized as 140NC, manufactured by Mirafi). Above the geotextile, the design plans specified for a 6" layer of Type C fill material which consisted

of rock smaller than 3” but larger than 3/8”. Type D fill material compacted between 98 and 100 percent of dry maximum density as determined by Tex-133-E was to be placed above the previous Type C layer. This material was specified in the design plans as salvaged asphalt pavement, which would pass a 2”sieve. The plans also specified for this material to be sprayed with water and emulsified asphalt (SS-1) mixture of 1 to 8 percent to guarantee the material bonded correctly. The following layers consisting of material Type D consisted of a 6.06” layer placed above the Type C material, a biaxial geogrid, and then another 6.04” layer of Type D material was placed with another biaxial geogrid placed above but this one extending from the embankment to the outer edge of the inner lane as shown in Figure 3.11. Following this an additional 3.5” layer of Type D material of was to be placed above after which a final 6” layer of cement treated base was to be placed. The final additions specified in the plans was a 3” layer of Type C HMA above which a final 1” thin overlay was placed. Figure 3.11 shows the final design selected by TxDOT for the reparation of SH-21 for the area pertinent for this study.

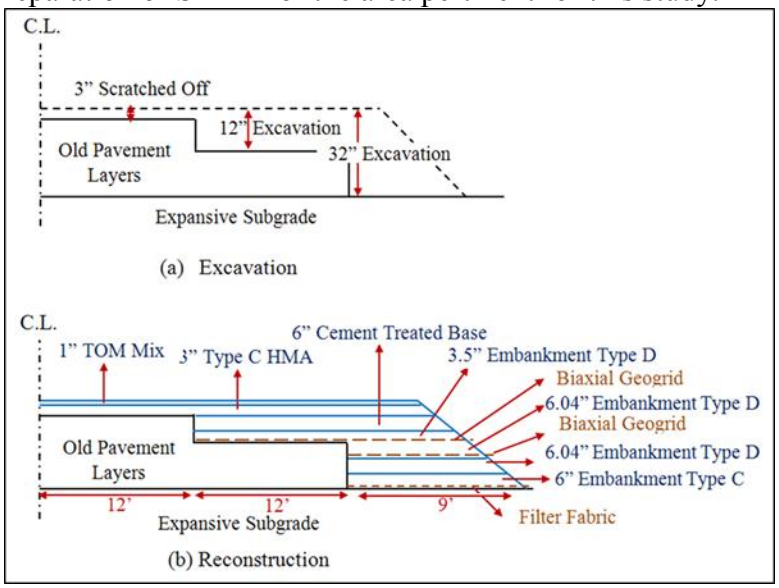

Figure 3.11: Detailed sketch of excavation and rebuild of SH-21

3.5 TEST SECTIONS EVALUATED BY UT-AUSTIN

The University of Texas at Austin (UT) became involved in this project by suggesting the use of various types of geotextiles instead of just the generic filter fabric initially included in the design plans (Zornberg, Roodi, & Azevedo, August 2013). The generic filter fabric is a "needlepunched nonwoven geotextile composed of polypropylene fibers" (Tencate Mirafi, 2014). This geotextile was to be used just for separation in the original design. The use of alternative geotextiles was incorporated in the study which could provide additional benefits such as reinforcement and enhanced lateral drainage, in addition to separation.

The additional geotextiles selected in this study, in addition to the control (GT1) geotextile (Mirafi 140NC) included Mirafi HP570 (GT2), RS580i (GT3), and H2Ri (GT4). The GT2 is "composed of high-tenacity polypropylene yarns, which are woven into a network" (Tencate Mirafi, 2010). This geotextile provides filtration, separation, and soil reinforcement. The GT3 has a "super high-tenacity polypropylene filaments formed into an innovative weave to provide superior reinforcement strength and soil interaction with high water flow and soil retention capabilities" (Tencate Mirafi, 2013). Finally the GT4 "is a revolutionary wicking geosynthetic created from super high-tenacity polypropylene filaments and patented wicking filaments formed into an innovative weave to provide superior reinforcement strength and soil interaction integrated with a high soil retention and wicking capabilities" (Tencate Mirafi, 2011). To wick is defined by the Merriam-Webster dictionary website as "to cause (fluid or moisture) to be pulled away from a surface". The GT4 geotextile is expected to wick moisture from a wetter area to a drier area and as a result balance out moisture in the area of the geotextile. In roads founded on expansive clays this will not prevent the vertical movement of the road but will reduce the differential movement thus reducing cracks in the pavement. Table 3.3 summarizes the

geotextiles used in this study as well as how they will be referred to from now on and the capabilities used for the marketing of each geotextile.

Table 3.3: Geotextiles used in this study

Geotextile	Commercial Name	Capabilities
GT1	Mirafi 140NC	Separation, Lateral Drainage
GT2	Mirafi HP570	Soil Reinforcement, Separation, Filtration
GT3	Mirafi RS580i	Soil Reinforcement, Separation, Filtration, Confinement
GT4	Mirafi H2Ri	Enhanced Lateral Drainage, Reinforcement, Separation, Filtration, Confinement

3.6 TEST SECTION LOCATIONS

Portion of SH-21 was selected for the construction of eight test sections where the various geotextiles would be incorporated in the final design chose by TxDOT. The selection of the study area was done in collaboration with the research group from The University of Texas at Austin and the TxDOT Bastrop office representatives. The final locations were chosen based on past performance of the existing road. The area where the test sections where finally constructed ranged from station 100+00 to 140+00, as shown in Figure 3.12. The test sections are arranged as shown in Figure 3.13.

Figure 3.12: Location of Test Sections on SH-21, Bastrop, Texas

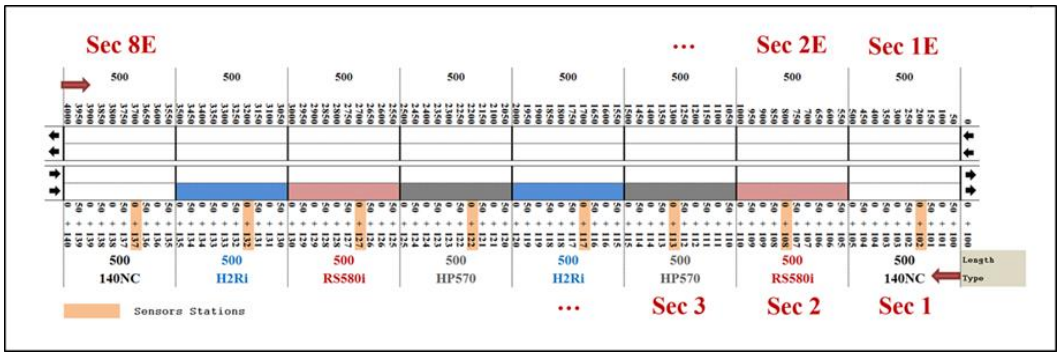

Figure 3.13: Arrangement of Test Sections on SH-21, Bastrop, Texas

3.7 MOISTURE SENSORS

Moisture sensors were installed during the construction of the test sections, before the installation of the geotextiles and placement of the base layers. The sensors were installed in the subgrade material, which consisted of expansive clays as shown in Figure 3.14. Decagon EC-5 and 5TE moisture sensors where installed in all the test sections. Both sensors measure volumetric water content using capacitance to define the dielectric permittivity of the soil in the vicinity of the sensors. In order to power the sensors and to record the sensor readings, Em50 Decagon data loggers were installed at the side of the road. The sensors were arranged in a similar arrangement in all 8 test sections, as shown in Figure 3.15. Sensor installation was finalized on January 25, 2013.


Figure 3.14: Image taken during installation of moisture sensors

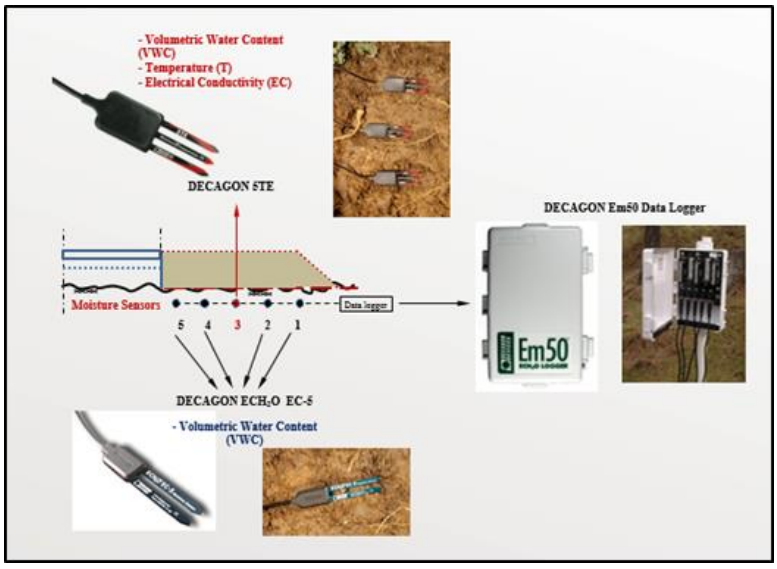

Figure 3.15: Moisture Sensor Array in Test Sections

3.8 SITE CHARACTERIZATION

During the installation of the moisture sensors, soil samples of the subgrade were obtained for each test section by the UT-Austin research team. These samples were then tested at the UT-Austin geotechnical laboratory. Atterberg Limit tests were run on soil samples from all 8 locations and are summarized in Table 3.4. These results showed that in general the subgrade soils in the area of the test sections have medium to very high swelling potential, based on the Plasticity Index values obtained from the soil samples.

Table 3.4: Results from Atterberg Limit tests on samples from subgrade soils in SH-21

Section	PI
1	38
2	35
3	24
4	52
5	24
6	36
7	36
8	58

3.9 GEOTEXTILE INSTALLATION

After installation of the moisture sensors, placement of the geotextiles commenced on January 26, 2013. The geotextile roles used had been previously cut to a width of 9'2" (Zornberg, Roodi, & Azevedo, August 2013). The geotextiles were cut to the specified width in order to cover the subgrade level for the newly constructed shoulder as shown in Figure 3.11. The geotextiles as shown in Figure 3.11extend from the outer end of the outer lane, where the white line at the edge of the traffic lane will be, and outwards 9 feet. Two rolls were used per section due to the rolls being 300 feet long and all test sections being 500 feet long. Figure 3.16 shows how the geotextiles were installed in the multiple test sections.

Figure 3.16: Image taken during installation of H2Ri in Section 7

3.10 COMPLETION OF PAVEMENT SHOULDER CONSTRUCTION

After the installation of the moisture sensors and the geotextiles, construction of the base layer components of the pavement structure continued until the pavement layer was placed and construction was finalized. Figure 3.17 and Figure 3.18 show the area of study on SH-21 after construction was finalized.

Figure 3.17: Images of finalized SH-21, Test Section 7

Figure 3.18: Images of finalized SH-21, Test Section 1

Chapter 4 : Moisture Sensor Installation/Layout and Results

As discussed in Chapter 3, a total of eight test pavement sections were instrumented with moisture sensors in order to obtain moisture data from the subgrade soils underneath the newly constructed shoulder. Sensors were installed following a horizontal array in order to allow evaluation of the hydraulic performance of the various geotextiles. Additional sensors were installed in a vertical array in order to provide additional information of moisture in the natural soils at each section. The eight test sections are located on SH-21 in Bastrop, Texas, as shown in Figure 4.1. The installation process for each location as well as the data and its analysis are presented below.

Figure 4.1: Locations of Test Sections

4.1 MOISTURE SENSOR INSTALLATION

4.1.1 Horizontal Sensor arrays

A total of eight test sections were instrumented with moisture sensors in order to evaluate the hydraulic performance of each geotextile used in the study. Five moisture sensors manufactured by Decagon Devices were placed per section in approximately the center of each test sections. All test sections have similar subgrade soils. The location of each array of sensors is shown in Figure 4.2. Unfortunately, during the construction phase

the sensor array in Section 2 was damaged and abandoned from the very beginning, leaving only 7 sensors arrays available for evaluation in this study.

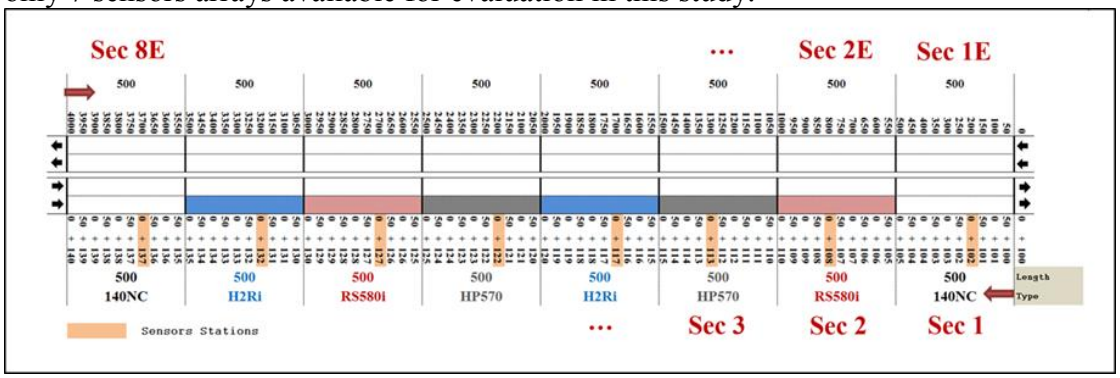

Figure 4.2: Location on Moisture Sensors per Test Section

The moisture sensors were placed approximately two inches below the surface of the finished subgrade in order to measure the moisture content of the subgrade material. Figure 4.3 was taken on January 2013 during the construction phase of SH-21 corresponding to construction of the sections evaluated in this study. The subgrade material was initially compacted and prepared. Before placement of the base material a trench was dug at each section in order to install the moisture sensors.

Figure 4.3: Installation of Sensors (Section 8)

The sensors were spaced horizontally 1.5 feet between each sensor, as shown in Figure 4.4. This spacing allowed for moisture measurements to be taken across the width of the geotextile underneath the road shoulder. Four of the five sensors measure volumetric water content (Decagon ECH2O EC-5 sensor). The fifth sensor is a Decagon 5TE sensor capable of measuring volumetric water content, temperature, and electrical conductivity. The sensors were installed as shown in Figure 4.5.

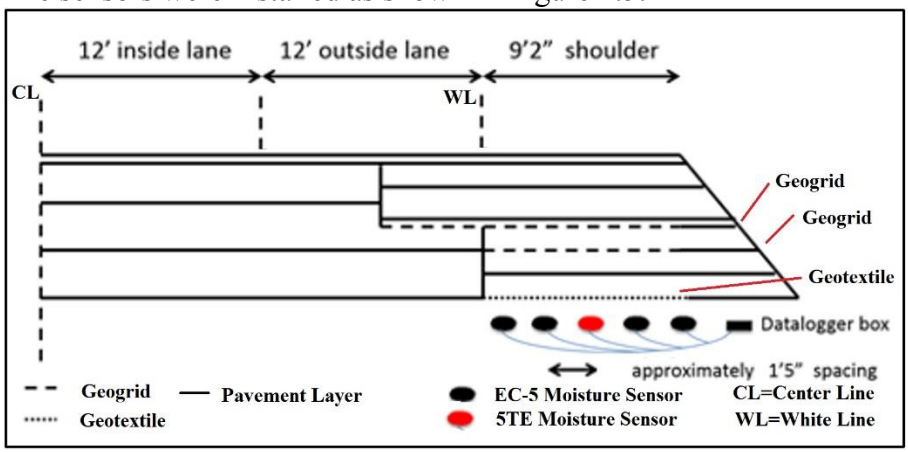

Figure 4.4: Sensor Layout

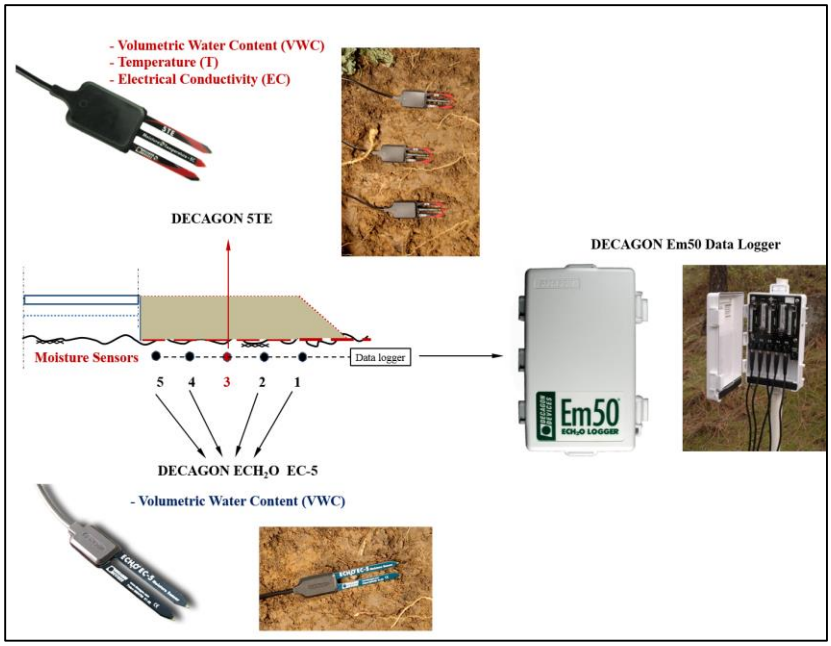

Figure 4.5: Equipment used in sensor array beneath pavement

As shown in Figure 4.5, sensors were connected to a data logger in order to power them and record the data. The cables connecting the sensors to the data loggers were placed along the same trench dug to install the sensors, as shown in Figure 4.6. After the sensors had been installed and the trenches had been refilled, the sections were re-compacted. The various geotextiles were placed in order to continue the construction process by placing the layer of base materials and finally the asphalt surface. Figure 4.7 shows the continuation of the construction process from the refilling of the trenches to the placing of the geotextiles and base layers. The geotextiles were placed solely over the subgrade material for the new shoulders. The geotextiles extend 9 feet outward from the where the white line at the outer edge of the outer lane is located, as shown in Figure 4.4. The hydraulic benefits of the geotextiles are expected to occur only under the geotextiles in the shoulder area where the sensors are located. This study was considered a pilot to evaluate the performance of the various geotextiles, even if the shoulder areas were the only ones that experienced any benefits from the geotextiles.

Figure 4.6: Connection of sensors to data logger (Section 7)

Figure 4.7: Placing of Geotextiles and Base Layers

The data loggers initially were buried at the side of the road for approximately the first year of the study. This was done by placing the data loggers in waterproof boxes as shown in Figure 4.8. The cables were passed through some openings that were installed in the boxes in order for the cables to enter the boxes while preventing water to pass. These openings are believed to have not performed as intended, as water ultimately entered the boxes, which led to damage in the data loggers. In most cases the data loggers were repaired and data was downloaded. However, in some cases the data loggers did not turn on again and data was ultimately lost.

Figure 4.8: Data logger placed in protective casing

In order to address this problem, the data loggers were removed from the ground and were placed at the side of the road on Saturday, May 17, 2014. The decision of placing the data loggers above ground took some time in order to perform the installation properly due to past bad experiences. In past studies data loggers had been placed in mail boxes, due to the excessive Texas heat, the batteries powering the data loggers exploded ruining the devices. There were concerns as well of the data loggers being vandalized and/or being stolen. Ultimately, the data loggers were installed in outdoor sprinkler boxes, which were placed on metal stakes at the side of the road. The boxes were placed within the brush or between the trees to protect the data loggers from the heat and hide them from people. They were placed high enough from the ground so as to prevent them from flooding during intense rain events and low enough to keep them out of the line of sight of drivers. Figure 4.9 shows the sprinkler box with two data loggers installed in

Section 7.

Figure 4.9: New data logger location

The sensors placed underneath the pavement for this study have 16 feet long cables, which were adequate when the data loggers were buried. In order to place the data loggers at the side of the road within the brush and trees, longer cables were needed. Decagon Devices provide extension cables with female and male stereo jack ends. The extension cables were bought as well as heat-shrink wrap which was moisture resistant. These connections could be sources of problems and because of this much care was taken in the planning for this modification in the location of the data loggers.

In order to minimize possible problems associated with moisture entering the connection point between the sensors and the extension cables, moisture resistant shrink wrap was used, which contained a lining of adhesive. This adhesive melts when heated, thus providing a good seal of the connection even against moisture. The shrink wraps were tested in the lab, an extension cable was connected using the shrink wrap and the connection was placed at the bottom of a bucket with about 2 feet of water. The connection was left under water for over a week and then removed then open and was found to have remained dry. In the lab, the heat-shrink wrap was heated using a heat gun, an approach that was not possible in the field. In order to perform the field installation, a small butane

torch was utilized. The heating of the shrink wrap using the butane torch was first practiced in the lab to make sure it worked properly. The actual field installation was subsequently performed. A visit to the field to recheck connections when some sensors were malfunctioning involved the splicing of the heat-shrink wraps to see if that was the source of problems. Once cut open the connections were found to be dry, proving that moisture resistant heat-shrink wraps did work for these installations.

In order to move the data loggers from where they were buried to their future location they had to first be excavated. The distance of the data loggers from the edge of the white line was painted on the side of the road where the data loggers were located with respect to the section of road as shown in Figure 4.10. The cables that are part of the sensors were connected to the extension cables and the connections were

Figure 4.10: Distance from data logger to edge of white line (Section 6)

buried where the data loggers were placed before. A trench was dug at each section in order to have the cable extensions at least 6" underneath the surface to protect them from being damaged. A metal stake was driven using a hammer and the sprinkler box was attached to

it using bolts and screws. Figure 4.11 shows the cables from the sensors on the left and on the right the extension cables in the trench in order to reach the location of the new data logger. An example of a finalized installation is shown in Figure 4.12. After the data loggers were removed from underground, no issues involving damaged data loggers was experienced.

Figure 4.11: Installation of extension cables and new data loggers

Figure 4.12: Finalized installation of new data loggers in Section 6

4.1.2 Vertical Sensor Array

An additional installation was performed between November and December 2014. This consisted of a vertical array of 5 Decagon EC-5 sensors installed at each of the 7 sections with functioning sensors underneath the pavement. The main purpose of this array was to record the moisture front migration in the shoulder and be able to compare the data from the vertical array to the horizontal array under the pavement. The sensors were installed in the subgrade soils and were spaced approximately 6 inches apart from each other. This arrangement was based from previous experience and was appropriate to be able to capture the migration of the moisture front in the natural soils at the site.

The installation was done in two phases, with the first one taking place on November 13, 2014. For this installation a two-man auger was used in order to drill holes using a 12" diameter auger with the addition of an extension in order to reach required depths. Three installations were conducted in order to complete the field effort. The two-man auger did not have enough power to perform the drill holes fast enough and without excessive effort from the operators. Installations at sections 8, 7, and 4 were done that day.

Figure 4.13: Phase 1 of installation of Vertical Sensors

The second phase took place on December 3, 2014, and a Bobcat Skid-Steer was used, which had a hydraulic auger installed on it, as shown in Figure 4.14. The auger had a diameter of 12" and was equipped with an extension as well. The additional power of the equipment used for the second phase allowed for a total of 4 installations to be done and a total of 8 holes were drilled. One hole per section was opened for purpose of installation of the sensors and a second hole was performed at each section in order to obtain soil samples. The soil samples consisted of cuttings from the auger from the natural soil as well as samples disturbed as little as possible. Compaction molds were pushed into the soil using the hydraulic system of the Bobcat in order to obtain samples as less disturbed as possible with the equipment accessible to the research group. Figure 4.15 shows sampling at Section 4, cuttings from the subgrade material were taken in sealed buckets and the compaction

molds were removed with as little disturbance to the sample as possible. The samples were taken for future work in case the soils at the site need to be further characterized.

Figure 4.14: Bobcat Skid-Steer equipped with 12” hydraulic auger

Figure 4.15: Sampling during second phase of installation of Vertical Array

Table 4.1 shows the distance from the edge of the outer white line of the road to the location where the vertical arrays were installed. The holes were drilled at the same distance from the edge of the white line but to the side of the past location of the data loggers to prevent possibly damaging the extension cables connecting the horizontal sensor array to the data loggers placed above ground which had been buried at those locations. During the drilling process, the thickness of each layer was documented and the sensors were installed below where the natural soil starts. The rational for this approach was to have the first sensor in the vertical array at a similar depth/elevation as the sensors in the horizontal array for purposes of comparing readings. The sensors were then inserted manually into the soil with a vertical spacing of 6 inches between sensors. Table 4.2 summarizes the depth of each sensor in the vertical arrays with respect to the surface of the fill material. Figure 4.12 shows all 5 moisture sensors installed for the vertical array in

Section 7. The cables for each sensors were labeled using colored electric tape so it was known to what sensor they belonged.

Table 4.1: Horizontal distance from edge of white line to Vertical Array

Section	Distance (ft)
1	16.58
3	18.17
4	15.92
5	17.58
6	15.67
7	17.00
8	17.00

Table 4.2: Depth of sensors in Vertical Array with respect to surface

	Depth from surface (in)				
Section	Sensor 1	Sensor 2	Sensor 3	Sensor 4	Sensor 5
1	7	13	19	25	31
3	8	14	20	26	32
4	10	16	22	28	34
5	12	18	24	30	36
6	22	28	34	40	46
7	22.5	28.5	34.5	40.5	46
8	18	24	30.5	36.5	42

Figure 4.16: Vertical Array of Moisture Sensors Installed in Section 7

An additional installation was done in Section 6, specifically 5 additional sensors were placed in order to obtain moisture data from the layer of fill. The layer of fill at this site consisted of 22” of fill and 5 EC-5 sensors were installed with a vertical spacing of approximately 3.5”.

After the sensors were installed, the soil that had been excavated was placed back into the hole in the same order it was removed. The mixing of the different soils encountered while drilled the holes was minimized as much as possible since the body of the sensors were not able to be inserted into the soil, only the prongs. The moisture readings of these sensors are influenced by the body of the sensor itself so the soil where the prongs were inserted had to be the same that surrounded the body of the sensors. The soil was placed in lifts to be able to compact as much as possible and much care was taken during compaction to not damage any sensor. Figure 4.17 below shows how the holes where the vertical arrays of moisture sensors were refilled and compacted.

Figure 4.17: Finalizing installation of Vertical Arrays of Moisture Sensors

Additional details on the sensors and data loggers work are provided in Chapter 2, including a description of how these sensors are able to perform the measurements of volumetric water content of the soil.

4.1.3 Soil Layering

Information on the soils present at each section was obtained during installation of both the horizontal and vertical arrays. During construction of the new shoulder, when the horizontal array of sensors and the geotextiles were installed, soil samples were obtained and the subgrade material was visually observed. Samples were collected where the moisture sensors were installed. The Atterberg Limits for these soil samples were obtained. The soils retrieved in all sections were found to be expansive with plasticity indexes (PIs) ranging from 24 to 58. Sections 1, 3, 5, 6, and 7 had PIs ranging from 24 to 38, while Section 4 had a PI of 52 and Section 8 showed the highest PI of 58. This may suggest that sections 4 and 8 have subgrade soils that are potentially more expansive than the other sections. From the visual inspection at the site during construction as well as the lab tests, it was concluded that the Cook Mountain formation is the prevalent soil in the test sections. This is a clayey soil formation with expansive properties. Chapter 3 provides details on the characterization of the soils at the test sections as well as the portion of SH-21, where the sections are located. Figure 4.18 shows the Cook Mountain formation subgrade, this photo was taken during the construction phase of the shoulders.

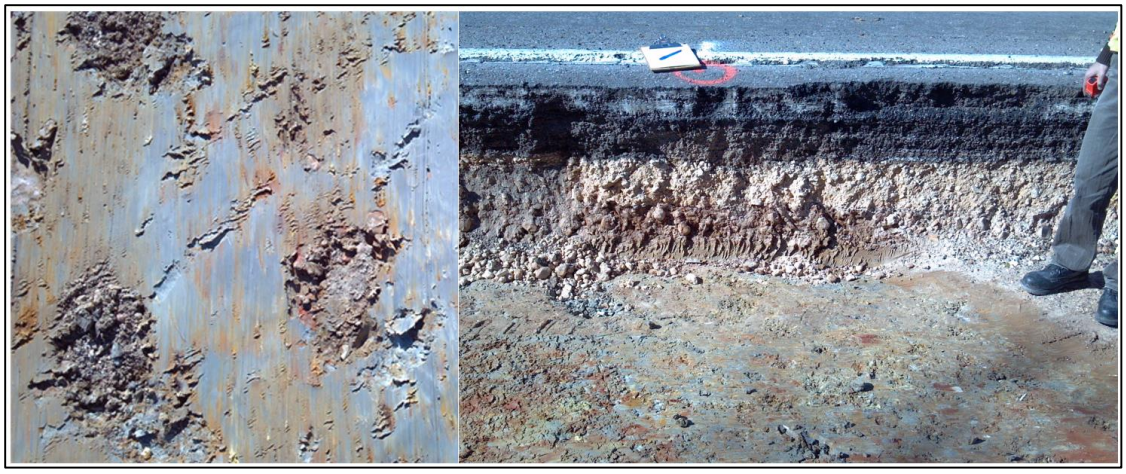

Figure 4.18: Cook Mountain subgrade soil in one of the Test Sections of SH-21

Soil stratigraphy information was obtained during installation of the vertical arrays of moisture sensors. During the drilling process, the thickness of each layer encountered was documented in order to establish the soils in which the moisture sensors are located. The data on what soils are present at the side of each section as well as their thicknesses was useful in the comparing performance of the various sections. Table 4.3 shows the layering documented during the installation. It should be noticed that Cook Mountain soils were not found in Sections 7 and 8. However, they were observed during the installation of the horizontal sensors, as shown in Figure 4.19. Possible explanations for this is that the

layer could have been thin and been excavated or that it was not observed at the shoulder due to natural variability.

Table 4.3: Soil Layering observed during installation of Vertical Arrays

	Depth to bottom of layer (in)						
Soil	Section 1	Section 3	Section 4	Section 5	Section 6	Section 7	Section 8
Fill	7	8	10	12	22	22	18
Cook Mountain/Reddish Brown Clay	36	21	22	20	40	N/O	N/O
Dark Brown/Greenish Clay	N/O	21+	22+	20+	40+	22+	18+
Sand	36+	N/O	N/O	N/O	N/O	N/O	N/O
N/O means Not Observed							

Figure 4.19: Cook Mountain formation in Section 8 during installation of Horizontal Array

Elevations were also measured at the each section were the sensors were placed. Survey measurements were conducted using a SOKKIA CX series total station (Figure 4.20). From the design plans it is known that there is 32" of material placed on top of the subgrade in the paved areas (Figure 3.10). Using the elevations measured with the total station and the information on the soil stratigraphy from both sensor installations, profiles

were prepared to better understand the characteristics of the test sections. Figure 4.21 shows the soil profile prepared for Section 8 where Cook Mountain was evident in the subgrade but not at the side of the road during the installation of the vertical array of sensors.

Figure 4.20: Total Station setup used to measure elevations on the shoulders of SH-21

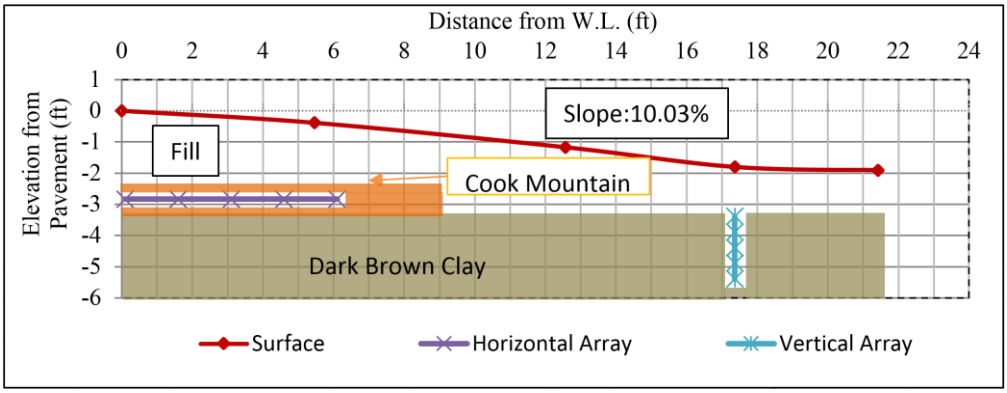

Figure 4.21: Soil Profile at Section 8

4.2 Weather Data

In order to assess the hydraulic performance of the various geotextiles, precipitation data was needed as this would be the main source of water infiltration into the pavement structure. The water table at this site is very deep, so it was not expected to be a source of moisture for the subgrade and base layers of SH-21. Weather records were collected from

the start of the project and data was obtained for over a year before the actual construction in order to understand what the weather trend was in this area.

Weather data was obtained from multiple sources because some of the sources often missed collecting data for some dates. At the beginning the data was obtained from a program called HydroDesktop, which is an open source GIS enabled program. It obtains data from multiple sources around the site of interest and interpolates to obtain values for the specific place for which data is asked for. Use of data generated using this program was subsequently replaced by use of data from the NOAA data base. The majority of the weather data for the site was obtained from three sources. The first one corresponds to the weather station in Squirel Run, just south of the test section. The data for this weather station was downloaded from the Wunderground website. The two other sources were weather stations of the NOAA network, NOAA Station 1.2 and 5.7. Figure 4.22 shows a Google earth map indicating the location of each weather station in relation to the test section locations. Table 4.4 includes the coordinates of each weather station as well as the links from which the data can be accessed.

Table 4.4: Principal Sources for Weather Data

Weather Station Name	Source Website	Coordinates of Station
Squirrel Run	Wunderground.com	30.168, -97.179
Bastrop 1.2 N TX US	Ncdc.noaa.gov	30.1709, -97.2373
Bastrop 5.7 SW TX US	Ncdc.noaa.gov	30.1306, -97.3025

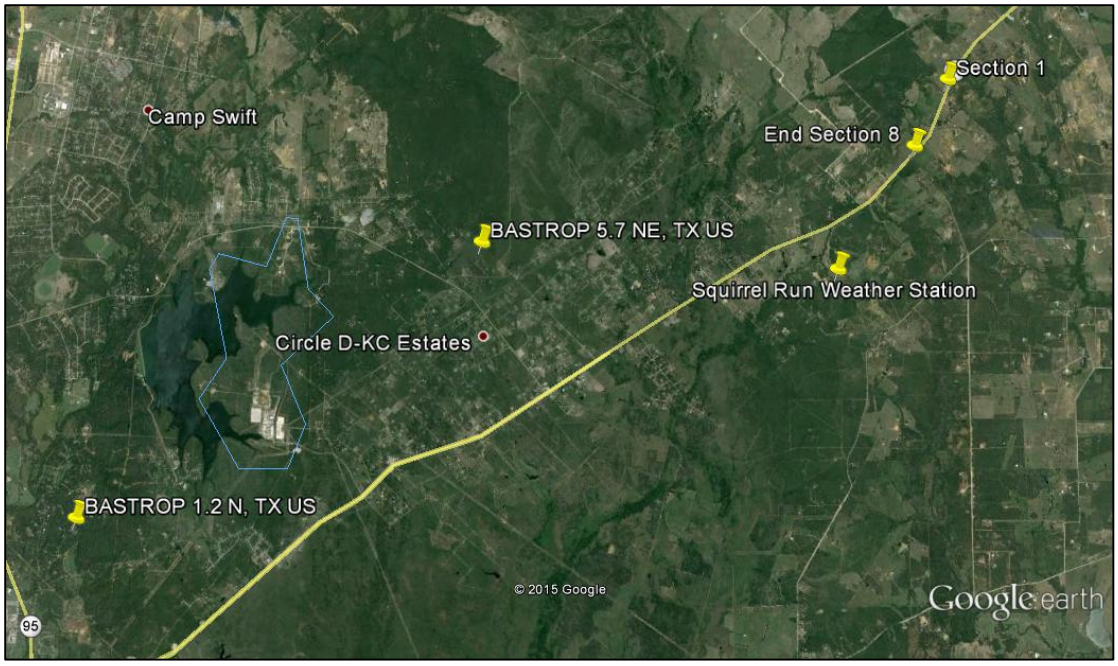

Figure 4.22: Location of Weather Stations and Test Sections

Data was downloaded from 2010 until March 27, 2015 in order to evaluate the weather trends in the area. Figure 4.23 shows that 2011 was the year of the record drought but that on average the area receives around 30” of rain and that since the SH-21 reconstruction it has been raining an average amount. Figure 4.24 shows the average precipitation for each month since 2010 until March 27, 2015. It can be observed that there is significant variability, but that a clear dry period between October and April occurs.

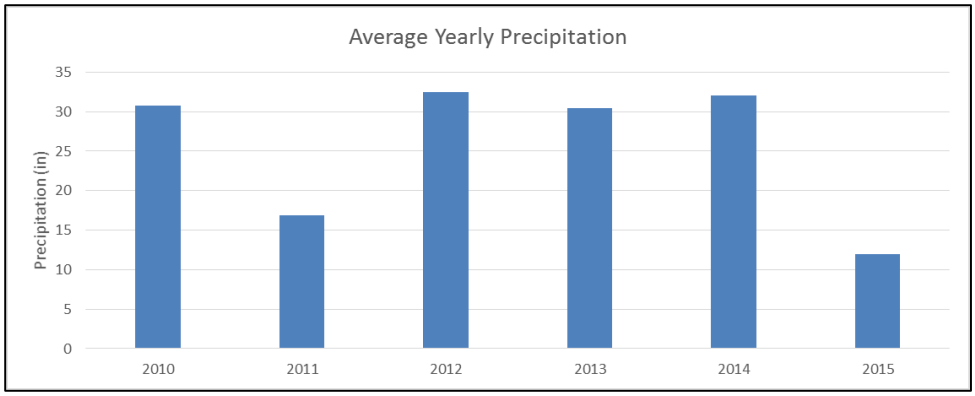

Figure 4.23: Average yearly rain from 2010 until March 27, 2015

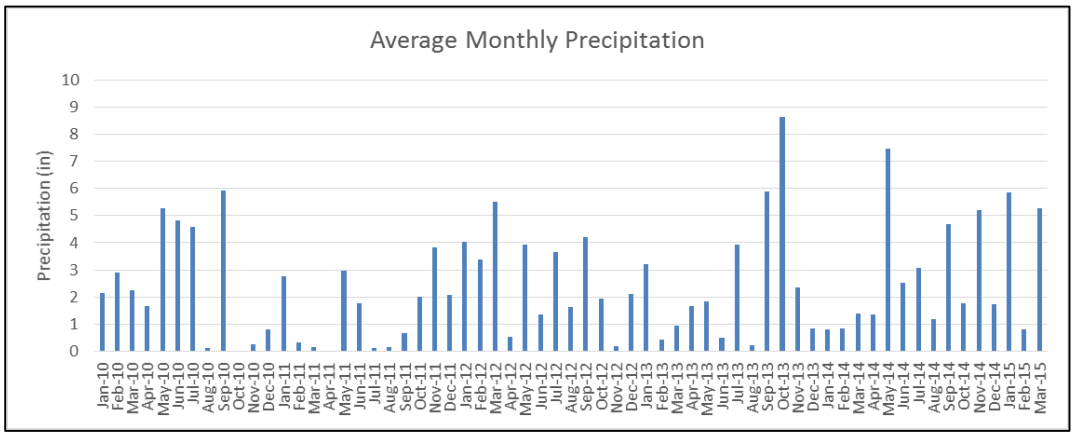

Figure 4.24: Average monthly precipitation since 2010 until March 27, 2015

4.3 GEOTEXTILES USED IN TEST SECTIONS

Before moving to the results of the moisture sensors, details on the four geotextiles used for this study are provided in order to understand what each one is designed for. The control geotextile, GT1 (Mirafi's 140NC geotextile), is the one that TxDOT had initially planned on using throughout the entire project. This is a needle punched nonwoven geotextile whose main purpose is for separation but is capable of lateral drainage with a permittivity of 2 sec^-1 and a flow rate of 140 gal/min/ft². **Error! Reference source not found.** shows the GT1 geotextile as was delivered to the site.

Figure 4.25: Photos of GT1 taken during rehabilitation of SH-21

The second geotextile used was GT3 (Mirafi's RS580i), which is made out of strong polypropylene filaments that provide high reinforcement strength as well as soil interaction. The specifications sheet provided by Tencate for the geotextile suggests it provides confinement, filtration, separation, and soil reinforcement but no lateral drainage. Among the 4 geotextiles used in this study, this geotextile is the one with the highest tensile modulus measured at 90,000 lbs/ft at a 2% strain. It has a lower permittivity than GT1 at 1 sec^-1 as well as a lower flowrate of 75 gal/min/ft². This geotextile different to GT1 is said to provide good soil interaction, its soil interaction coefficient is 0.9 as suggested by its specifications sheet. **Error! Reference source not found.** shows a close up of GT3 as well as a picture during the actual installation of the geotextile in one of the test sections.


Figure 4.26: Pictures of GT3 geotextile

The third geotextile used was GT2 (Mirafi's HP570), which as GT3, is made of high tenacity polypropylene yarns. This geotextile is capable of providing filtration, separation, and soil reinforcement but just like GT3 does not provide lateral drainage. The GT2 is the second strongest geotextile in the study, it has a tensile modulus of 1300 lbs/ft at a 2% strain. This geotextile has an even lower permittivity than GT3 at 0.4 sec^-1 and a flowrate of 30 gal/min/ft². **Error! Reference source not found.** below shows a close up of the geotextile as well as a photo taken during the actual installation of the geotextile in one of the test sections.

Figure 4.27: Pictures of GT2 geotextile

The fourth geotextile used was GT4 (Mirafi's H2Ri geotextile), which was the main focus for this study. This geotextile has special hydraulic properties due to the combination of its hydrophilic and hydrophobic fibers. This geotextile is capable of redistributing moisture by using its wicking fibers and transporting excess moisture through capillarity to areas of lower moisture content. This geotextile is capable of providing reinforcement with a tensile strength of 75 lbs/ft at 2% strain which is lower than GT3 and GT2 but higher than GT1. It can provide filtration as well as separation and confinement. GT4 is expected to provide enhanced lateral drainage, 0.24 sec^-1 and 15 gal/min/ft², but is capable of wicking moisture. It was tested using ASTM C1559 and was able to wick water 6" above

the water surface after 24 minutes as reported in the specifications sheet provided by Tencate. It was also tested with the same ASTM manual but wicking was measured horizontally and GT4 wicked water a total of 73.3 inches in the horizontal directions after 983 minutes. Testing is currently under way on these types of measurements at The University of Texas at Austin to better characterize the wicking properties of GT4 geotextile. **Error! Reference source not found.** shows images taken during the installation of the geotextile in one of the test sections.

Figure 4.28: Pictures of GT4 during installation

4.4 MOISTURE SENSOR DATA

The hydraulic performance of different geotextiles was evaluated in this study for the case of pavement sections founded on expansive clays. When these expansive clays are wetted they tend to expand and when they are dried out they contract. The resulting vertical movement is not expected to be uniform within the pavement section with most of the displacements occurring at or near the shoulder. These differential movements lead to stresses in the pavement, which ultimately result in longitudinal cracks and accelerated pavement deterioration.

Sensors were installed underneath the pavement of the new shoulder, built as part of the reconstruction of a segment of SH-21 in Bastrop, Texas. These sensors have been

used to collect moisture data since late January 2013 until present. Moisture readings along with weather data were used to assess the potential effect of the different geotextiles on the subgrade soil moisture contents.

The main focus was on comparing the performance of different sections with that of the sections with a geotextile with enhanced lateral drainage (Section 4 and 7). The GT4 geotextile was expected to drain water through enhanced lateral drainage due to its wicking fibers. Accordingly, water was expected to migrate from where there is an excess of it to where there is lack of it. In the case of roads on expansive clays this would suggest that GT4 is able to maintain or generate an approximately uniform moisture content underneath the textile thus imparting uniform vertical movements in expansive clays. From the case histories discussed in Chapter 2, GT4 was able to provide reinforcement, separation, and improved lateral drainage when it was daylighted. The performance of H2Ri was proven with the performance of the sections which contained the textile within its structure.

The geotextiles installed in SH-21 were installed and enclosed by soil, meaning that they did not daylight at the shoulder. Accordingly, the GT4 geotextile will not drain the soil underneath the pavement structure causing shrinkage, but is expected to equalize the moisture content and cause uniform movements. This uniform vertical displacements would prevent the formation of longitudinal cracks due to tensile stresses in the pavement.

4.4.1 Horizontal Moisture Sensor Data

Horizontal arrays of sensors were placed below the pavement sections, as shown in Figure 4.29, to monitor moisture changes over time. Data has been periodically downloaded from the data loggers from late January 2014 until March 27, 2015. The data is downloaded from the data loggers using a program provided by Decagon Devices called

ECH2O Utility. This program downloads the data and automatically converts it into a Microsoft Excel spreadsheet as shown below in Table 4.5.

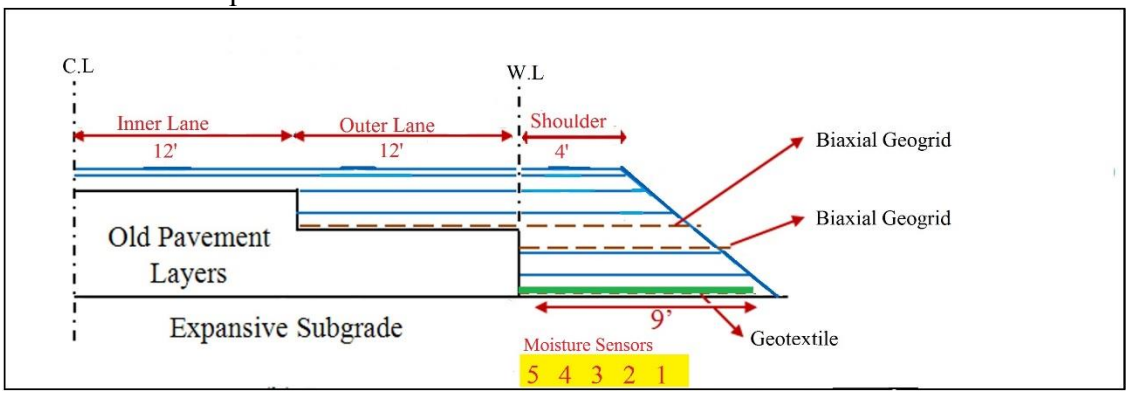

Figure 4.29: Sketch of Reconstructed SH-21 pavement structure with Sensor Installation

Table 4.5: Example of downloaded data using ECH2O Utility

EM23217	Port 1	Port 2	Port 3	Port 3	Port 3	Port 4	Port 5
2735 records	EC-5 Soil Moisture	EC-5 Soil Moisture	5TE Moisture/Temp/EC	5TE Moistur	5TE Moisture/Te	EC-5 Soil Moisture	EC-5 Soil Moisture
Measurement Time	m³/m³ VWC	m³/m³ VWC	m³/m³ VWC	°C Temp	mS/cm EC Bulk	m³/m³ VWC	m³/m³ VWC
1/25/2013 8:00 AM	0.000	0.000	0.000	16.6	1.42	0.000	0.000
1/25/2013 9:00 AM	0.014	0.001	0.000	16.4	1.54	0.004	-0.003
1/25/2013 10:00 AM	0.027	0.006	0.000	16.4	1.57	0.023	0.018
1/25/2013 11:00 AM	0.039	0.014	0.003	16.6	1.69	0.064	0.018
1/25/2013 12:00 PM	0.042	0.018	0.005	17.4	1.73	0.070	0.022
1/25/2013 1:00 PM	0.047	0.022	0.007	18.6	1.73	0.075	0.026
1/25/2013 2:00 PM	0.050	0.025	0.008	19.5	1.73	0.078	0.029
1/25/2013 3:00 PM	0.054	0.028	0.009	20.3	1.73	0.082	0.029
1/25/2013 4:00 PM	0.058	0.028	0.010	20.7	1.74	0.082	0.025

Data was downloaded every 2 to 3 months on average and was then combined with data downloaded previously. The data was plotted against time together with precipitation data. The data was also plotted as change in volumetric water content by subtracting the readings to the first reading ever taken. This was done for all 7 sections in order to evaluate how moisture changed below the pavement with time and weather patterns. Figure 4.30 below shows the raw data up to March 27, 2015, plotted along with precipitation data.

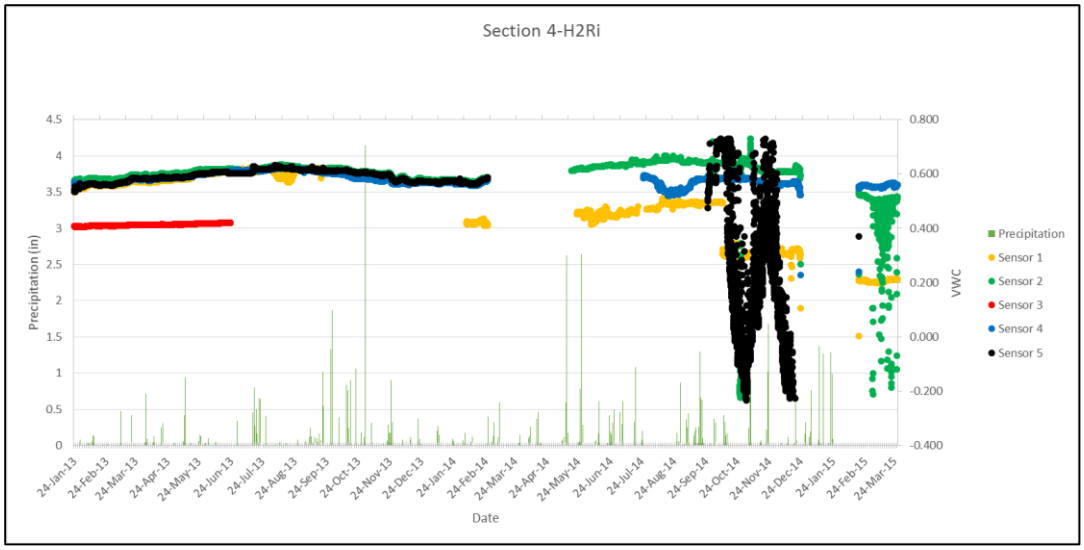

Figure 4.30: Raw Moisture Data from Section 4 together with Precipitation Data

As shown in Figure 4.34Figure 4.26, there are data points that are seemingly incorrect. This is due to possible sensors malfunctioning because of a number of multiple possible reasons. Some of these sensors may be not be adequate for the stresses in this project (induced by 32" of compacted material above them). It is possible that stresses may have led to cracking of the sensor body. This facilitates moisture to seep into them which would explain sensors still functioning but giving abnormal readings. In other occasions the sensors were reading correctly but had occasional abnormal readings. In both cases the data points corresponding to faulty reading were removed. This can be noticed in Figure 4.31, which was processed by deleting points that could be determined to be faulty readings.

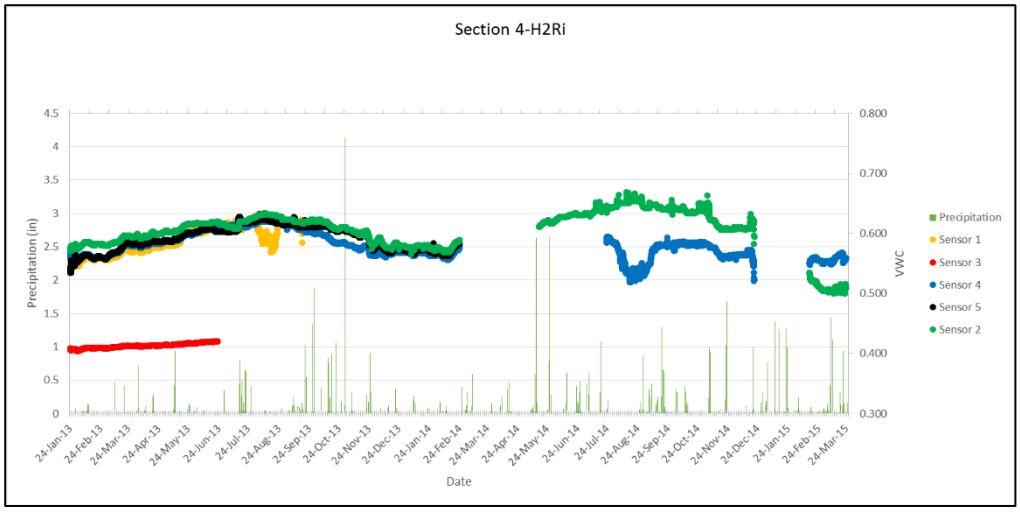

Figure 4.31: Processed Moisture Data from Section 4 together with Precipitation Data

The actual processing of the data involved identifying points that were significantly different from the trend values. Peaks that appeared in the data were mostly deleted if there wasn't a significant rain event to justify the increase in moisture. Sudden increases or decreases were often identified as erroneous. Cook Mountain clays have very low hydraulic conductivities, which would not allow significant increases or decreases in moisture content within a few hours.

From plots such as the one shown in Figure 4.31, a trend was noted in which readings peaked between June and September and then hit a low point around January and February. This trend was evaluated and found to correspond to changes in temperature. In order to verify this, air temperature was plotted against the readings from the sensors in order to confirm this. Figure 4.32 shows data from Sensor 2 in all 7 test sections and the air temperature data obtained from the weather records. The similarity in the trend of the air temperature and the moisture readings is obvious.

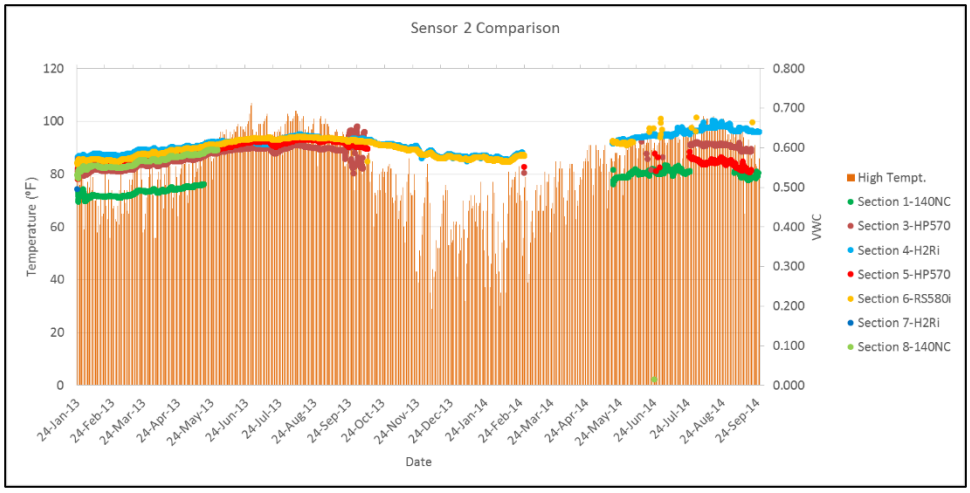

Figure 4.32: Data from all Sensor 2's compared with Air Temperature

In order to correct for temperature effect, research was conducted on the effects of temperature on volumetric water content readings. "The temperature sensitivity is not caused by the ECH2O sensors themselves which are almost perfectly insensitive to temperature changes, but rather the electrical characteristics of the soil, which can be quite sensitive to temperature changes" (Cobos, 2015). The literature suggests that the reason for the measurements being affected by temperature is the interaction of the water with the soil and temperature. Kocarek (2012) performed studies on how temperature affected ECH2)-TE sensors and determined that it should be considered a "linear relationship between the $\Delta\theta$ and Δt". Thus a linear equation could be used to correct the data. Kocarek (2012) suggested equation (4.1), where θref is the corrected volumetric water content while θm is the measured one. The constant coefficient of 0.002 was determined experimentally in a study conducted by Kocarek (2012). In this study, the coefficient was determined that would minimize the temperature induced oscillations shown in Figure 4.31. Data from Sensors 3, which measures temperature of the soil, was used, and t_{ref} was assumed 20ºC as suggested by Kocarek (2012).

$$\theta ref = \theta m - 0.002(tm - tref) \quad (4.1)$$

This coefficient was determined for both types of sensors, EC-5 and 5TE, since they had slightly different calibrations, which is the reason why their readings are slightly different. The form of Equation (4.1) was used in this study, but, instead of using 0.002, the values in Table 4.6 were used for correction. Figure 4.33 shows the data after correction for temperature effects, this plot can be compared with the processed data shown above in Figure 4.31.

Table 4.6: Coefficients used for temperature correction of Moisture Data

	c	tref (°C)
EC5	0.002615	20
5TE	0.00229	20

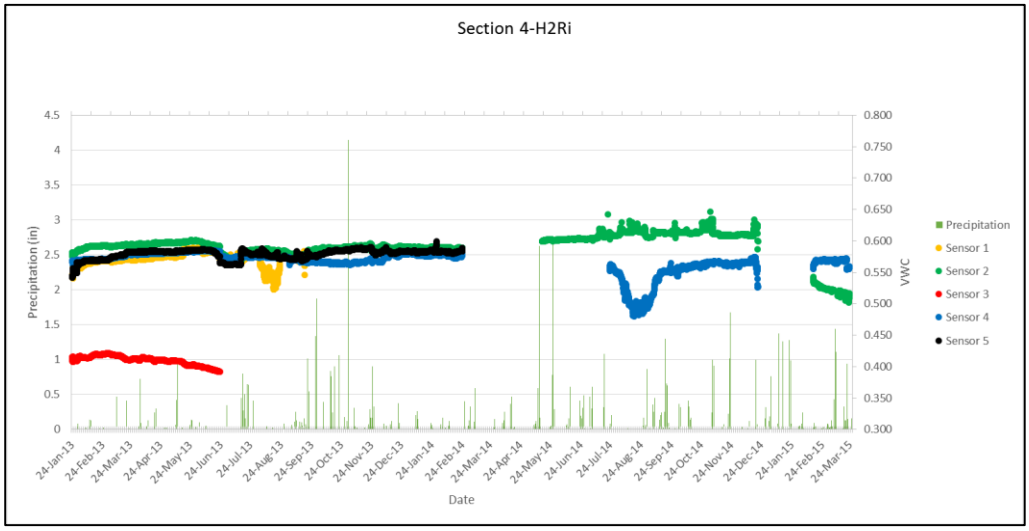

Figure 4.33: Temperature corrected Moisture Data for Section 4

The data from all 7 sections was processed to account for temperature corrections in order to then evaluate the hydraulic performance of the different geotextiles. Moisture profiles were prepared in order to see just how temperature changed over the geotextile and shoulder. Figure 4.34 illustrates the moisture profiles prepared for Section 8, which

turned out to be the best way to evaluate the performance of the geotextiles since over time the changes in moisture content were small and not very noticeable on a large scale as that shown in Figure 4.33.

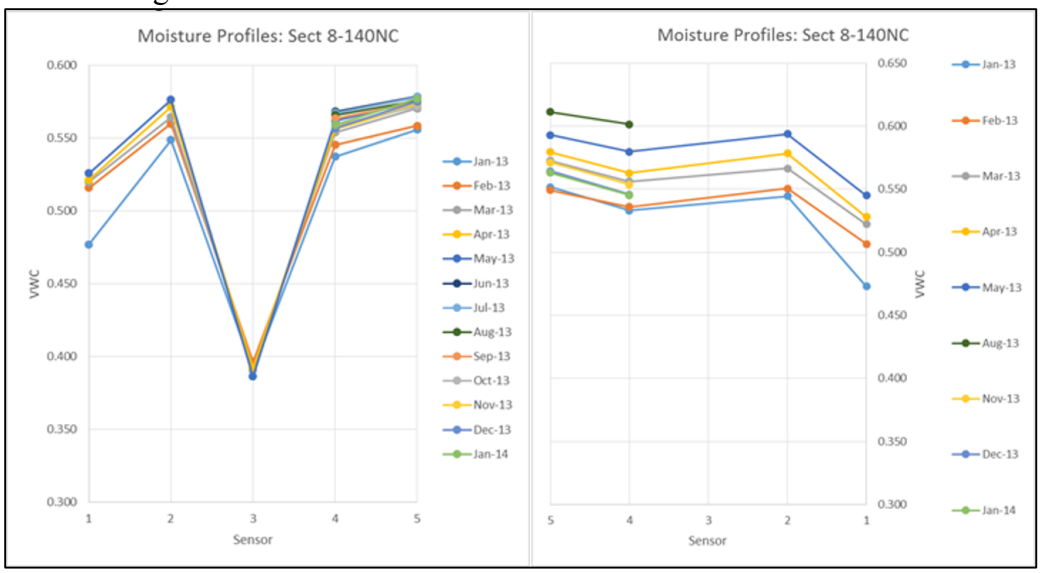

Figure 4.34: Moisture profiles for Section 8

4.4.2 Vertical Moisture Sensor Data

In addition to the horizontal array of moisture sensors installed from the beginning of the study, an additional array of vertical sensors were installed in the natural soils located on the shoulder of the road. The objective of this additional set of sensors was to assess the water infiltrated into the subgrade during rain events. These sensors were installed at the end of 2014, so only initial data can be reported at this point. The data so far was plotted in two ways to help analyze the data.

The first way used to present the data is the same as that used for the moisture in the horizontal array. This has been useful to see the big picture, jumps in moisture content can be observed in these sensors during rain events, unlike the sensors underneath the pavement. By plotting the data this way the response time of the sensors with respect to the rain event can be assessed. In order to better assess how the moisture in these soils

changes with time, the data has been plotted for specific weeks as shown in Figure 4.35 which allows to see how moisture changes in the soils as you go down and with time.

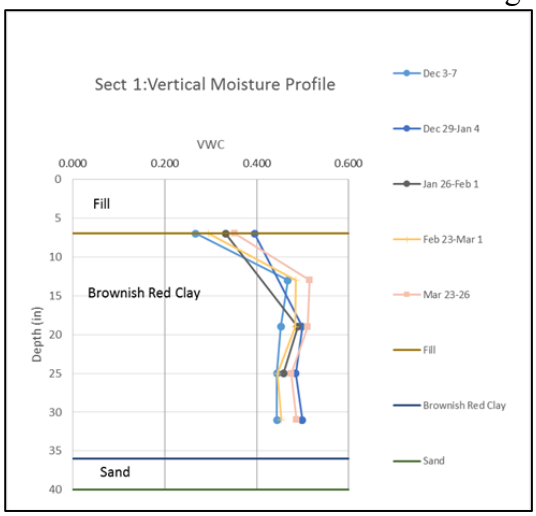

Figure 4.35: Data from vertical array of sensors from Section 1

4.5 Results from Moisture Sensors

After analyzing the data from both arrays, the sections were evaluated to assess the relative performance of the sections with different geotextiles. The first section evaluated was Section 1 which has a GT1 geotextile, which has no significant in-place drainage capacity. This geotextile is considered the control geotextile since it is the one installed in all SH-21. This geotextile is mainly for separation.

The following sections provide a discussion of the moisture data collected in the 8 pavement test sections with GT1, GT2, GT3, and GT4 geotextiles.

4.5.1 Section 1-GT1

For Section 1, relevant data was lost between late May 2013 and late May 2014 due to the flooding of the data loggers. The data for this section is showed in Figure 4.36. Since the data loggers started recording data, a significant difference in moisture content between

the extremes of the shoulder was observed. This change is of about 5% and was maintained over time as shown below in Figure 4.37.

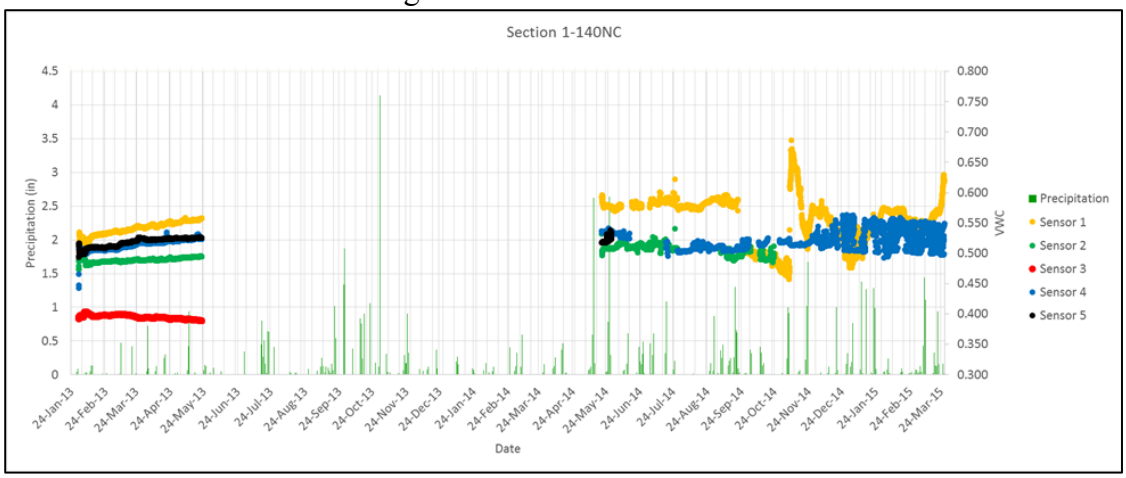

Figure 4.36: Data from Horizontal Array of Sensors beneath Section 1

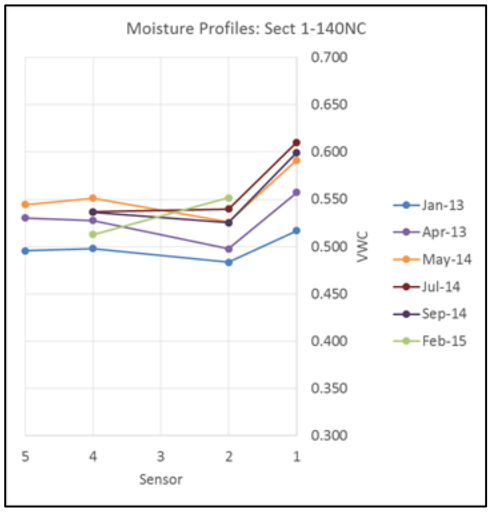

Figure 4.37: Moisture Profiles from Section 1

From the moisture profiles shown in Figure 4.41, it can be observed that there was around a 5% difference in moisture content between Sensor 5 and 1, which was maintained over time with the profiles shifting up and down over time. This vertical shifting of the profiles is most probably due to seasonal variations in moisture content.

The data from the vertical array of sensors was also evaluated, in spite of its recent installation compared to the horizontal array. Profiles of the shoulder were prepared in order to better understand the drainage condition of the section. Figure 4.39 shows the profile from Section 1. It shows that the vertical array was unintentionally installed in a low point on the shoulder, which could make the readings from this sensors not very reliable. Figure 4.39 shows the data from the vertical array of sensors and as expected the largest changes in moisture content occur for Sensor 1, which is closest to the fill/subgrade interface. The other sensors do not experience significant changes and show dryer moisture contents than those read by the sensors beneath the pavement.

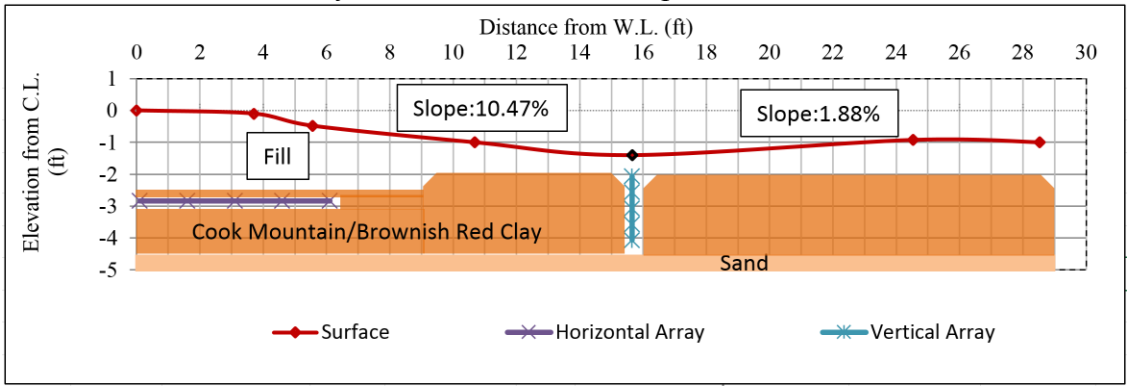

Figure 4.38: Profile of Section 1

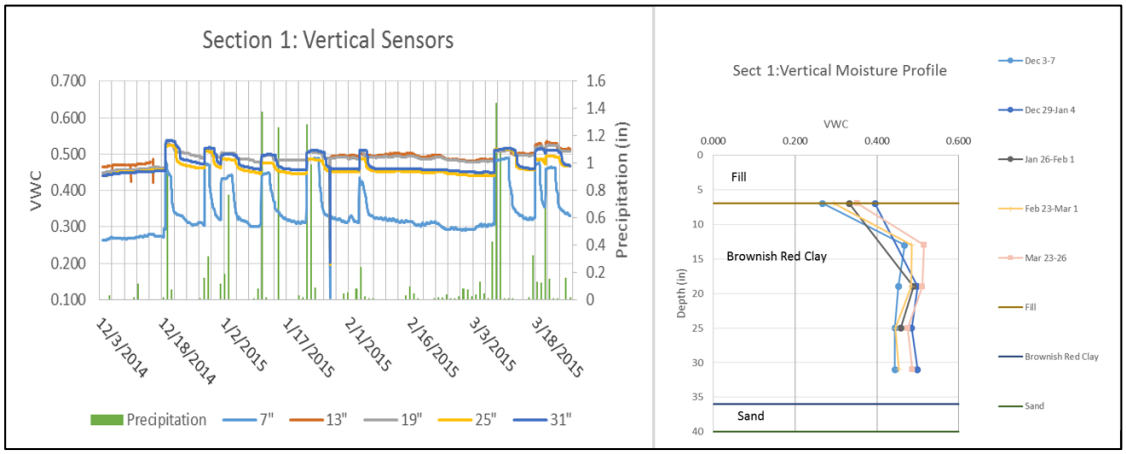

Figure 4.39: Data from Vertical Sensors in Section 1

One of the objectives of the vertical sensors was to compare the readings from the top sensor to the Sensor 1 from the horizontal array. This was not possible for this section since the sensors are installed at different elevations/depths. Sensors 2 and 3 from the vertical array seem to compare better with Sensor 1 from the horizontal array but they show different moisture contents and there is still too little data from the vertical arrays to be confident in the data it is producing. Preferential flow may have affected the readings from the vertical array which would amplify the changes in moisture contents during rain events.

4.5.2 Section 3-GT2

Section 3 has the same sensor arrangement as all other sections. This section was constructed using GT2 as geotextile under the newly constructed shoulder (see Figure 4.2). This geotextile is marketed as having filtration, separation, and soil reinforcement properties. Data from the sensors below the pavement for this section was complicated, the data is not very clean as shown in Figure 4.40. The better data was obtained from January 2013 until around October 2013. The gap in data between October 2013 and May 2014, as in Section 1, was due to flooding of data loggers. Unfortunately, data obtained after the new data loggers were installed looks worse than before due to possible sensor malfunctions.

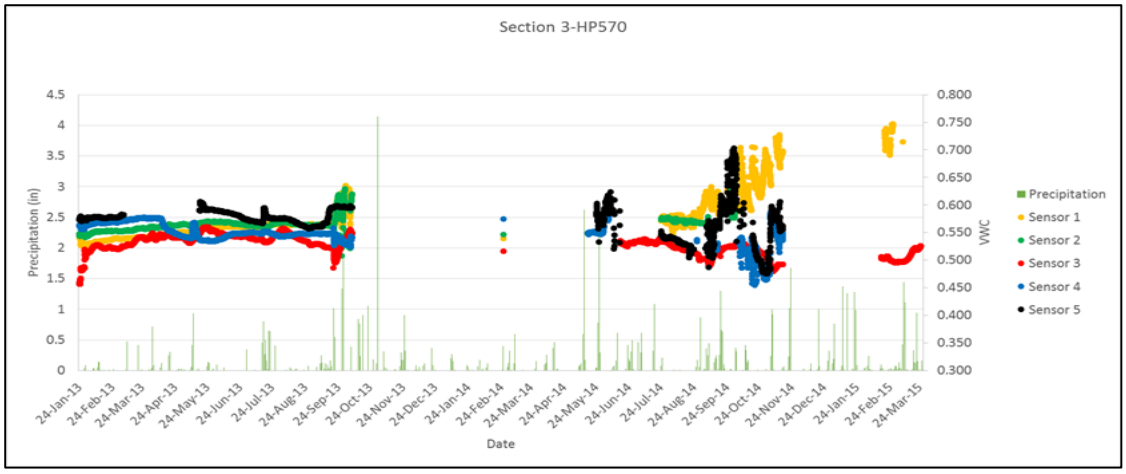

Figure 4.40: Data from Horizontal Array of Sensors beneath Section 3

In order to better understand the moisture response, moisture profiles like the ones for Section 1 were done. Figure 4.41 shows the moisture profiles from the periods of best data. The data shows an average change in moisture content between Sensors 5 and 1 of around 5% and this is increased for the data from October 2014. The moisture readings below the geotextile shows large differences in moisture content occurring throughout the shoulder and especially at Sensor 1 which is located at the edge of the shoulder as shown in Figure 4.29. These large moisture changes at the shoulder edge could lead to the formation of longitudinal cracks in the pavement.

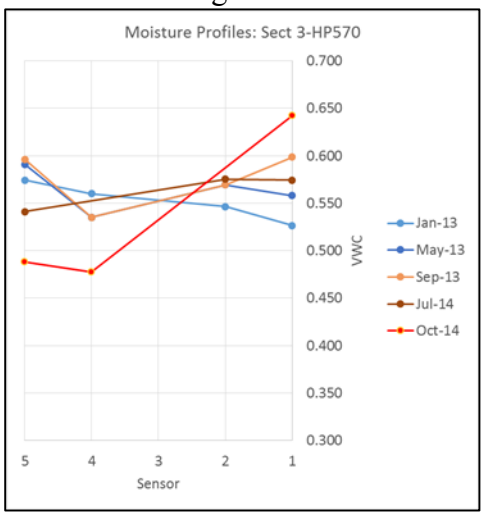

Figure 4.41: Moisture profiles from Section 3

The data from the vertical array installed at this section was assessed along with the profile of the section shown in Figure 4.42. From the profile it can be observed that there is a significant slope on the shoulder, suggesting that much of the water that falls on the shoulder would drain to the side. This is consistent with the data of the vertical array which shows only slight changes in moisture content suggesting that this array is not as sensitive to rain events. Unfortunately, the data from the vertical array collected so far was not as helpful, but could become relevant with continued readings.

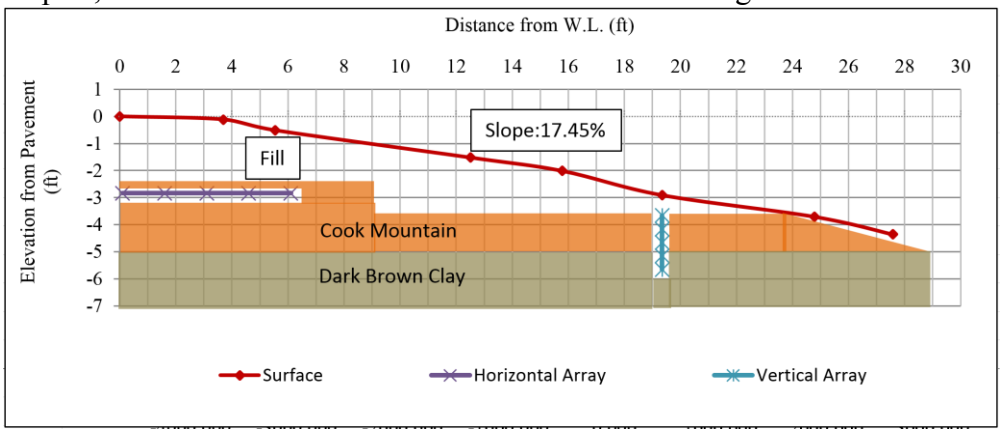

Figure 4.42: Profile for Section 3

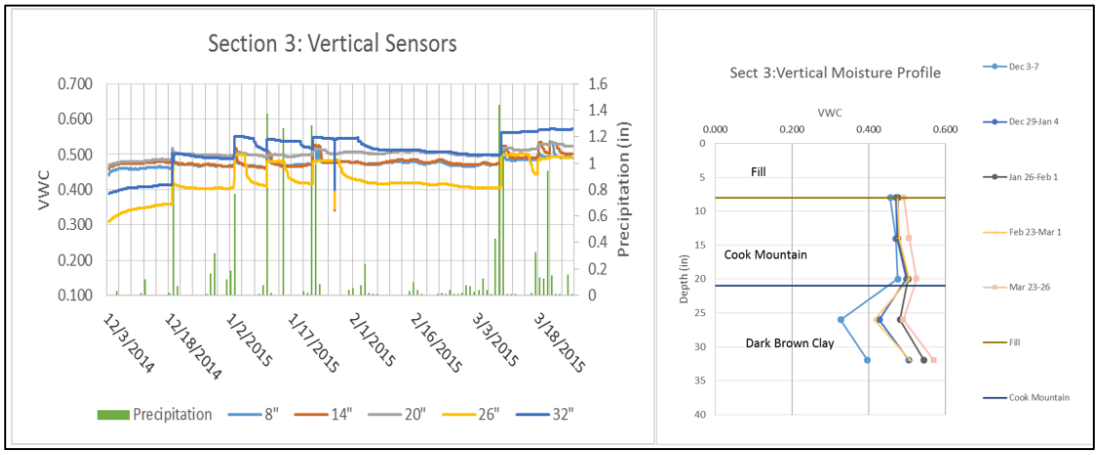

Figure 4.43: Data from Vertical Sensors in Section 3

4.5.3 Section 4-GT4

Section 4 is one of the two sections with the GT4 geotextile, which has the enhanced lateral drainage capability due to its wicking fibers. The data from the sensors below the pavement in this section is showed in Figure 4.44. Data collected for this section uninterrupted until around late February 2014 when the data loggers were flooded and when the new ones were installed Sensor 4 was showing lower than before data. From Figure 4.44 it can be observed that the data from sensors 1, 2, 4, and 5 were very similar suggesting a uniform moisture content under the pavement for a significant period of time. Sensor 3 shows lower moisture readings but this has been attributed to a slightly different calibration since Sensor 3 is a 5TE sensor and sensors 1, 2, 4, and 5 are all EC-5 sensors.

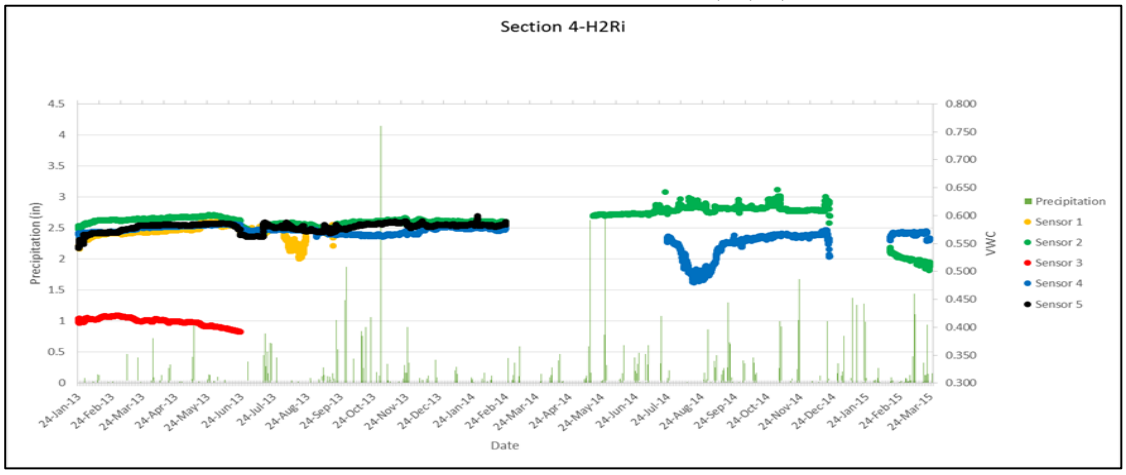

Figure 4.44: Data from Horizontal Array of Sensors beneath Section 4

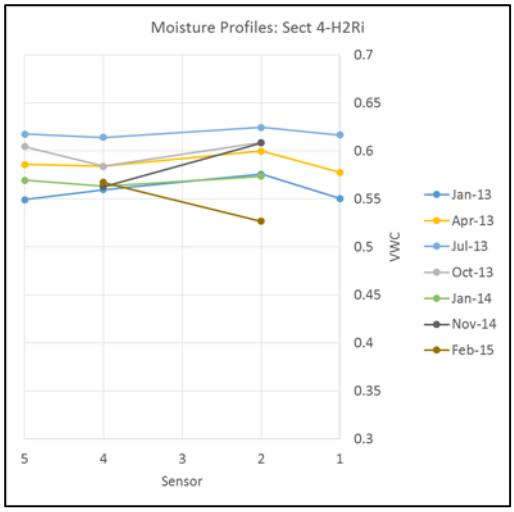

Figure 4.45: Moisture profiles from Section 4

In order to better analyze the data from Section 4, moisture profiles were also evaluated for this section, as shown in Figure 4.45. These profiles all show approximately uniform moisture contents for various periods of time. The moisture profiles seem to shift vertically all together with seasonal variations in moisture content, always maintaining a reasonably constant moisture content. This may suggest that GT4 is capable of maintaining a uniform moisture content below it when it starts that way.

Profiles for the section as well as the vertical data from the vertical sensor array at this section were evaluated. Figure 4.47 shows the profile for Section 4, which suggest a slope of 13.16 percent, adequate for good drainage just like Section 3. In this case, the vertical array shows significant changes in moisture content throughout the entire array suggesting possibly some influence from preferential flow. The drainage condition in Section 4 is similar to that of Section 3 due to them both having similar shoulder slopes as shown in Figure 4.42 and Figure 4.46. Yet in Section 4 with the GT4, moisture is kept almost constant underneath the geotextile only changing with seasonal variations.

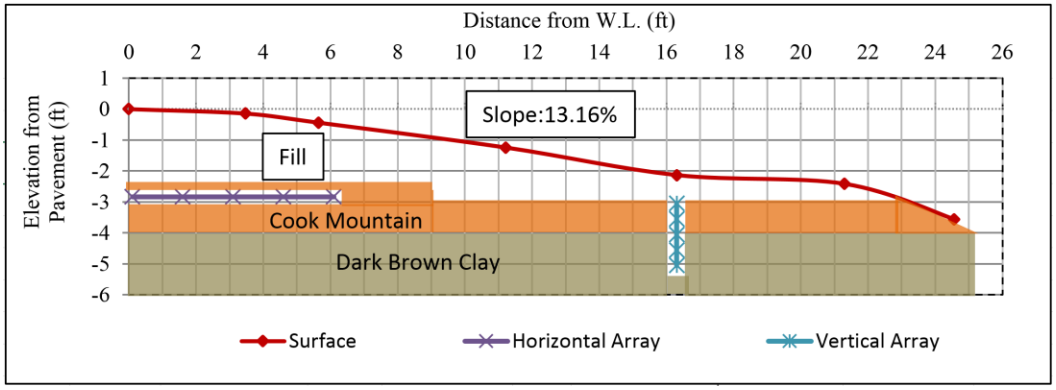

Figure 4.46: Profile for Section 4

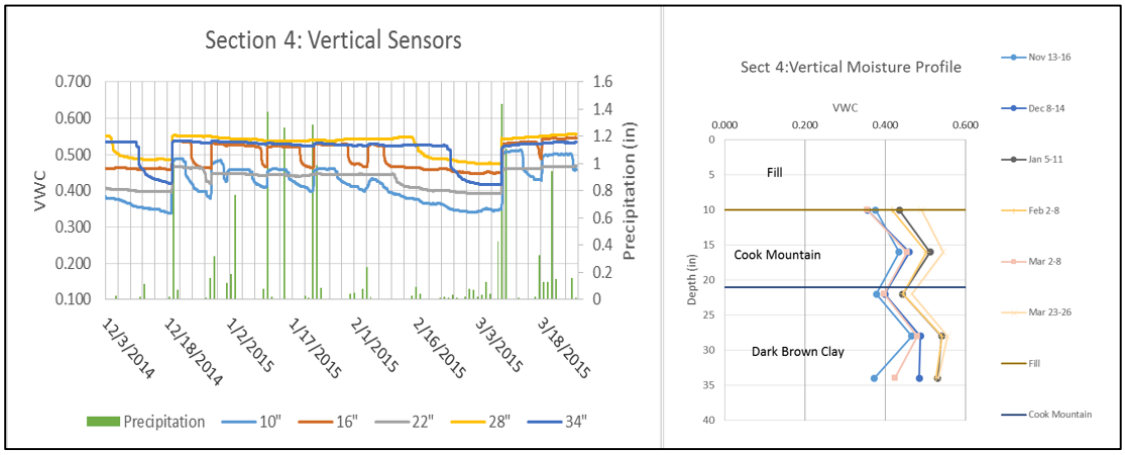

Figure 4.47: Data from Vertical Sensors in Section 4

4.5.4 Section 5-GT2

Section 5, as Section 3, involved installation of the GT3 geotextile. This geotextile provides filtration, separation, and soil reinforcement, but not enhanced lateral drainage. This section, as Section 3 has good data until around October 2013 as can be seen below in Figure 4.48 after which there is a gap in the data and then continues again on May 2014. After May 2014 the sensors that appear to be working are 1, 2, and 4 with 1 and 2 having some sporadic jumps and drops but maintaining readings within the average. On December 2014 Sensor 1 stopped working and only Sensor 2 ended up providing moisture content readings. Even this sensor showed some unexplainable increases in moisture content towards the end of the data set.

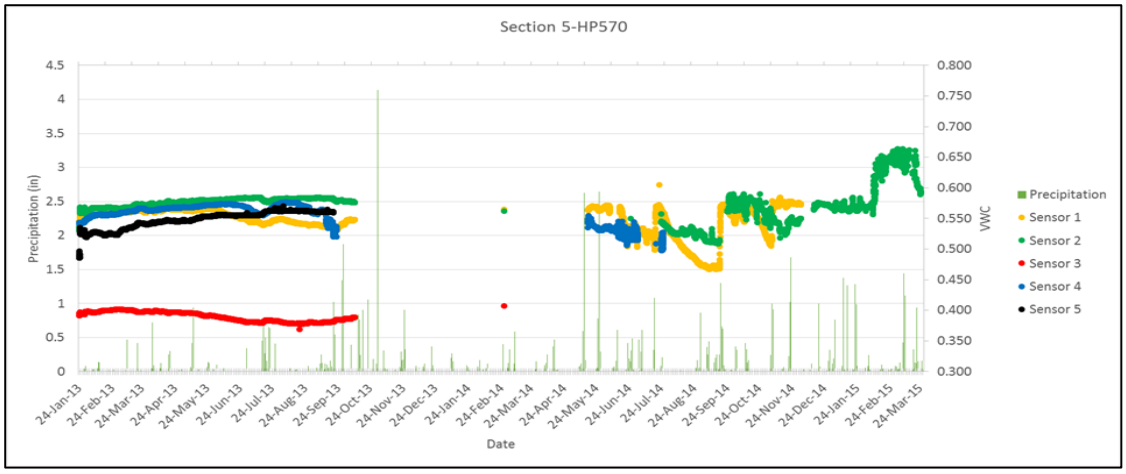

Figure 4.48: Data from Horizontal Array beneath Section 5

In order to better understand this data, moisture profiles were compiled. Figure 4.49 shows that the moisture content on January 2013 started off around 0.52 where Sensor 5 is located and increased towards Sensor 1 to 0.55. The shape of this profile was maintained until for around 8 months after which Sensor 2 and 5 stopped working and not enough data was available to prepare the moisture profiles. From the profiles that were compiled, it is evident that the moisture profile's shape seems to be maintained and the difference in moisture contents between the extremes of the shoulder is never decreased. This can lead to longitudinal cracks.

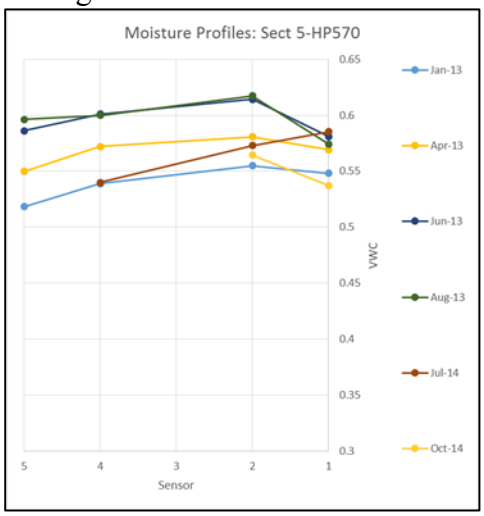

Figure 4.49: Moisture profiles from Section 5

In an attempt to try to better evaluate this data the vertical sensors were included in the analysis together with the section profile which both are included below, Figure 4.50 and Figure 4.51. The profile shows a drainage condition similar to that of sections 3 and 4 with similar shoulder slopes. Even though the drainage condition in this section is similar to that of section 3 and 4, the sensors from the vertical array in this installation show significant changes in moisture content at the top 2 sensors which decreases with depth as is to be expected. The sensors seem to show the soils moistening over time and then maintaining moisture contents ranging from 0.4 to 0.5. Unfortunately comparisons of this data to that from the horizontal array cannot be done with only Sensor 2 working below the pavement and showing some strange readings.

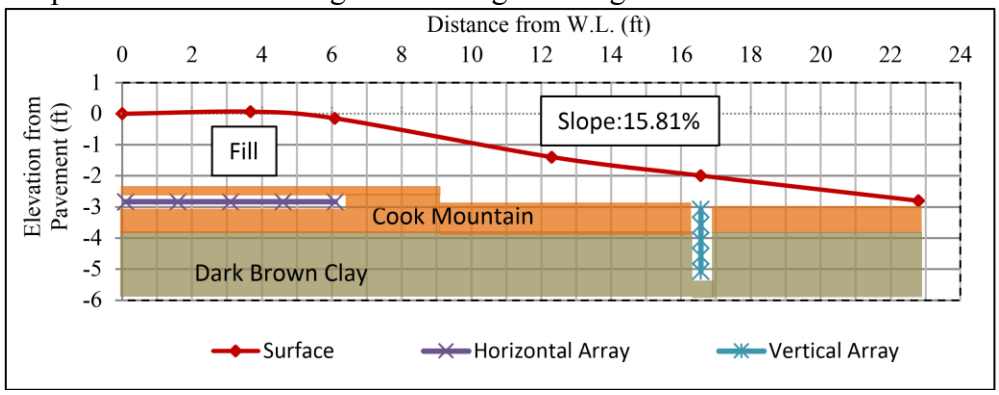

Figure 4.50: Profile for Section 5

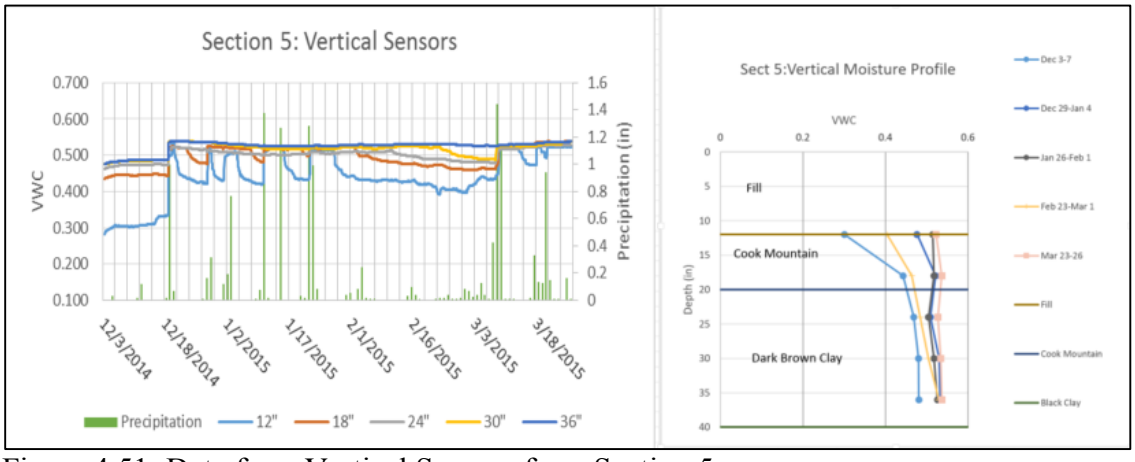

Figure 4.51: Data from Vertical Sensors from Section 5

4.5.5 Section 6-GT3

This section includes GT3 geotextile, which was developed to provide soil confinement, filtration, separation, and soil reinforcement but not lateral drainage. Data from this section like the other is rather good until December 2013 after which there is a gap until May 2014 when the new data loggers were installed. The data for the sensors placed below the pavement in this section is shown in Figure 4.52. Similar to Section 5, the shoulder seems to have been constructed with varying moisture contents throughout its width as shown in the data in Figure 4.52 for January 24, 2013. From the early data, it can be seen that Sensors 1 and 4 show similar readings while Sensor 2 shows higher values and Sensor 5 lower values. It appears as time progresses towards around September 2013, the moisture contents difference becomes smaller. Unfortunately, Sensor 5 is the only sensor working after late September 2014 and like other sensors, data looks less consistent after late 2014. This makes it impossible to see how moisture has varied below the geotextile after late September 2014.

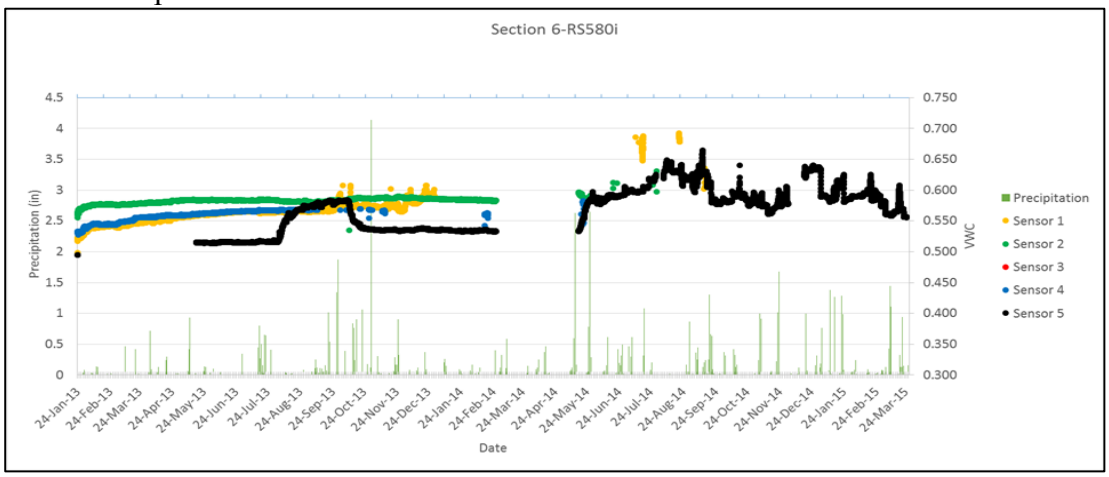

Figure 4.52: Data from Horizontal Array beneath Section 6

The horizontal moisture profiles shown in Figure 4.53 shows a trend similar to that shown in Figure 4.52 with regards to moisture contents below the geotextile becoming similar. What Figure 4.52 does not show is the changes in moisture concentrating around

Sensor 1 which, as previously mentioned, could lead to vertical movements around the shoulder which tend to cause longitudinal cracks. Data from February 2014 reinforces this fact that RS580i is not helping with the possible drainage or at least equilibration of moisture below the pavement.

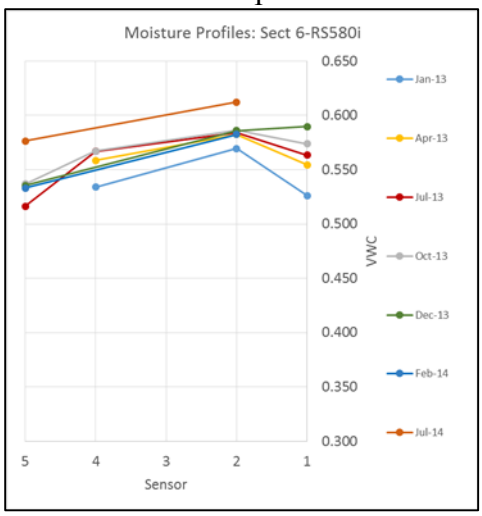

Figure 4.53: Moisture profiles from Section 6

The vertical data together with the section profile were evaluated. This section, unlike Section 1 through 5 and 7 and 8, contains 5 additional moisture sensors in the vertical array in order to capture moisture changes in the fill. The reason for this was that this section had a significant layer of fill which was found adequate for this installation.

The profile for this section shows similar drainage conditions as those observed in sections 3, 4, and 5 though the slope of the shoulder is steeper as shown in Figure 4.54, suggesting better drainage which would lead to less rain water infiltration. This is not as clear from the data shown in Figure 4.55, with some changes occurring in the fill layer and the most significant moisture changes occurring in the actual Cook Mountain formation. Data from the vertical array again, was not able to be compared to the data from the horizontal array due to lack of enough sensors in the horizontal array. In this case the only

sensor still working under the pavement after late September 2014 is Sensor 5 which is the one furthest toward the center of the road as shown in Figure 4.2.

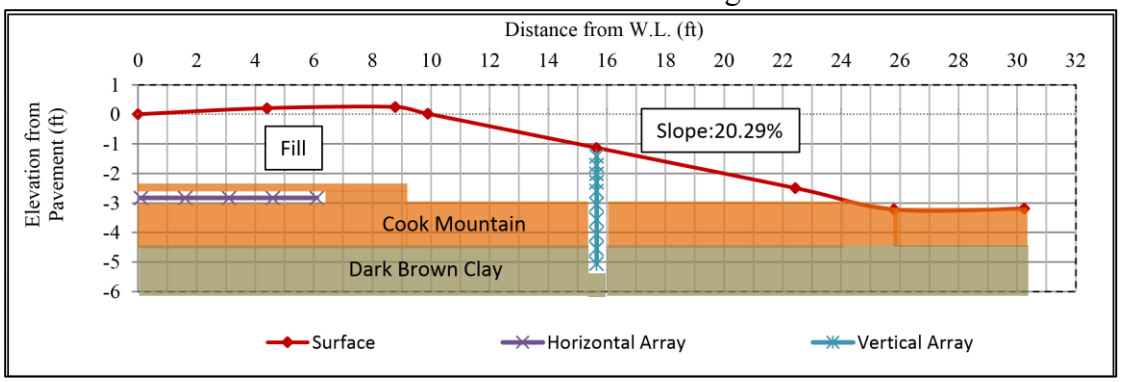

Figure 4.54: Profile for Section 6

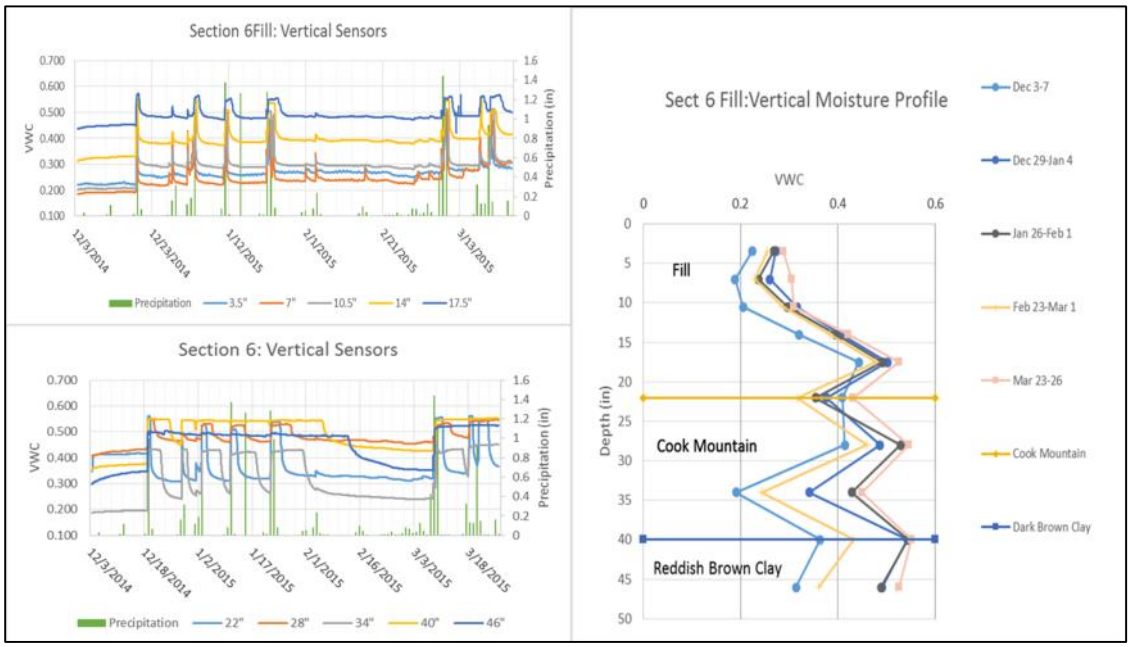

Figure 4.55: Data from Vertical Sensors from Section 6

4.5.6 Section 7-GT4

Section 7 is a section with the GT4 geotextile in addition to Section 4, which is able to better distribute moisture throughout its coverage thanks to its wicking fibers. The data from the sensors underneath the pavement for this section like other is not ideal. Moisture date from the sensors was consistent from January 2013 until about July 2013, after which

the data started wandering from the trends based on the initial data. From the data for the period where the sensors were working very well, it can be observed that from the beginning there was a substantial difference in moisture content in the shoulder. The data suggest that moisture contents were around 5 to 10% lower than those registered by Sensors 1 and 2, as shown in Figure 4.56. It is noticeable with time that moisture readings from the sensors seems to become similar as time passes. This is more noticeable in Figure 4.57, which shows moisture profiles for beneath Section 7 using Sensors 1, 2, 4, and 5 which are all EC-5 sensors.

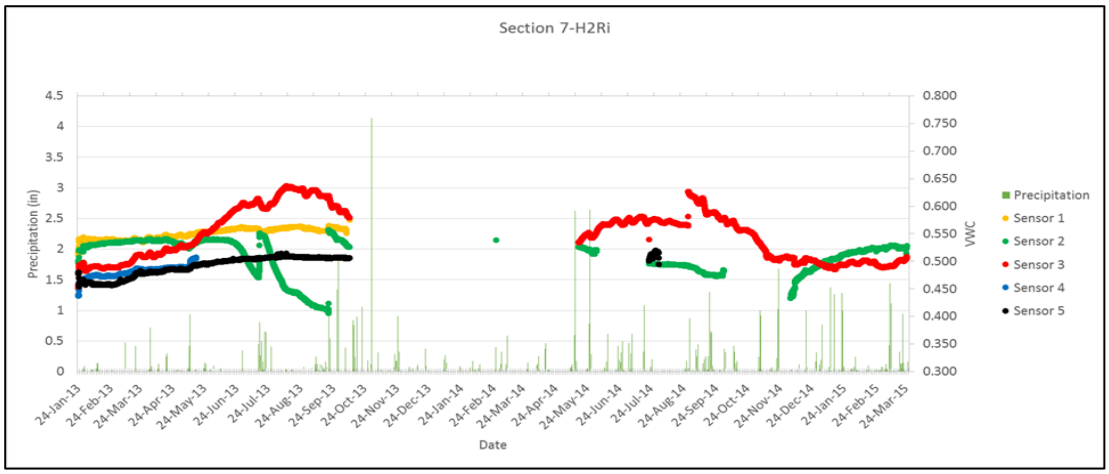

Figure 4.56: Data from Horizontal Array beneath Section 7

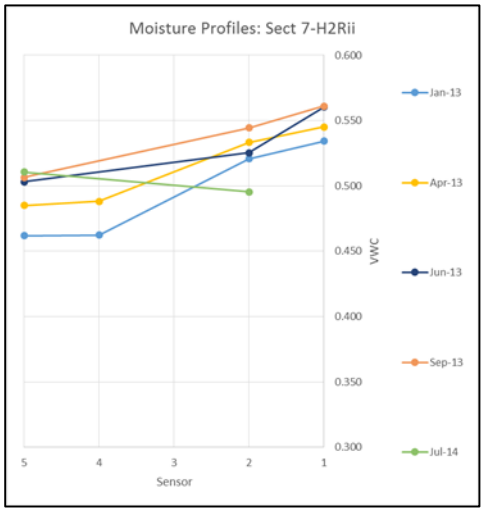

Figure 4.57: Moisture profiles from Section 7

Figure 4.57 shows the moisture profile for January 2013 as the light blue line. At this date, the difference in moisture content between Sensor 5 and 1 was approximately 7%. Later in April 2013, this difference went down to around 6% and seems to be progressively decreasing. The profile for July 2014 unfortunately lacked data from Sensor 1, which could have possibly reinforced this idea. By what the data shows it seems that this section with the GT4 geotextile is performing as expected, by equalizing the moisture content beneath the geotextile. Section 7, like Sections 1, 3, and 5, showed differences in moisture contents between Sensor 5 and 1 under the geotextile. Section 7, unlike Sections 1, 3, and 5, seems to be reducing this difference overtime due possibly to the enhanced lateral drainage provided by GT4. If more sensors were working beneath the geotextile, the data would possibly show the moisture equilibration over time better.

Data from the vertical array as well as the section profile were looked at to see if something else could be observed to provide data on the performance of GT4. The profile shown in Figure 4.58 shows similar drainage conditions to Sections 3 and 5 due to similar slopes on the shoulder. This confirms that the difference in the moisture profiles cannot be attributed to different drainage conditions. The data from the vertical array shown in Figure 4.59 was evaluated as well. In this case, all the sensors were installed in the natural soil which did not appear to be the Cook Mountain formation based on observations done during the opening of holes for the installation of the vertical sensor array in Section 7. The soils were much darker and lacked the reddish and greyish colors typical of Cook Mountain clays. The data from these sensors was attempted to be compared to data from the horizontal array but they were installed at different elevations/depths and in different soils. The one things that was noticeable is that moisture content readings for both arrays are similar, though the vertical sensors are showing higher moisture readings after the period of December 2014.

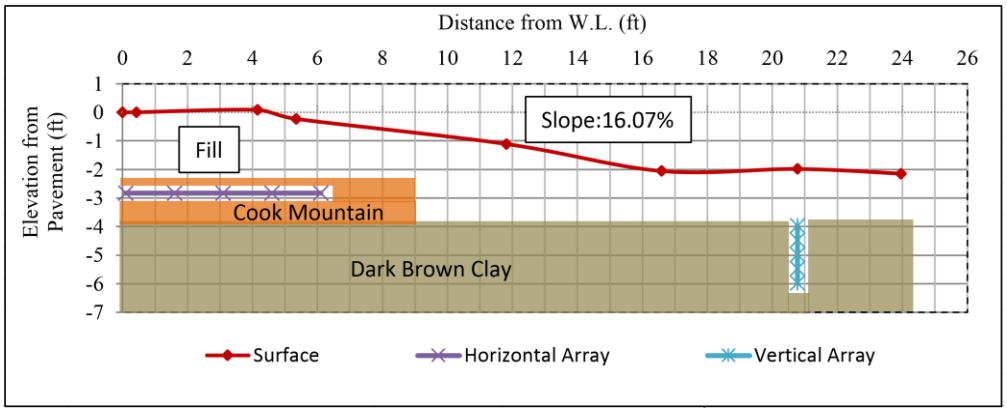

Figure 4.58: Profile for Section 7

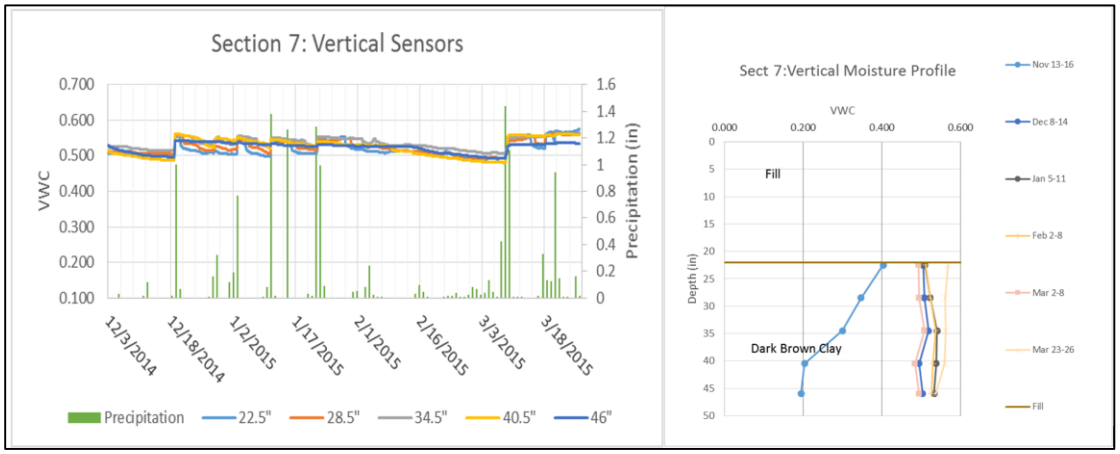

Figure 4.59: Data from Vertical Sensors from Section 7

4.5.7 Section 8-GT1

This last section is an additional control section with GT1, which as stated is expected to provide separation as well as lateral drainage. This section has been particularly hard to analyze since moisture sensors have performed very poorly. Data quality was excellent up to around June 2013, as shown in Figure 4.60. The sensors that lasted the most were 4 and 5, which is good but not adequate for the construction of moisture profiles which have showed to be very helpful in evaluating the hydraulic performance of the other sections.

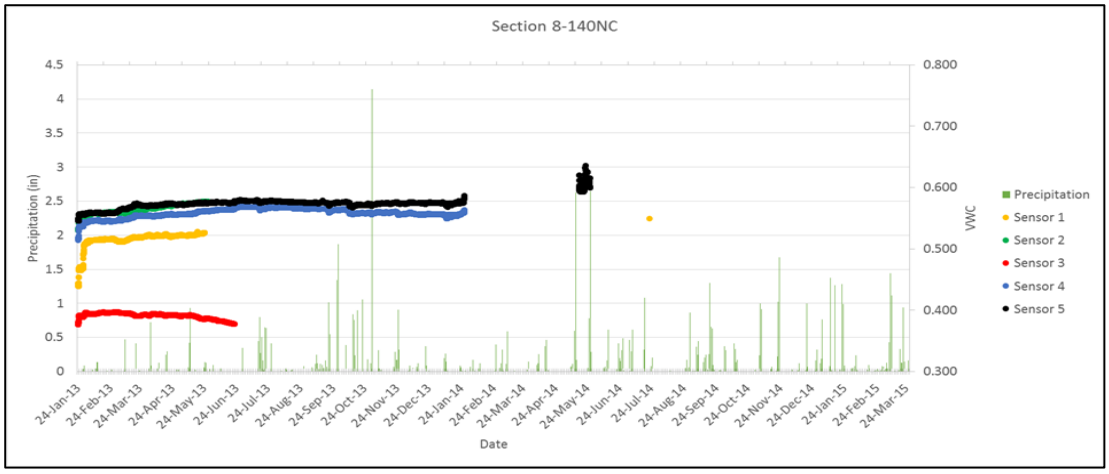

Figure 4.60: Data from Horizontal Array beneath Section 8

The moisture profiles for this section are showed in Figure 4.61, and include data from January 2013 until January 2014 which was the more consistent data acquired from this section. It can be observed that the section, like others, started off with differences of around 7% or more between Sensor 5 and 1 underneath the geotextile. Unlike the data from Section 7, in this case, this difference is maintained over time, with the profiles just shifting up and down with seasonal changes in moisture in the soil as shown in Figure 4.61. It can be observed, that in some of the cases, the differences in moisture between time periods was amplified in the area closer to Sensor 1. This could suggest larger changes in volume can take place close to the outer edge of the paved shoulder, leading to the formation of possible longitudinal cracks in the shoulder pavement. This performance is similar to that observed in Section 1, which also has the GT1 geotextile.

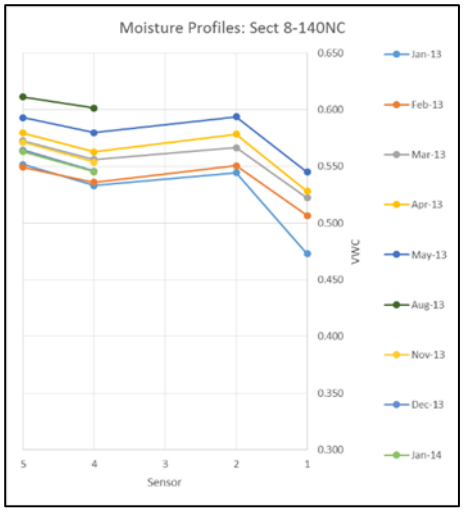

Figure 4.61: Moisture profiles from Section 8

The profile of Section 8 is shown in Figure 4.62, which shows a different shoulder slope compared to Section 1 as well as the presence of slightly different soils beneath the pavement structure. The moisture data beneath the geotextile still shows similar trends for both, Sections 1 and 8, with the only similarity being the geotextile.

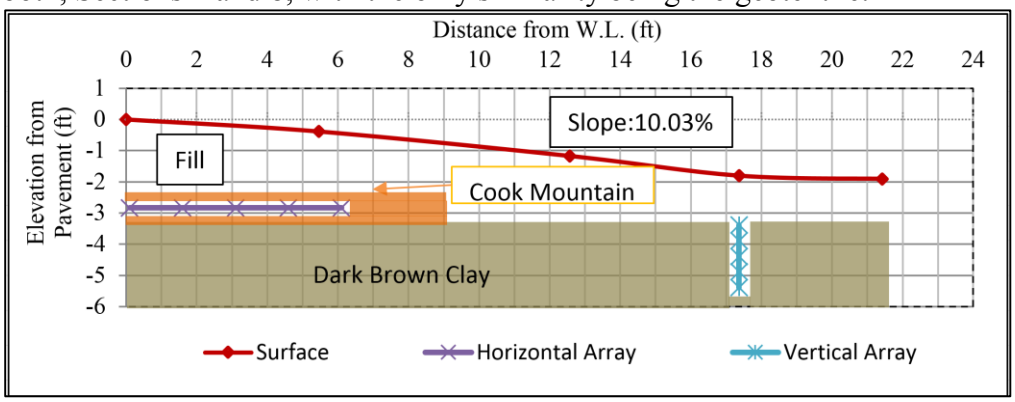

Figure 4.62: Profile for Section 8

Data from the vertical array of sensors was evaluated in order to see if anything else could be learned from them. The data included in Figure 4.63 was analyzed, while looking at the data from the horizontal array, in order to see if there were any similarities in the data. Unfortunately, Sensor 1 from beneath the geotextile in Section 8 stopped working early on during the study. From the little data that was recorded from it, the readings from

Sensor 1is similar to those being measured by the top sensor in the vertical array, even do it appears to be installed in a different soil. Other than this nothing else was noted.

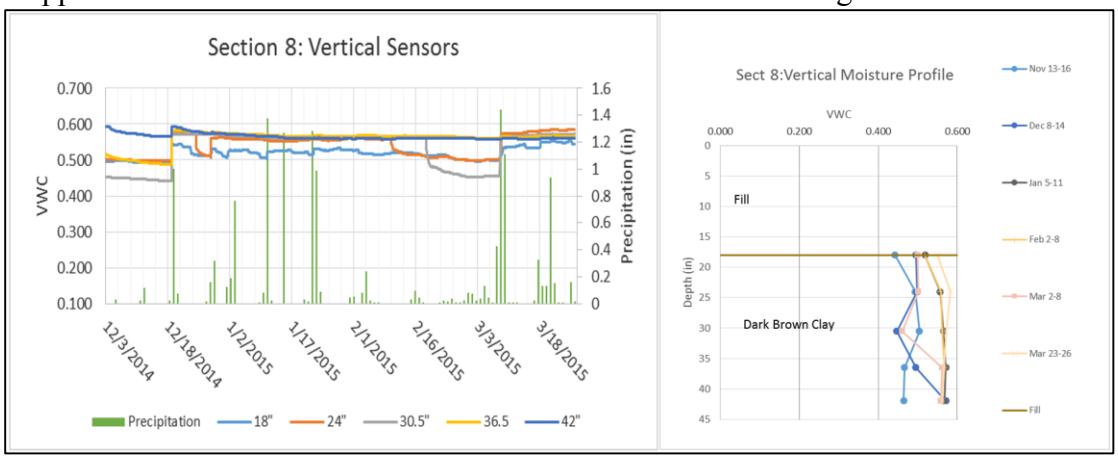

Figure 4.63: Data from Vertical Sensors from Section 8

4.5.8 Comparison of sections with and without enhanced lateral drainage

The two GT4 sections, 4 and 7, show promising results regarding the ability to move moisture from where there is an excess of it to where there is lack of it. This property has been used in several case histories to drain pavement layers by daylighting the geotextile. In this case it was installed beneath the pavement and surrounded by soil so it does not have outlet. The idea of GT4 draining the top of an expansive subgrade is not favorable, it could lead to shrinkage by drying out the soils, resulting in more possible stresses on the pavement built above. The GT4 geotextile if daylighted, could transport water into the section through capillarity as well, leading to expansion of the soils and thus again resulting in more stresses on the pavement built above GT4.

Data for Section 4 shows how GT4 has maintained a uniform moisture content in the subgrade below it as shown in Figure 4.45. Sections 1, 5, and 8, show moisture profiles that were maintained over time like Section 4, but these sections show differences of at least 5% between Sensor 5 and 1 while in Section 4 the moisture profiles are kept almost horizontal over time.

Section 7, unlike Section 4, started off with a significant difference in moisture content between Sensor 1 and 5 similar to Sections 1, 5, and 8. The one difference between Section 7 and the other 3 is the presence of the GT4 geotextile. GT4 appears to have equalized the moisture content below the geotextile and shoulder as shown in Figure 4.57. This is unlike what is observed from the moisture profiles from sections 1, 5, and 8 shown in Figure 4.37, Figure 4.49, and Figure 4.61.

Chapter 5 : Visual Condition Survey Procedures and Results

The presence of expansive clays below the pavement structure in SH-21 has left it susceptible to extensive cracking, particularly longitudinal cracks. In order to evaluate the effectiveness of the various geotextiles being used in this study, visual condition surveys were performed periodically. These surveys were conducted using an established protocol previously used in other field projects. The procedures are mainly based on the TxDOT Pavement Management Information System, Rater's Manual (Texas Department of Transportation, 2010). Using these surveys the various sections of this study can be rated based on their condition.

5.1 Focus of visual condition surveys

The Rater's Manual identifies various flexible pavement distresses like rutting, alligator cracking, and longitudinal cracks among a few others. For this study the main focus was longitudinal cracks. In turn, these cracks were grouped into longitudinal cracks in the wheel path as well as in the edge of the pavement, and shoulder cracks. The edge of the pavement for this study was defined as the white line on the outer edge of the outer lane, this is where the geotextile starts and extends outward 9 feet, as shown in Figure 4.29. The purpose of this was that the typical cracks associated with distresses caused by expansive clays are longitudinal cracks parallel to the centerline. These cracks tend to form as the outer edges of the asphalt are displaced vertically due to the expansion and contraction of the subgrade. These vertical movements generate longitudinal cracks which tend to start closer to the edge of the asphalt and move inwards as the cracking progresses and water seeps into the cracks.

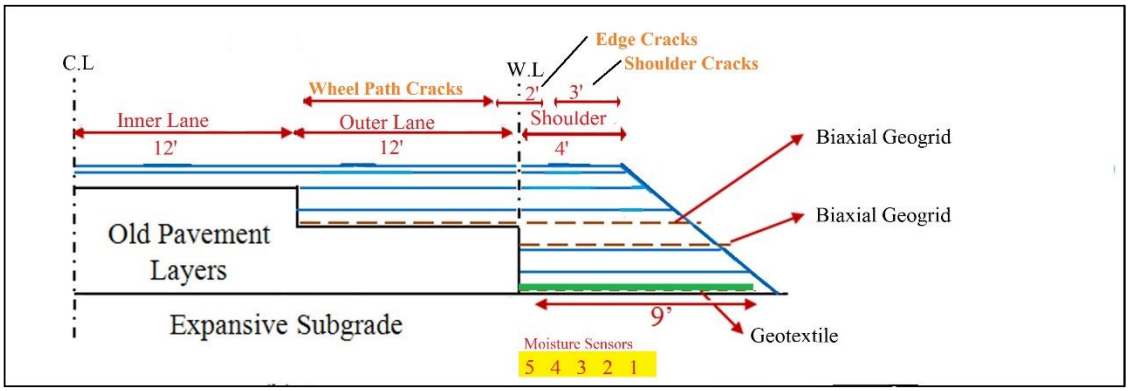

Figure 5.1: Pavement structure in SH-21 pavement test sections

During the condition surveys 3 main types of cracks were documented, the location and names of these cracks are shown in Figure 5.1. Figure 5.2, Figure 5.3, and Figure 5.4 below show examples of these cracks. Edge cracks in this study, include cracks on the white line or 1 feet from it as shown in Figure 5.1. Wheel path cracks for this study were cracks located within the outer traffic lane. Finally, shoulder cracks for this study included cracks that formed further away than 1 foot from the white line towards the shoulder as shown in Figure 5.1. Shoulder cracks for this study did not include the cracks at the very edge of the asphalt since these can be due to construction defects like poor compaction at the edge but were still documented. Rutting was measured as well at the beginning of the study but was then decided it was too dangerous due to traffic conditions.

Figure 5.2: Example of Wheel Path Cracks in Section 8

Figure 5.3: Example of Edge Crack in Section 7

Figure 5.4: Example of Shoulder Crack in Section 6

5.2 EQUIPMENT AND PROCEDURES

The visual condition surveys were conducted based on procedures already established from previous field projects. They were based on the Rater's Manual from TxDOT Pavement Information System. In order to perform these surveys the equipment described below was required in order to document the distresses as well as for safety precautions.

A distance measuring wheel was utilized in order to document where within the 8 test sections shown in Figure 5.5 were the distresses located as well as to measure the length of each crack. As part of the procedure, cracks measuring less than 3 mm wide were documented but not considered when rating the sections. In order to measure these cracks, a metal 6 inch ruler with millimeters was used. A camera was used in order to document with pictures the different cracks, distresses, or particularity that was thought adequate to document. The majority of the images taken for this study were obtained using a Canon T1i DSLR camera capable of taking 15.1 megapixel images. This quality of images was

useful in order to evaluate cracks. Figure 5.6 shows the equipment used to document the distresses in the pavement surface.

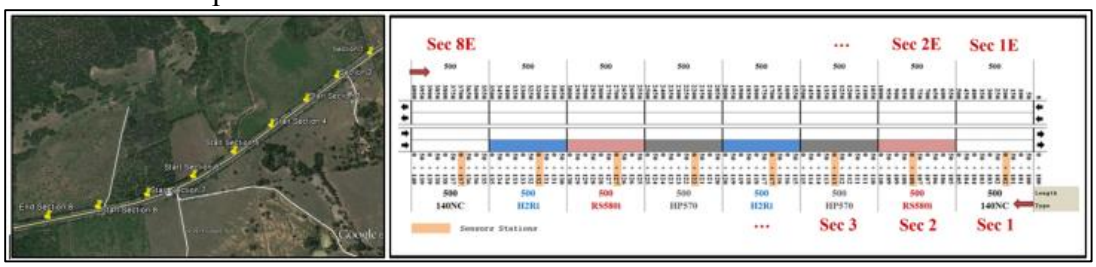

Figure 5.5: Location of Test Sections

Figure 5.6: Equipment used for Visual Condition Surveys

A survey form was developed for this study, where all the information from the condition surveys was to be documented in order to keep proper records. Figure 5.7 shows a sheet of one of the condition survey forms. There is space to document from what distance reading the distress starts and where it ends as well as the pictures taken and details on the distress type. This survey sheet was the one used for all 10 surveys performed for this study yet in the discussion the cracks will be separated in slightly different categories. For future surveys a survey form based on the distresses analyzed in the following sections of the text is recommended.

Condition Survey 2 *Date: Dec 16 2013*

SECTION 1: 140NC (STA 100+00 to 105+00) (0 to 500ft)

LOCATION		Pic	Cracking (note: W = Width)									Patching / Patched shoulder	Surface Defects		Pothole	Rutting		Comments
Dist. Readg (ft.)			Longitudinal			Edge/ Shoulder	Transverse		Alligator		Block		Flush	Ravel	Dim.	Depth (mm)		
From	To	#	W (mm)	@ YL	@ Wheel Path	E/S W (mm)	W (mm)	# cracks	% Area	Seve rity	% Area		Width	Width	(in.)	W.L.	Y.L.	

YSE = Yellow Straight Edge, Height = 59 mm; if Rutting < 65 mm → NO Rutting. If > 110 mm →Failure
BSE = Blue Straight Edge, H = 73 mm; if Rutting < 79 mm → NO Rutting. If > 124 mm → Failure

Edge Cracking = within 2 feet from Edge Stripe
Shoulder crack = > 2 feet from Edge Stripe

Figure 5.7: Example of Condition Survey Forms

5.3 WEATHER DATA

As part of the surveys, weather data was utilized in order to correlate formation and/or changes in distresses with weather events. Weather data recorded for the analysis of the data from the moisture sensors was utilized for this analysis as well. This data, as described in Chapter 4, was obtained from more than one source in order to compensate for missing data from some of the sources. Data on precipitation was recorded since 2010 all the way to March 26, 2015. Figure 5.8 below shows the yearly precipitation and Figure 5.9 shows the monthly precipitation, both since 2010.

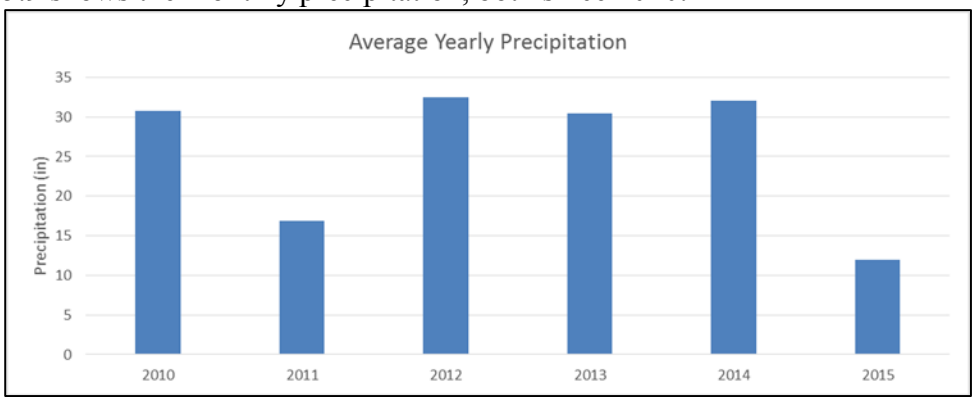

Figure 5.8: Yearly precipitation since 2010 until May 26, 2015

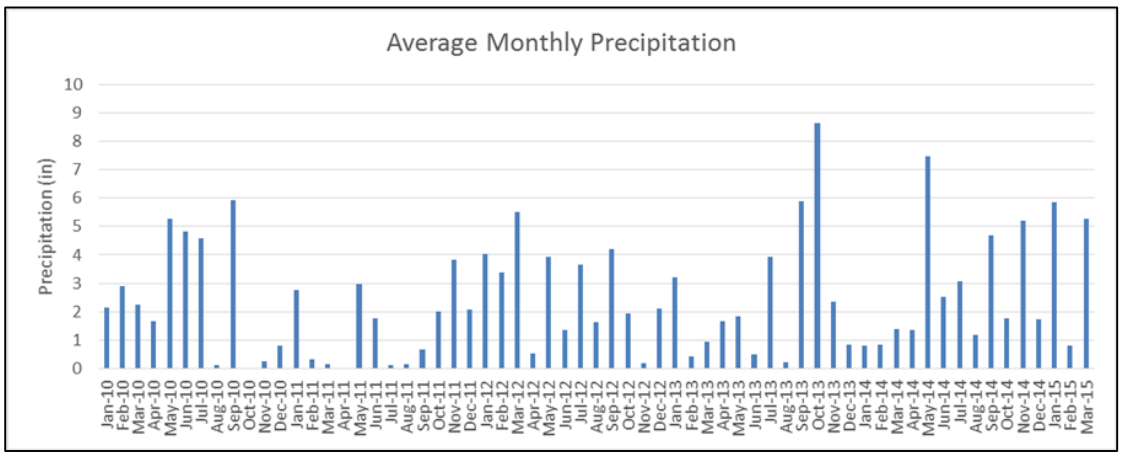

Figure 5.9: Monthly precipitation

The year 2011 was a record drought in Texas, which was responsible for significant distress in many roads founded on expansive clays, including SH-21. In 2011 the total

amount of precipitation at the end of the year totaled around 17 inches, while the average precipitation for the area of Bastrop, Texas, is around 30". The reconstruction of SH-21 was completed during 2013.

5.4 GEOTEXTILES USED IN TEST SECTIONS

The geotextiles used in the pavement test sections are named in this study GT1, GT2, GT3, and GT4. Chapter 4 discusses in detail the capabilities and properties of each geotextile. GT1 is the control geotextile in this study which provides separation and is installed in Sections 1 and 8. GT2 is installed in Sections 3 and 5, this geotextile provides reinforcement like GT3 which is installed in Sections 2 and 6. GT3 though, is a stronger geotextile compared to GT2, thus providing more reinforcement. GT4 is the main focus of this study and is installed in Sections 4 and 7. GT4 is capable of enhanced lateral drainage as well as reinforcement, filtration, separation, and confinement. Table 3.3 summarizes the geotextiles used in this study as well as their commercial names and the capabilities they provide.

5.5 RESULTS

In order to obtain adequate records of how the sections are performing in terms of distresses, a total of 10 visual conditions surveys have been done since the road was reconstructed until March 26, 2015.

Table 5.1 summarizes the dates of all the surveys done as part of this study. The objective of this evaluation was to go and document all distresses periodically and after any significant weather event, be it a dryer or wetter than normal period.

Table 5.1: Dates of Visual Condition Surveys performed

Visual Condition Surveys	
Survey #	Date
1	10-Oct-13
2	17-Dec-13
3	16-Feb-14
4	9-Jun-14
5	27-Jun-14
6	8-Aug-14
7	25-Sep-14
8	13-Nov-14
9	27-Jan-15
10	26-Mar-15

These surveys were conducted overt time in order to be able to compare the data more efficiently. The surveys were always started from the South side of the road where traffic goes northeast towards Paige from Section 1. From here the distance on the distance measuring wheel was set to cero and the surveys were started. The starting and ending of each section was documented. Each section is 500 feet long so for example, the beginning of Section 2 should be documented as 500 feet and the end of Section 2 and beginning of Section 3 as 1000 feet. This procedure was continued until reaching the end of the test sections were the distance measuring wheel should show a value close to 4000 feet at the end of Section 8. After the test sections were surveyed, the other side of the road was also evaluated since the other side of the road was constructed using the GT1 geotextile, which is the control in the test sections.

For this study the north side of the road where traffic goes towards Bastrop, Texas, was surveyed but not considered. The north side of the road is performing much better that the south side and is probably due to different drainage conditions. From the design plans it appears that water flows northward toward the test sections so this side will experience

larger moisture variations and be susceptible to more vertical displacements due to the expansive soils. Figure 5.10 and Figure 5.11 show the location of the test sections as well as the direction of surface runoff and drainage paths that go below the pavement structure. The location of these drainage paths located in Section 4 and 6 probably suggest low points to where water will drain to which could have some effect on the performance of these sections.

The results are grouped into 3 main distresses considered in this study, shoulder cracks, edge cracks and longitudinal cracks in the wheel path cracks. The data for the last survey was documented but not presented in this document. The majority of the cracks were sealed by TxDOT personnel so for this study data up to January 27, 2015 was used.

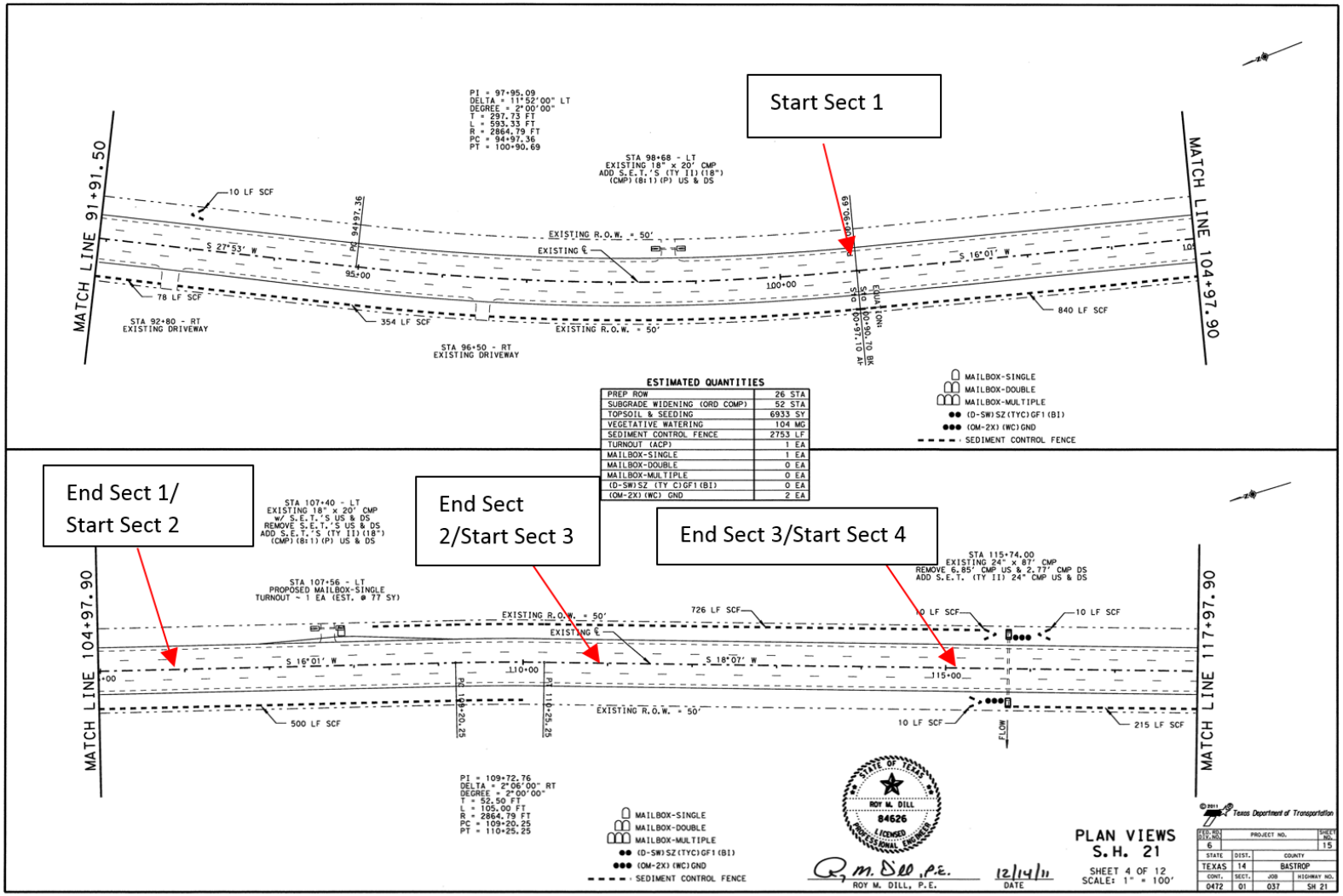

Figure 5.10: Design plans showing location of test Sections 1 through 4 and direction of surface runoff

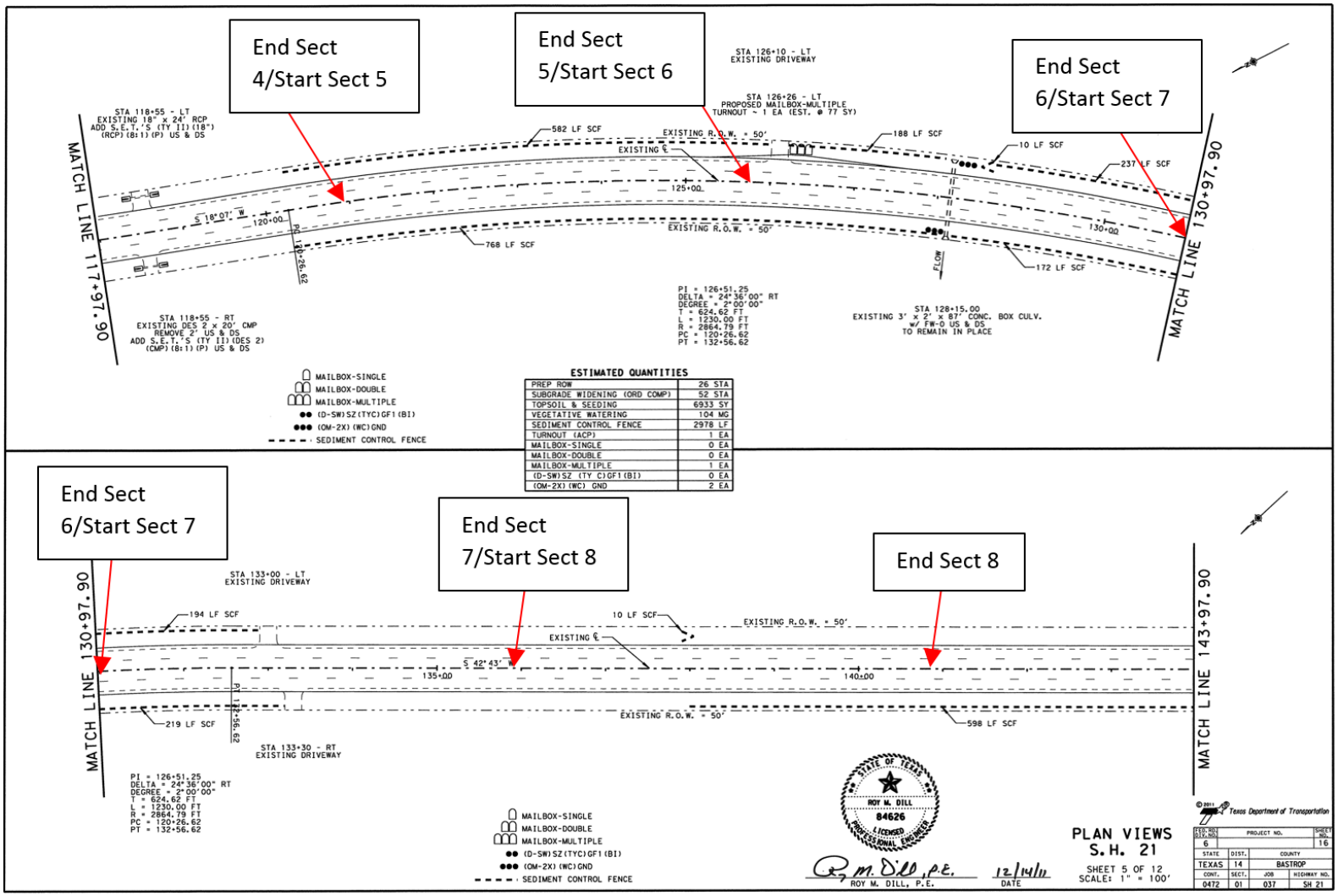

Figure 5.11: Design plans showing location of test Sections 4 through 8 and direction of surface runoff

5.5.1 Shoulder Cracks

As described in 5.1, shoulder cracks for the purpose of this study are considered longitudinal cracks that are 1 foot or further from the white line as shown in Figure 5.1. Shoulder cracks as defined for this study, will be located within the shoulder, above the geotextile, and far enough from the edges of the asphalt, so that any cracks in this zone can be attributed to expansive clays with more certainty. It's important to point out, that cracks in the very edge of the asphalt were not included in shoulder cracks. The outer edge, where the asphalt ends is a zone where poor compaction of the material tends to happen and the asphalt can crack in this area for other reasons other than expansive clays.

Based on this definition of shoulder cracks, the surveys showed that Section 4 and 7, both with GT4 installed, showed no shoulder cracking. These results may suggest that the GT4 geotextile may be causing the paved shoulder, built above the geotextile, to be displaced vertically as a single mass. The moisture data for these sections, discussed in Chapter 4, shows GT4 promoting a uniform moisture beneath it. This uniform moisture content beneath GT4 would result in the soils in this area expanding or contracting the same amount. The paved shoulder built above GT4 in this case, will move up and down all together and not experience differential movements which would possibly result in no longitudinal cracking in the shoulder area as the survey data shows. Figure 5.12 and Figure 5.13 show pictures taken of the shoulder areas of both Section 7 and 4 during the survey done on January 27, 2015. Both images show no cracking in what was defined as the shoulder area. Results appear to suggest that GT4 is able to prevent cracking in the shoulder, by equilibrating moisture beneath the geotextile through enhanced lateral drainage.

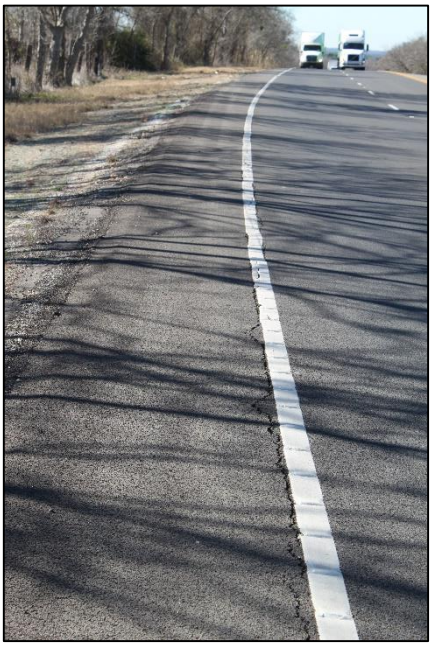

Figure 5.12: Shoulder area of Section 7 in January 27, 2015 Survey

Figure 5.13: Shoulder area of Section 4 in January 27, 2015 Survey

Sections 3 and 5, both have GT2 installed, which as previously said mainly provides soil reinforcement. Section 3 has not showed any cracking in the shoulder area suggesting that GT2 may be helping in the minimization of longitudinal cracking in this area but Section 5 has showed minor cracking. The cracking in the shoulder area in Section 5 is located towards the end of the section and has yet to exceed the 3 mm threshold used to

decide if the crack is included in the survey data or not. As previously mentioned, cracks with a width of less than 3 mm are typically not reported, but in this case it was plotted since this cracking will only increase with time. Figure 5.14 shows that shoulder cracking is a small portion of the total distresses, but the presence of this type of cracking suggest the expansive clays are still having some detrimental effects even with the presence of reinforcement.

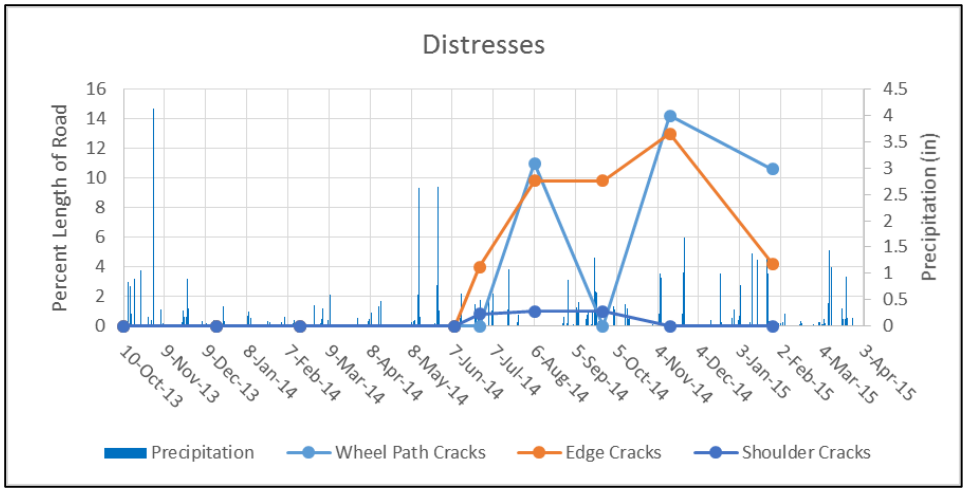

Figure 5.14: Condition Survey data from Section 5

Sections 2 and 6 have GT3 installed which like GT2 provides soil reinforcement but has a higher tensile modulus as discussed in 4.3. Section 2, like Section 3, did not show any shoulder cracking. Section 6 showed cracking in the shoulder area at the beginning of the section as showed in Figure 5.16, which connects to the shoulder crack in Section 5. Unlike the crack in Section 5, the portion of it in Section 6 has been wider than 3 mm. Figure 5.15 shows the data from the condition surveys done in Section 6 which show cracking in the shoulder which is most probably due to expansive clays since the crack appears to close after various rain events.

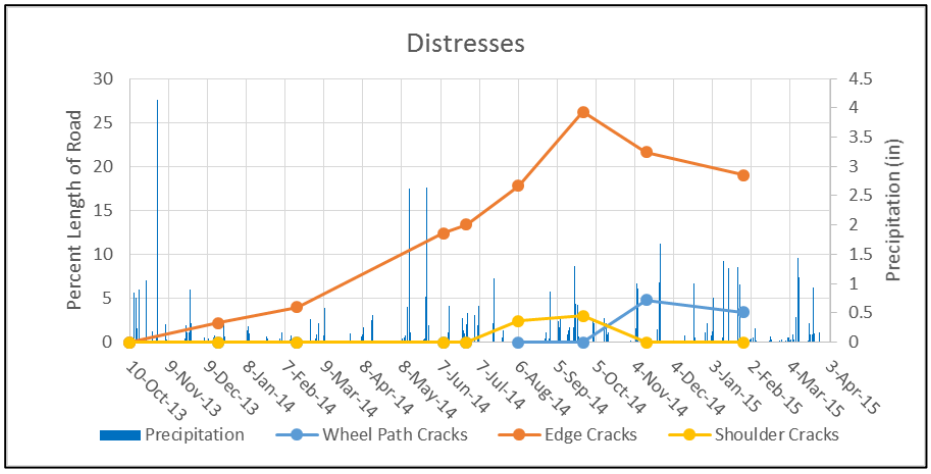

Figure 5.15: Condition Survey data from Section 6

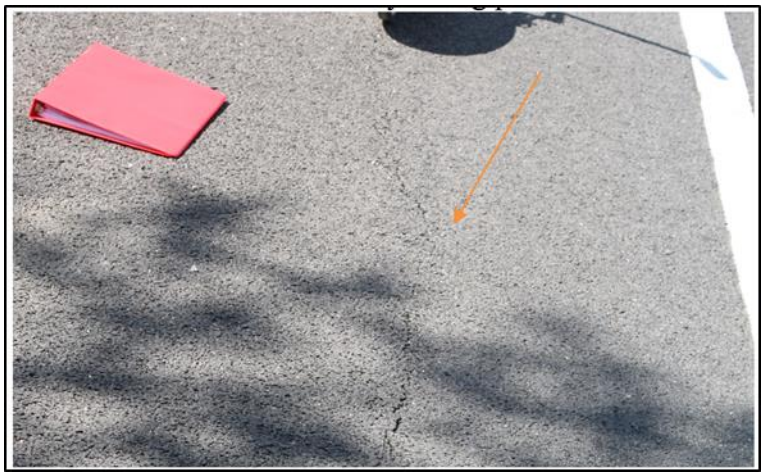
Figure 5.16: Shoulder Crack at the beginning of Section 6

Sections 1 and 8, which has GT1 installed, showed no shoulder cracking during the 10 condition surveys performed. Section 1 appears to be founded on a different subgrade soil compared to the other sections which was noticed when the installation of the sensors in the vertical array was done. Section 1 as will be discussed further along has shown less cracking than other sections suggesting it may be related to the subgrade since this section has the control geotextile which provides no benefits other than separation. Section 8 on the other hand is believed to be founded on the Cook Mountain formation but when the drilling for the installation of the vertical array took place, this formation was not found as

shown in Figure 4.62. Instead, a dark clay was found but this was at the side of the road where possibly the Cook Mountain formation may have been excavated. From the soil characterization data, the PI at Section 8 was determined to be 58 which is very high suggesting very expansive soils which makes the lack of shoulder cracking in this section interesting. One of the ideas discussed was the possibility of the shoulder founded above GT1 is more flexible due to GT1 not providing any reinforcement, and this has prevented shoulder cracking until the moment.

5.5.2 Edge Cracks

As described above, edge cracks are defined for the purpose of this study as cracks that are within 1 feet of the white line at the outer edge of the outer lane as shown in Figure 5.1 and Figure 5.17. This type of crack was the one most observed during the surveys, appearing the earliest. Figure 5.18 shows the progression with time of the edge cracks documented in all 8 test sections plotted together with daily precipitation and accumulative precipitation. Before going into the discussion, survey data until January 27, 2015 was used due to TxDOT sealing the cracks between this date and March 26, 2015. Figure 5.17 shows an example of one of the cracks sealed by TxDOT at some point between January 27 and March 26, 2015.

Figure 5.17: Image taken in Section 7 on March 27, 2015

From the figures it can be said that Section 7 shows the highest number of edge cracks. This section was studied more carefully because the tendency of cracks due to expansive clays is that they will open during dry periods and close during wet periods. For Section 7 the progression of the cracks appeared to be unrelated to weather events suggesting another cause for the cracks. Figure 5.19 shows 2 images taken during a survey performed on November 13, 2014. These pictures show how the crack progresses perfectly parallel to the white line where the geotextile ends as shown in Figure 5.1. There is some vertical displacement evident also which could be due to consolidation of the new shoulder structure.

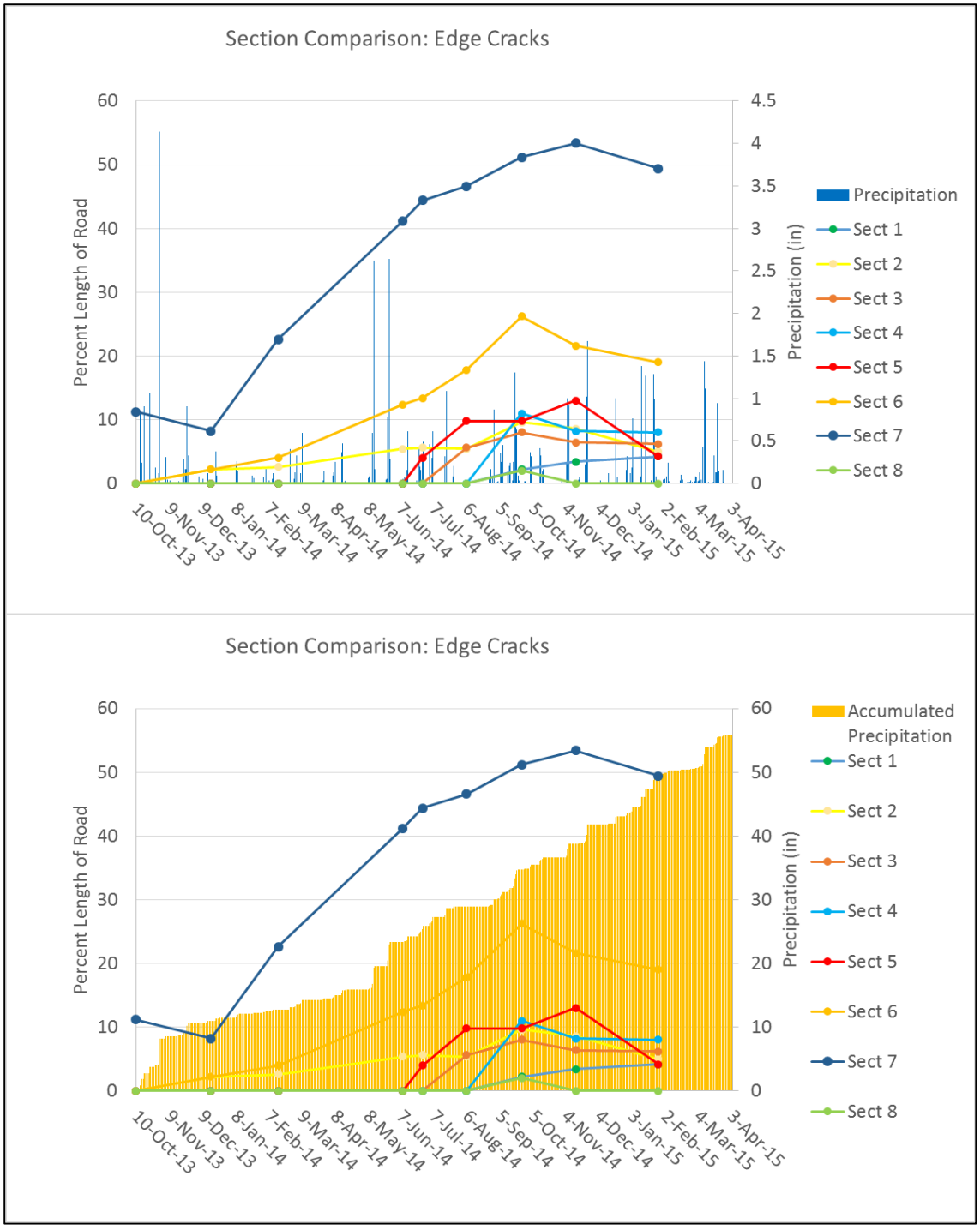

Figure 5.18: Comparison of Edge Cracks in each section over time

Figure 5.19: Pictures of Edge Crack in Section 7

These edge cracks in Section 7 are probably due to the discontinuity that takes place below the white line, where the GT4 geotextile ends and the old pavement structure starts as shown in Figure 5.20. This cracking is to be expected where the geotextile ends. In addition, the shoulder which is a new structure can be settling which could explain the vertical displacement observed in the image on the right in Figure 5.19. One more possibility is that these cracks can be due to GT4 causing the shoulder to move vertically as a single mass with moisture variations in the soils beneath the geotextile. These longitudinal cracks along the white line could be due to shear generated as the shoulder moves vertically suggesting GT4 is performing as expected and leading to uniform vertical movements beneath it.

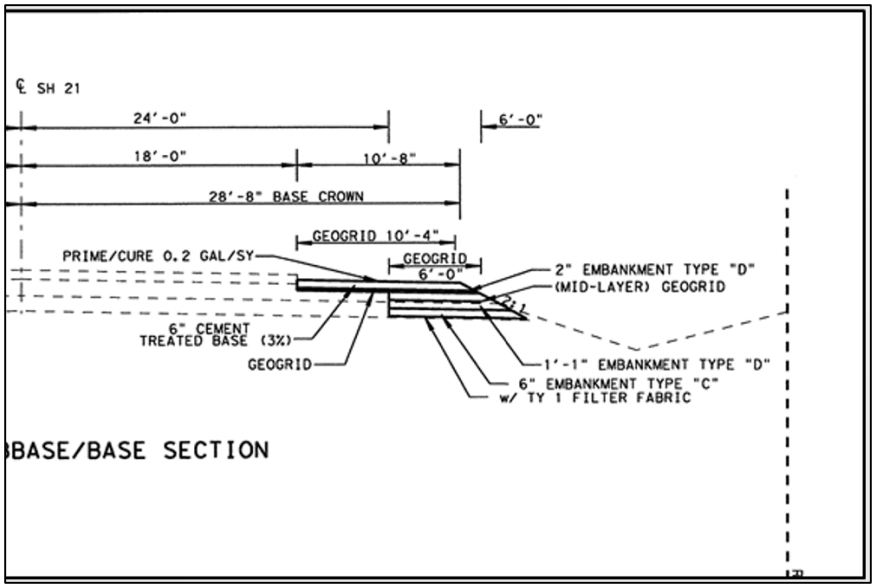

Figure 5.20: Pavement section from design plans for SH-21, Bastrop, Texas

Some parts of the edge cracks in Section 7, could be due to expansive clays as well as data from condition surveys may suggest. There is a reduction in percentage cracking between October 10 and December 17, 2013, for which a significant amount of rain fell in Bastrop, Texas. This reduction in cracking could be due to human error while doing the condition surveys or that there was a portion of the cracking due to expansive clays which may have expanded and closed the cracks. Something similar was observed between November 13, 2014 and January 27, 2015 as shown in Figure 5.18.

Section 6 which has GT3 installed, has shown some significant edge cracking as well. This section like Section 7, has progression of cracks that appear to be independent of rain events, which could suggest a situation similar to that of Section 7. This idea is reinforced by photos taken from the last surveys that show the edge crack from Section 7, progressing into Section 6 as shown below in Figure 5.21.

Figure 5.21: Edge Crack from Section 7 progressing into Section 6

Section 6 does have edge cracks that can be attributed to expansive clays, since like Section 7, there are cracks that are closing with wetter periods as shown after September 25, 2014 in Figure 5.18.

Section 5, which has GT2, shows less edge cracking with around 10% of its length cracked for a time period between August 8 and November 13, 2014. This section has cracking which runs along the white line like Section 6 and 7, but can be better related to rain events suggesting that it may be due to both, boundary condition and expansive clays. Individual plots to summarize distresses for each section were done as shown in Figure 5.22 which summarizes the distresses documented only in Section 5. It can be observed, that the cracking progresses after periods of dryness, the only detail is that many of the surveys after the one done on August 8, 2014, were performed after significant rain events. This makes the source of cracking not as evident.

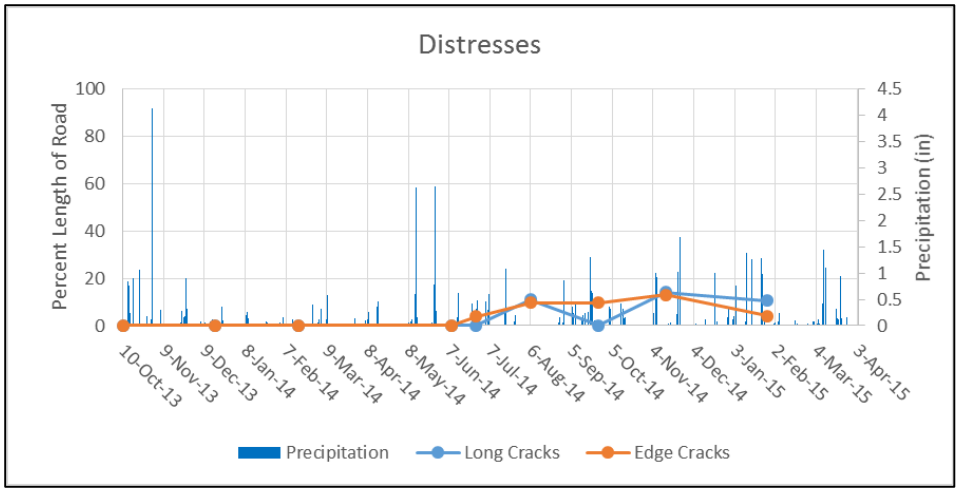

Figure 5.22: Summary of distresses in Section 5

Section 2, which has GT3 like Section6, showed around 10 percent edge cracking when most cracked. This section started cracking at some period between October 10, 2013 and December 17, 2013, and has grown steadily until reaching a maximum of around 10% cracking. The progression of cracks in this section, is more obviously related to dry periods, as shown in Figure 5.18.

Section 4, which has GT4 like Section 7, showed cracking similar to Section 2 peaking slightly above 10% on September 25, 2014. Section 4 had no edge cracking previous to this survey and seems to have cracked after approximately a month with minor to no rain events. The percentage of cracking seems to have peaked on September 25, 2014 and then stayed constant or decreased. The analysis of the data for this section like others, is not easy due to the surveys being done after significant rain events that could have caused cracks to close. This could lead to cracks being measured when portions of them are closed and create some confusion. Soil samples taken from Section 4 were obtained during the installation of the moisture sensors and a PI of 52 was obtained, exceeding all other sections except Section 8. This could suggest soils at this section are more expansive and capable of more vertical displacements that would results in more cracking. If this is the case then

this section might be performing better that others when considering that it is cracked the same amount as Section 5 and 2, which have PI's of 24 and 32.

Section 3 has GT2 installed as its geotextile underneath the shoulder. This section has very similar cracking to Section 2, even do it starts showing cracks around 9 months later. There actually is an edge crack that continues from Section 2 into Section 3 as shown below in Figure 5.23. Similarly to Sections 2 and 4, the cracking percentage peaks on the survey performed on September 25, 2014, and decreases after this date, possibly due to various significant rain events happening before the surveys were done as shown in Figure 5.18.

Figure 5.23: Edge crack in Section 3

Sections 1 and 8, both with GT1 installed, were the sections that cracked the least until the time this report was prepared. Section 1 seems to be founded on a different soil than the other sections, so it's not surprising that it is showing different performance. Section 8 on the other hand, is not very clear why it has practically no edge cracks. The only documented edge cracks in Section 8 were observed during the September 25, 2014 survey which is when multiple other sections had their percent cracking peak. The PI at this section is very high, 58, which would suggest highly expansive soils. A possibility for

no edge cracks is that the presence of the GT1 geotextile, which provides no reinforcement, has some effect and possibly decreases the boundary condition's effect on the section's performance.

5.5.3 Longitudinal Cracks in the Wheel Path

For the purpose of this study, longitudinal cracks in the wheel path or wheel path cracks, were those that occurred within the traffic lanes. These type of cracks, are typical of pavements founded on expansive clays as well. In this study these cracks are located past the extent of the geotextiles as shown in Figure 5.1 so they cannot be fully attributed to the performance of the geotextiles though they can be possibly related to it. Wheel path cracking occurring in these 8 test sections cannot be attributed to poor performance of the geotextiles since they occur outside of the coverage area of the textiles. 8 test sections where surveyed for wheel path cracks, taking note of any cracks in the traffic lanes, and the width of the cracks were measured when traffic allowed it and reported.

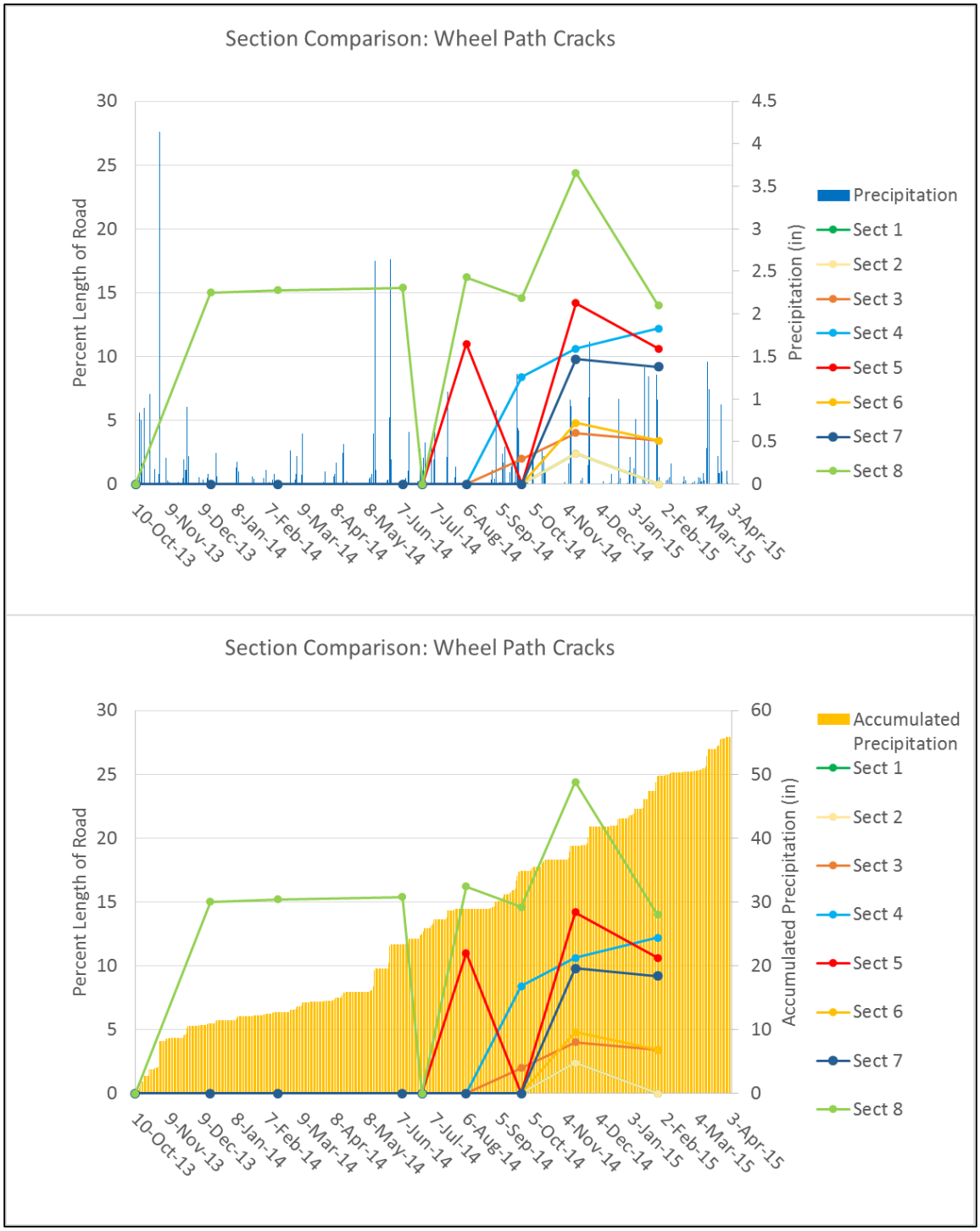

Figure 5.24: Comparison of Longitudinal Cracks in each section over time

Figure 5.24 shows the progression of wheel path cracks in all 8 test sections plotted against time together with daily precipitation, and accumulated precipitation. Unlike edge cracks, Section 8 did have significant wheel path cracks. This section has installed GT1 which only serves for separation and provided some lateral drainage. The section showed rapid cracking between October 10 and December 17, 2013, going from 0 to 15% longitudinal cracking after which cracking did not increase much over time. On the fifth survey on June 27, 2014, the longitudinal cracks appeared to have all closed up due to various significant rain events and then are open again during the 6th survey on August 8, 2014. There was a dry period approximately during the two weeks previous to the August 8, 2014 survey, suggesting that the cracks closed up after the rain events and opening back up after 2 weeks of no rain. This would confirm that these cracks are due to expansive clays which obviously are present in this section with samples tested from this section having a PI of 58. The increase and decrease of cracking percentage shown in Figure 5.24 after the survey done on August 8, 2014 shows how the cracks open and close with relation to rain events. Figure 5.25 shows how extensive the longitudinal cracking is in Section 8, reaching almost 25% of the entire section length on November 13, 2014.

Figure 5.25: Wheel path cracks in Section 8

Section 5 which has installed GT2 showed significant wheel path cracking also. This geotextile does not provide any hydraulic benefits but does provide reinforcement which should provide added stiffness in the shoulder area and help with cracking, unfortunately in this project these wheel path cracks are located past the extent of the geotextile which may be a reason for the wheel path cracking with wheel path cracking reached almost 15% on November 13, 2014. The cracking progression for this section again shows tendencies of cracks closing and opening with relation to rain events as shown in Figure 5.24, which as in Section 8, suggests they are related to expansive clays.

Sections 4 and 7, which both are GT4 sections, showed very similar wheel path cracking. Section 4 cracks sometime between August 8 and September 25, 2014 during which there was a significant dry period. Section 7 cracks sometime between September 25 and November 13, 2014 for which, there was another dry period that lasted almost a month and a half. Figure 5.26 and Figure 5.27 show the data from the surveys for both sections, since the cracking percentage is not very high Figure 5.24 may show a clearer picture with the larger scale.

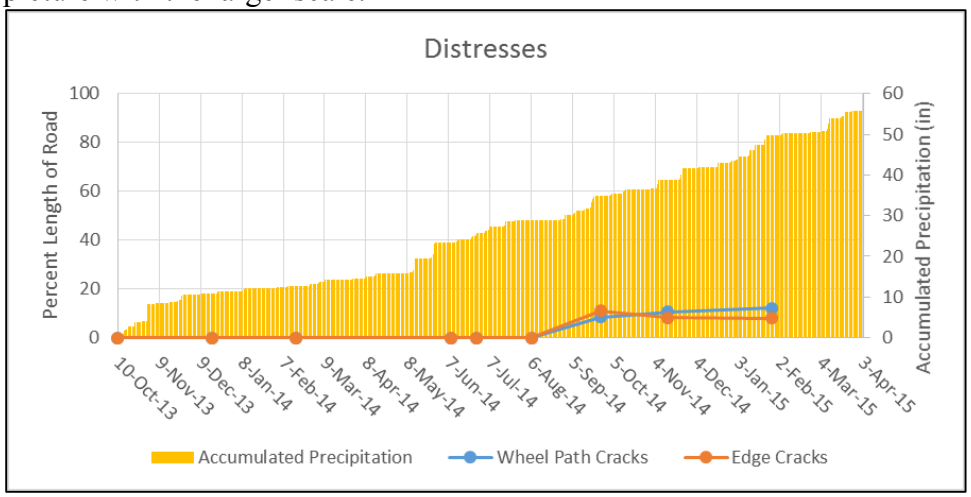

Figure 5.26: Summary of distresses in Section 4

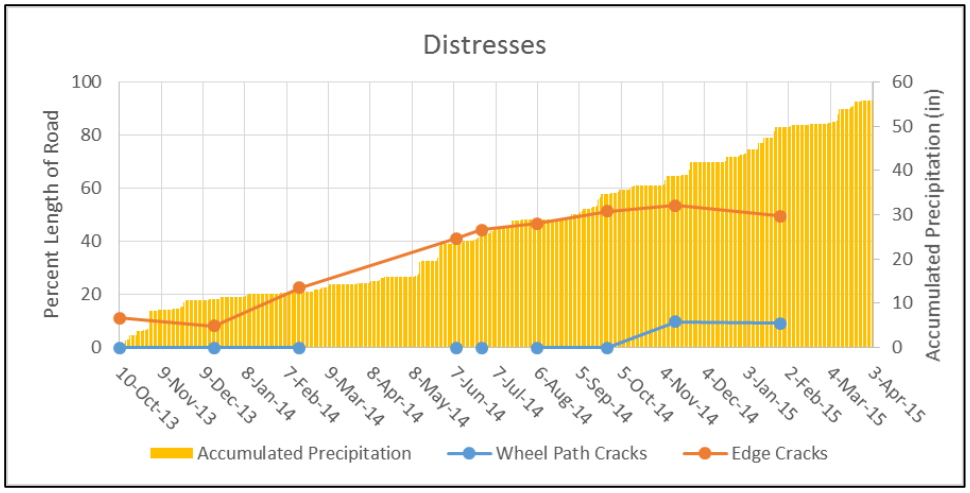

Figure 5.27: Summary of distresses in Section 7

The cracking in the sections with the GT4 geotextile, in terms of wheel path cracking, was something that was suspected as the study progressed. The GT4 geotextile, as already said, has shown to be able to equalize moisture contents underneath the coverage zone of the geotextile itself. This was shown in Chapter 4 when discussing the data from the moisture sensors. Section 4 showed that GT4 was maintaining a uniform moisture front underneath the geotextile while Section 7 appeared to show GT4 slowly equalizing moisture beneath the geotextile. In the case of Section 7, the sensors closer to the white line showed this area being less humid compared to the shoulder of the road. Thus in order to equilibrate the moisture, GT4 will have to bring water towards that area and increase the moisture content. This increase in moisture could lead to expansion of the clay in this area generating stresses in the pavement. The equalizing of moisture below the geotextile will prevent cracking in the area above the geotextile but will not prevent cracks in the outer areas.

Since both sections with GT4 are showing similar cracking in terms of wheel path cracks, it is believed that the way they were installed in the test sections is not the best for pavements founded on expansive clays. Possibly, the result will be that the vertical

displacements, instead of being concentrated at the outer edge of the pavement which is expected in the section without GT4 since they don't provide enhanced lateral drainage, will now take place further inwards in the pavement, thus still generating cracking but within the traffic lanes. The idea is that the shoulder will now be vertically displaced as a single mass due to equal moisture beneath the geotextile on which the shoulder is founded, and generate stresses in the asphalt closer to the traffic lanes resulting in wheel path cracks. If the entire pavement were built with GT4 below it, the entire road would ideally move vertically as a single mass with fluctuations in moisture content and would possibly not crack longitudinally.

The sections with less wheel path cracking, all have geotextiles capable of providing reinforcement. Section 6 and 2 both have installed GT3, which as mentioned previously is the strongest of all the geotextiles used in this study. The wheel path cracks in both sections appear to be due to expansive clays as they appeared after periods of dryness and show decreases in length after November 13, 2014 after which various rain events took place. Section 3 which has installed GT2, which also is capable of providing reinforcement, has cracking that also seems to be due to expansive clays for the same reasons as the cracks in Sections 6 and 2. Figure 5.24 shows clearly the tendency of the longitudinal cracks in these 3 sections to open up during times of little to no rain and close up during wet periods.

Section 1, which has the control geotextile, GT1 installed, showed the less wheel path cracking of all the sections. As explained before, this can be due to the presence of a different subgrade material. For this section, the first longitudinal cracks appeared just recently and were documented in the last survey done on March 26, 2015 as shown in Figure 5.24.

5.5.4 Comparison of Geotextiles

The performance of the geotextiles was evaluated as well in order to see how each geotextile performed. In order to evaluate each geotextile, averages of the distress data for the sections with the same geotextile was used. Figure 5.29 and Figure 5.30 below shows the data on the performance of each geotextile based on edge crack and longitudinal cracks independently.

GT4 showed the least cracking in terms of shoulder cracking with none at all. The only two sections at the moment showing some shoulder cracking are Sections 5 and 6 which have installed GT2 and GT3. This suggest that GT4 may be causing the shoulder to move vertically as a single mass thus preventing bending stresses in the asphalt in the shoulder above GT4 as was expected. Figure 5.28 shows the data for shoulder cracking until the writing of this report, these cracks will most probably only grow with time and possibly provide more insight on the performance of the geotextiles in these expansive soils.

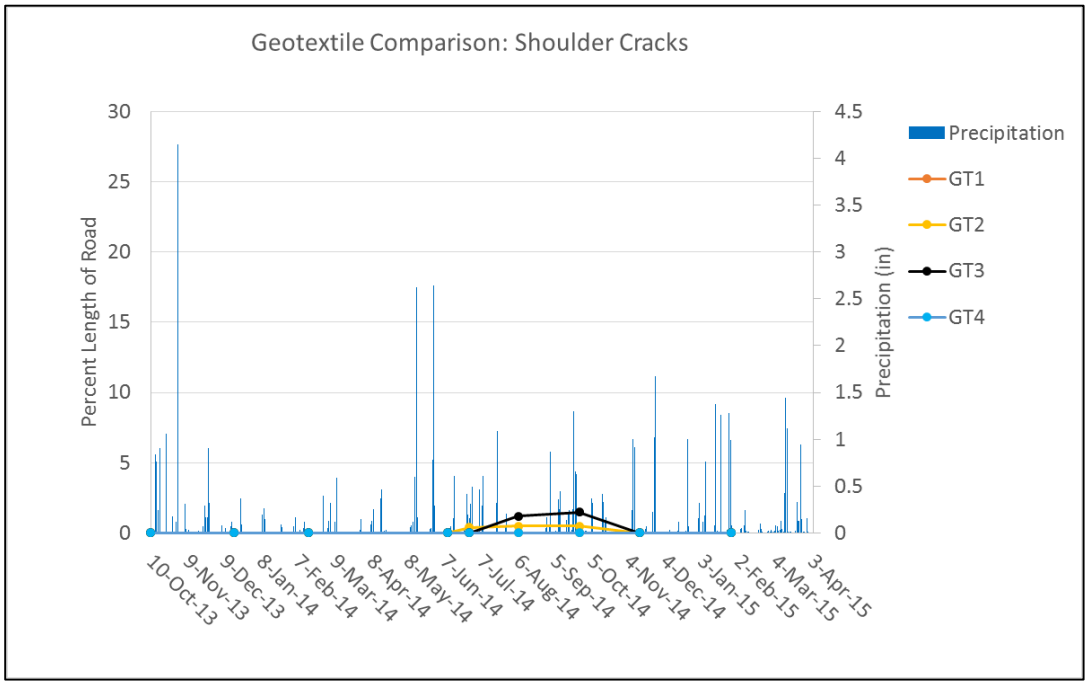

Figure 5.28: Comparison of Geotextiles in terms of Shoulder Cracking

In terms of edge cracking, Figure 5.29 suggest that GT4 has the most edge cracking, which is not necessarily bad. This average is mostly due to the large amount of cracking in Section 7, which as explained previously is believed to be driven by factors related to the boundary condition where the geotextile ends and the old pavement structure starts as shown in Figure 5.1. The fact that all the edge cracking in Section 7 is concentrated along the white line where the geotextile ends, suggest the edge cracks may not be related to expansive clays and as previously mentioned, cracking at the end of the geotextile is to be expected. This area is one that poor material compaction could have taken place which could explain the location of the crack perfectly above the boundary where the new structure ends and the old one starts. One other idea mentioned above is that these cracks which are prevalent in GT4 sections, could be due to shearing from the shoulders moving vertically as a single mass as data seems to suggest. So the fact that the GT4 sections show the most edge cracks could possibly be a sign that the geotextile is performing as hoped for.

The two geotextiles which are capable of providing the most reinforcement from all the 4 geotextiles used in the study, showed edge cracking ranging from around 10 to 20 percent. GT3 sections had more edge cracking than GT2 sections, even though GT3 is stronger. GT1 showed on average less edge cracking than all other geotextiles as shown in Figure 5.29. The main reason for this is that Section 8 for some reason which is still not understood very well, showed little to no edge cracking during the period of this study and Section 1 being founded on a slightly different subgrade performed better than the other sections.

The one thing to be noted is that much of what was recorded as edge cracks during the condition surveys as mentioned, are cracks that run along the white line. Just like for

Section 7, these cracks are due to the discontinuity of the geotextile ending at that point. A better way to evaluate performance of the geotextiles in terms of cracks, is the shoulder area. These cracks could be said to be due to the expansive clays with more assurance since the presence of a discontinuity is eliminated. As shown in Figure 5.28, these cracks are still not that abundant suggesting the study should be continued for more time, especially until a significant dry period occurs which would cause large tensile stresses in the pavements leading to longitudinal cracking.

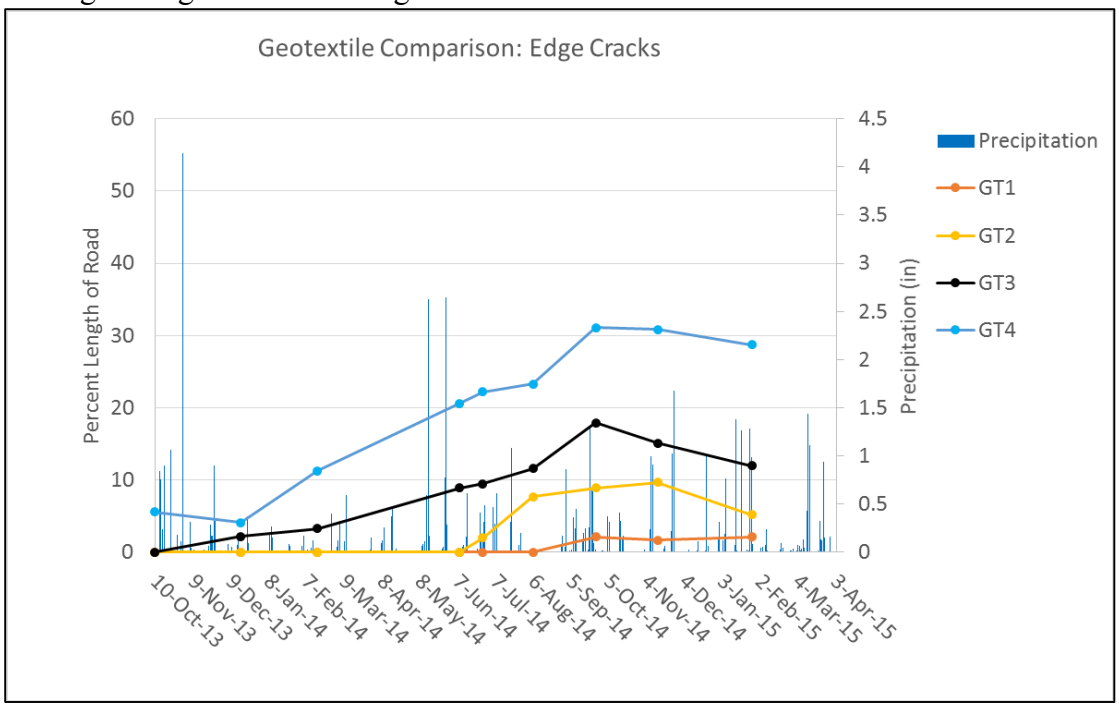

Figure 5.29: Comparison of Geotextiles in terms of Edge Cracking

In terms of longitudinal cracking, Figure 5.30 suggests that the control geotextile, GT1, cracked the most. These results were to be expected taking into consideration that the GT1 only provides separation, while the other geotextiles are capable of providing reinforcement, confinement, and GT4 in particular has the enhanced lateral drainage capabilities.

The GT4 sections showed significant wheel path cracking as well, but as mentioned before, this could be due to GT4 performing as hoped. GT4 was installed only under the shoulder which data shows prevents longitudinal cracks within the shoulder but possibly not in the surrounding pavement. The shoulder will move up and down together as moisture in the soil changes but the outer lane, where the wheel path cracks developed, will not, thus generating shear stress and bending moments which can lead to the formation of the wheel path cracks. What these results show is that possibly this type of installation of GT4 is not adequate for pavements founded on expansive clays, the ideal case would be to have GT4 underneath the entire road and see how it performs then.

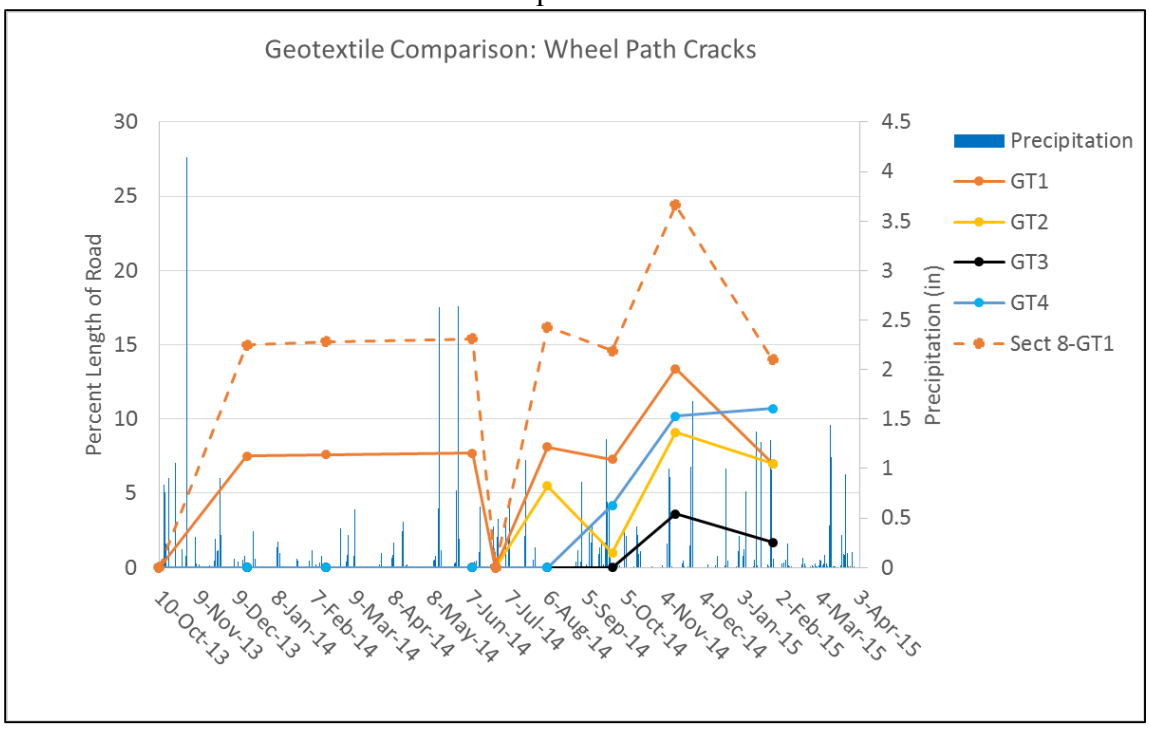

Figure 5.30: Comparison of Geotextiles in terms of Longitudinal Cracks

The geotextiles that showed the least wheel path cracking where the two that are able to provide the most reinforcement in the pavement structure and no hydraulic benefits like GT4. This was suspected after the consequences of having the GT4 geotextile only

under the shoulder were realized. The inability of both, GT2 andGT3, to transport moisture proved to be better in this type of installation. The concentration of moisture changes with these two geotextiles will happen closer to the edge of the pavement, further away from the outer traffic lane, causing most of the vertical displacement to take place in that area. The addition of the reinforcement which results in a stiffer pavement together with the movements happening further from the traffic lanes resulted in both GT3 and GT2 sections to have less wheel path cracks.

Chapter 6 : Conclusions and Recommendations

There is a significant presence of expansive clays in the United States as well as in the state of Texas. The weather conditions and significant number of roads founded on expansive clays in Texas pose a serious and costly problem for TxDOT. The prolonged periods of no rain fall accompanied by short periods of strong rainfall cause these roads founded on expansive clays to experience large stresses imposed by differential vertical displacements occurring under the roads.

6.1 SUMMARY OF RESEARCH OBJECTIVES

The main objective of this study was to evaluate the hydraulic performance of the GT4 geotextile in expansive clays and compare it to other geotextiles in the same soils. From previous research there was an idea that this geotextile could spread moisture more evenly under a road founded on expansive clays. The second objective was to quantify the ability of GT4 to prevent cracks from developing in pavements founded on expansive clays compared to other geotextiles. These two objectives were achieved with a field installation in a road called SH-21 in Bastrop, Texas, founded on a known expansive formation called Cook Mountain. The comparisons were done as follows:

- Data from moisture sensors below the geotextiles installed in the subgrade was evaluated. Profiles showing how moisture changed over time below the geotextile was used to compare the hydraulic performance of each of the 4 geotextiles.
- Visual condition surveys were done periodically and records were kept. The progression of cracks was plotted against time and precipitation to correlate the performance of the sections with weather cycles.

6.2 CONCLUSIONS

From the analysis of all the data from both the moisture sensors the following conclusions were made.

- GT4 seems to be able to maintain a uniform moisture front below roads founded one expansive clays as seen in data from Section 4
- GT4 appears to have the ability to equilibrate moisture in areas beneath it when there are significant difference in moisture content as seen in data from Section 7
- No other geotextile appeared to be generating any changes in moisture content that would suggest they are developing a uniform moisture content under the textile

From the multiple visual conditions surveys done in the test sections multiple observations were done and the following conclusions were made.

- GT4 sections showed not shoulder cracks, suggesting GT4 is able to reduce longitudinal cracking due to expansive clays in pavements founded above it
- GT4 sections showed more edge cracks than other sections, these cracks are mostly due to a boundary condition where a new and old structure meet as well as the end of the geotextiles occurring there as well, but the edge cracking in the GT4 sections could have possibly been amplified due to shear stresses of the shoulder built over GT4 moving vertically while the neighboring pavement structure did not
- GT4 sections showed some longitudinal wheel path cracking which was suspected, the enhanced lateral drainage provided by GT4 has shown to generate a uniform moisture content beneath it which causes soils in this area to expand or contract by the same amount, this may have resulted in the shoulder built above GT4 to move

vertically as a single mass while the outer lane next to it which is not built above GT4 did not, thus possibly generating tensile stresses and bending moments which led to the cracks

- GT3 and GT2 sections showed little longitudinal wheel path cracks, vertical movements with these geotextiles surely were concentrated closer to the end of the asphalt and the added stiffness these geotextiles kept longitudinal cracks in the wheel path to a minimum
- GT2 and GT3 sections showed some shoulder cracks which reinforces the conclusion stated above, vertical movements were concentrated at the edges in these sections leading to more cracks within the shoulder

Overall, from this study it appears that the GT4 geotextile is capable of the generating and maintaining a uniform moisture content in the soil beneath it even in expansive clays. This has been demonstrated by the data from the moisture sensors in Sections 4 and 7 as well as by the data obtained from the visual condition surveys. The lack of shoulder cracks and presence of edge and wheel path cracks in Sections 4 and 7 seems to suggest the shoulder in these sections may be moving vertically as a single mass due to the uniform moisture profile that GT4 has shown it can generate. The factor that H2Ri was enclosed in soil may possibly be the best way to install it since it appears to be able to equilibrate the moisture in the soil below it and have the structure built over GT4 move vertically as a single mass resulting in a minimization of longitudinal cracks as this study appears to suggest.

6.3 RECOMMENDATIONS FOR FUTURE RESEARCH

This is an ongoing study, based on previous experiences these sections will be monitored for several more years. In order to keep obtaining data from these sections and possibly confirm GT4's capabilities, it would be very beneficial that the moisture sensors that as mentioned have stopped working be revived. Talks have been started with Decagon Devices, which are the manufactures of all the equipment used for monitoring moisture beneath the sections but due to time constraints, not much has been done besides discussing the issues. The acquisition of what Decagon calls a Pro Check system would be beneficial since it appears to be able to trouble shoot sensors.

Since this will be an ongoing study, a recommendation is that any conclusions done in this document with regards to the visual condition surveys be revised after some time. As shown in Chapter 5 when discussing the weather data, there has not been any significantly dry year since the test sections were completed in early 2013. A more than normal dry year, like 2011, will truly test these geotextiles and provide much insight since SH-21 was damaged the most due to the 2011 drought.

The use of a 3-D scanning truck is recommended. Such technology if used periodically could provide much valuable information showing possibly the actual vertical movement of the shoulder with respect to the center line of the road. This could be used to confirm this phenomenon of the shoulder movements due to expansive clays and be used to correlate appearance of new cracks or progression of new to ones to these vertical movements or not. This in particular is at the moment in the works by other students in the research group.

For future projects similar to this one there are two main suggestions to make the project more successful. The first one is the use of more rugged moisture sensors. The sensors used for this study have a very good history in similar applications but for some

reason they did not perform well for this particular project. Decagon Devices produces more rugged sensors which are compatible to the data loggers used for this study. The GS1 sensors look promising with an epoxy coated body, stainless steel needle like prongs, and the cable exits the sensor body to the side decreasing chances of cable damage from the cables been bent during installation. One last recommendation for future projects like this one is the use of wireless data loggers which can send data over the internet. These data loggers are the same as the ones used for this study but they have the capability to send data through the internet using cellphone service. The benefit of these data loggers is that data can be seen in real time and if anything occurs it can be noted instantly and measures can be taken. Unfortunately these data loggers are significantly more expensive and the wireless service has to be paid as well but the possible benefits from using them could make them worthwhile.

In the case an opportunity to perform a project like this one, with a pavement on expansive clays, GT4 could be tested and placed underneath the entire pavement structure. From the results of this study, this appears to be the ideal way to incorporate GT4 in a pavement structure and would confirm if GT4 is a feasible way of dealing with pavements in expansive soils.

Appendix A: Description of conditions of SH-21 prior to reparation

Figure A.1: Longitudinal cracks in SH-21 prior to reparation

Figure A.2: Edge cracks in SH-21 prior to reparation

Figure A.3: Longitudinal cracks in SH-21 prior to reparation

Figure A.4: Class 1 distresses in SH-21 (Texas Transportation Institute, 2010)

Figure A.5: Class 3 distresses in SH-21 (Texas Transportation Institute, 2010)

Figure A.6: Class 4 distresses in SH-21 (Texas Transportation Institute, 2010)

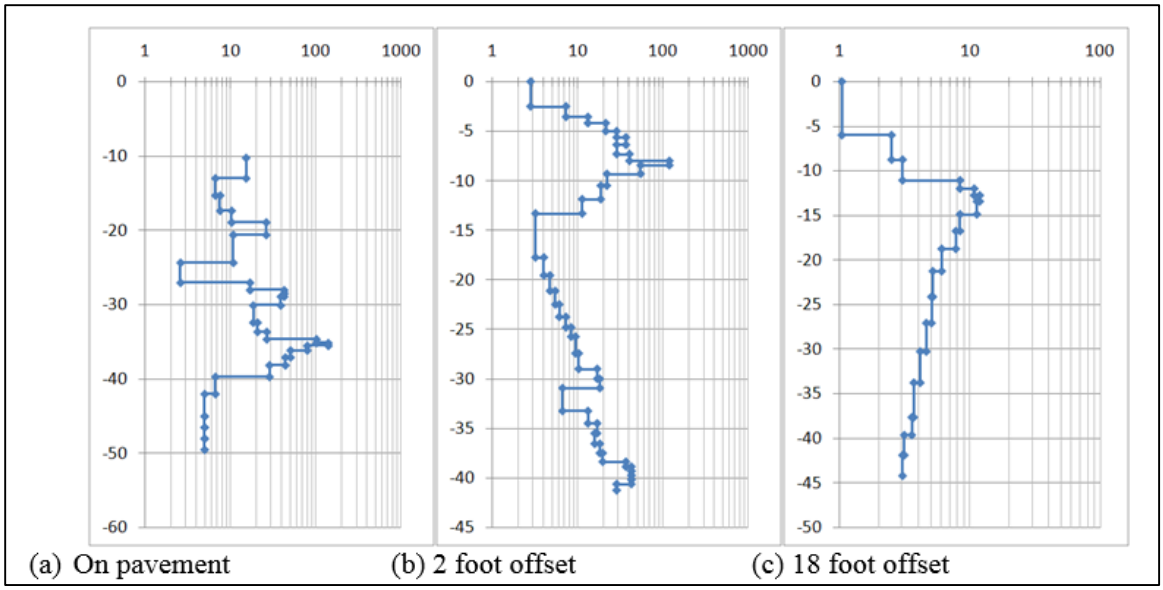

Figure A.7: DCP results from boring SB1 (Texas Transportation Institute, 2010)

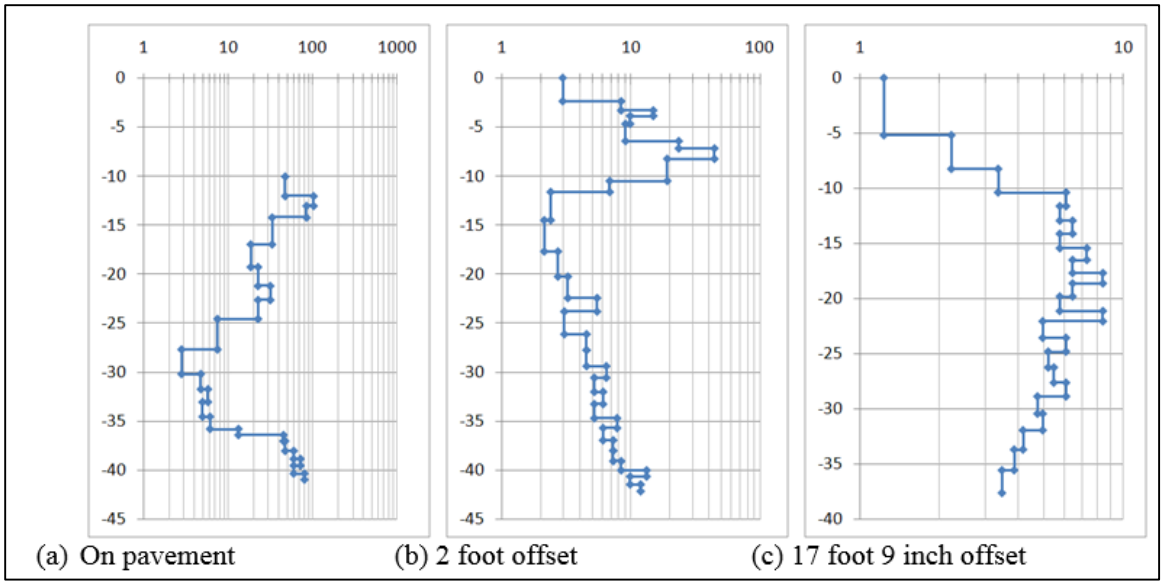

Figure A.8: DCP results from boring SB2 (Texas Transportation Institute, 2010)

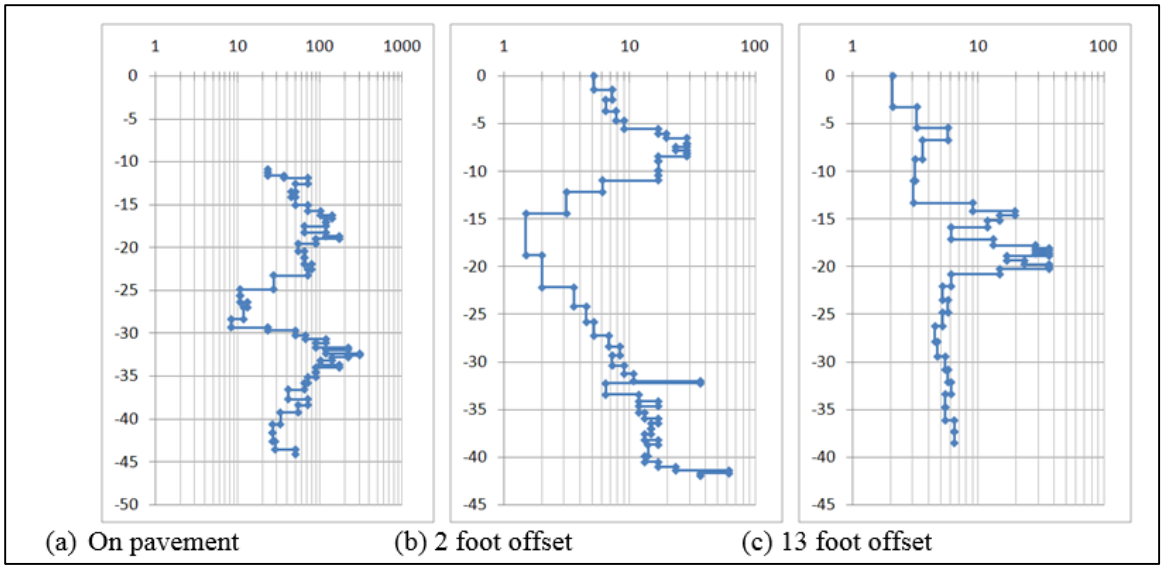

Figure A.9: DCP results from boring SB3 (Texas Transportation Institute, 2010)

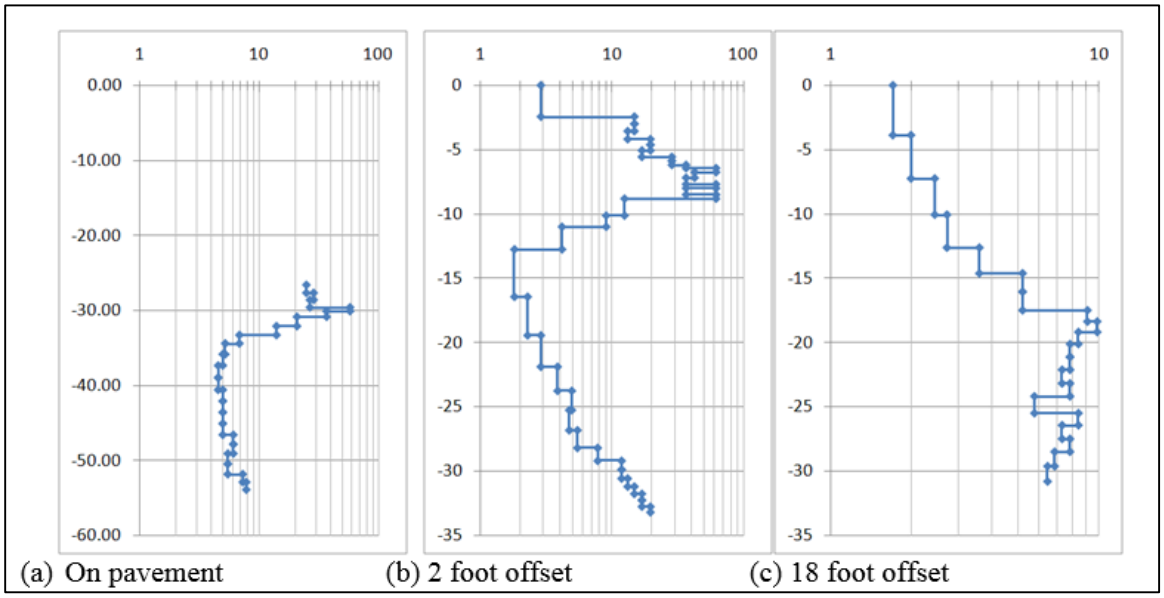

Figure A.10: DCP results from boring SB4 (Texas Transportation Institute, 2010)

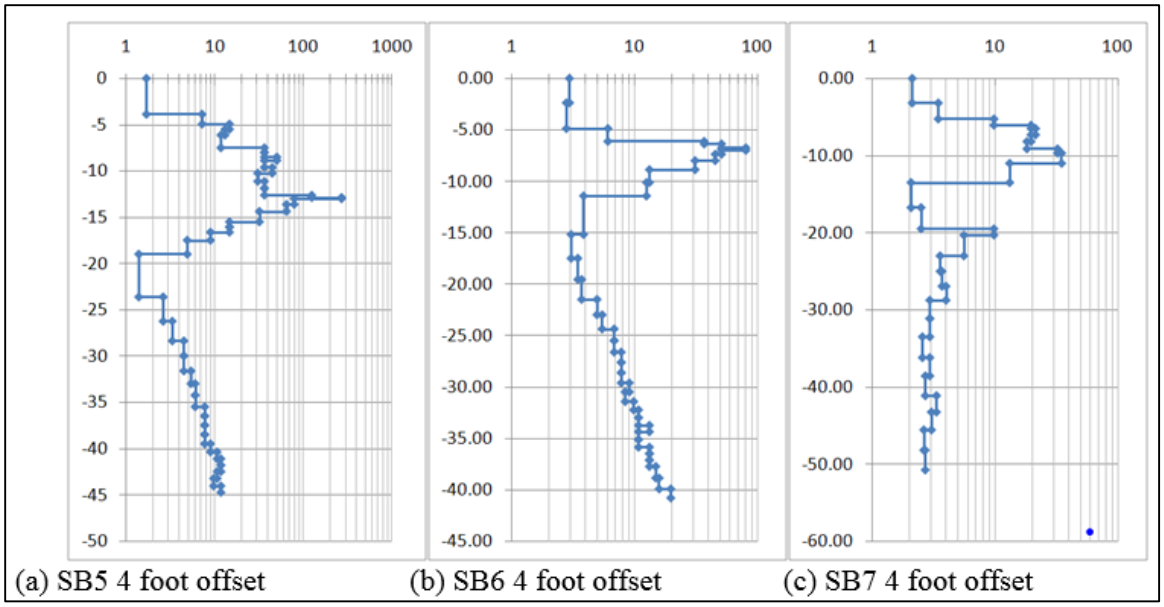

Figure A.11: DCP results from borings SB5, SB6, and SB7 (Texas Transportation Institute, 2010)

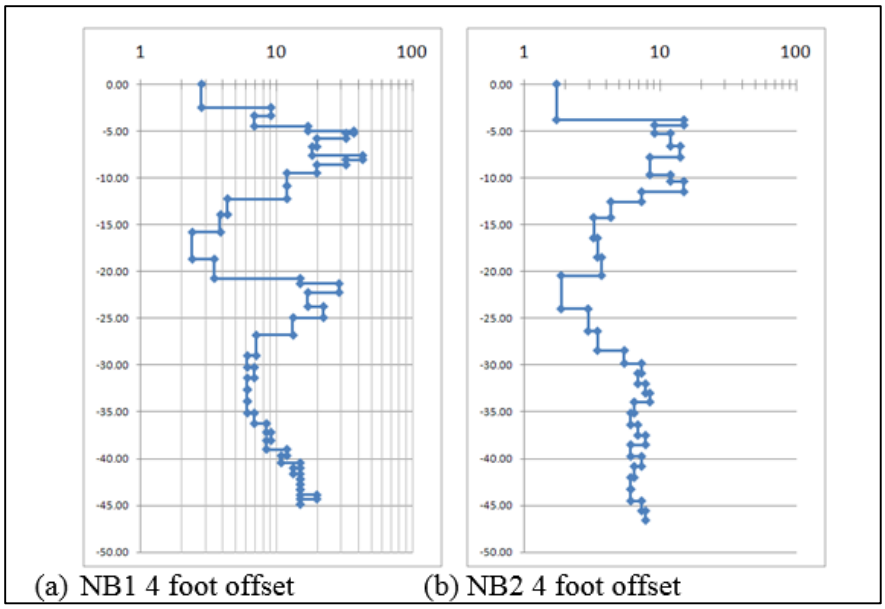

Figure A.12: DCP results from borings NB1 and NB2 (Texas Transportation Institute, 2010)

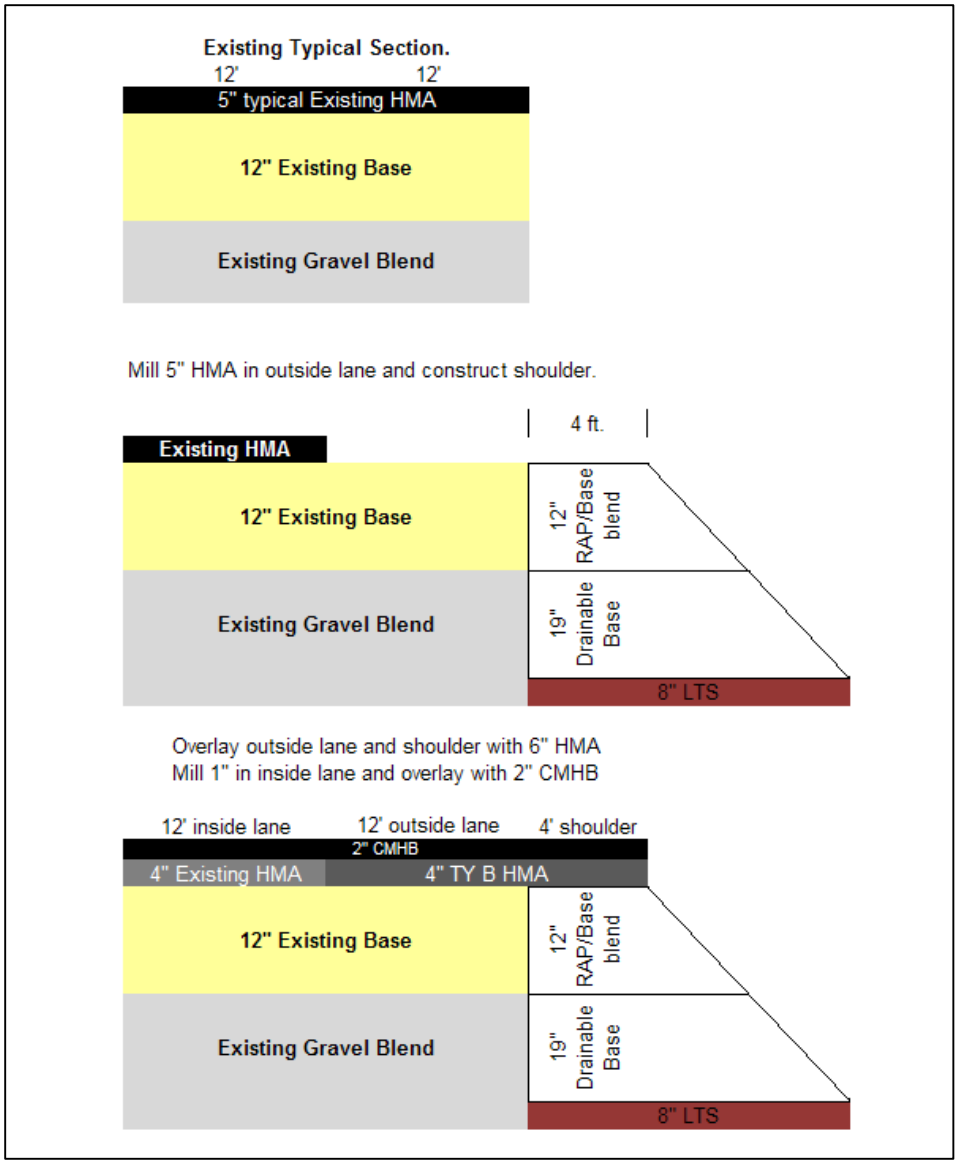

Figure A.13: Recommendations for SH-21 at 0 to 1400 feet from Southern Project Limits (Texas Transportation Institute, 2010)

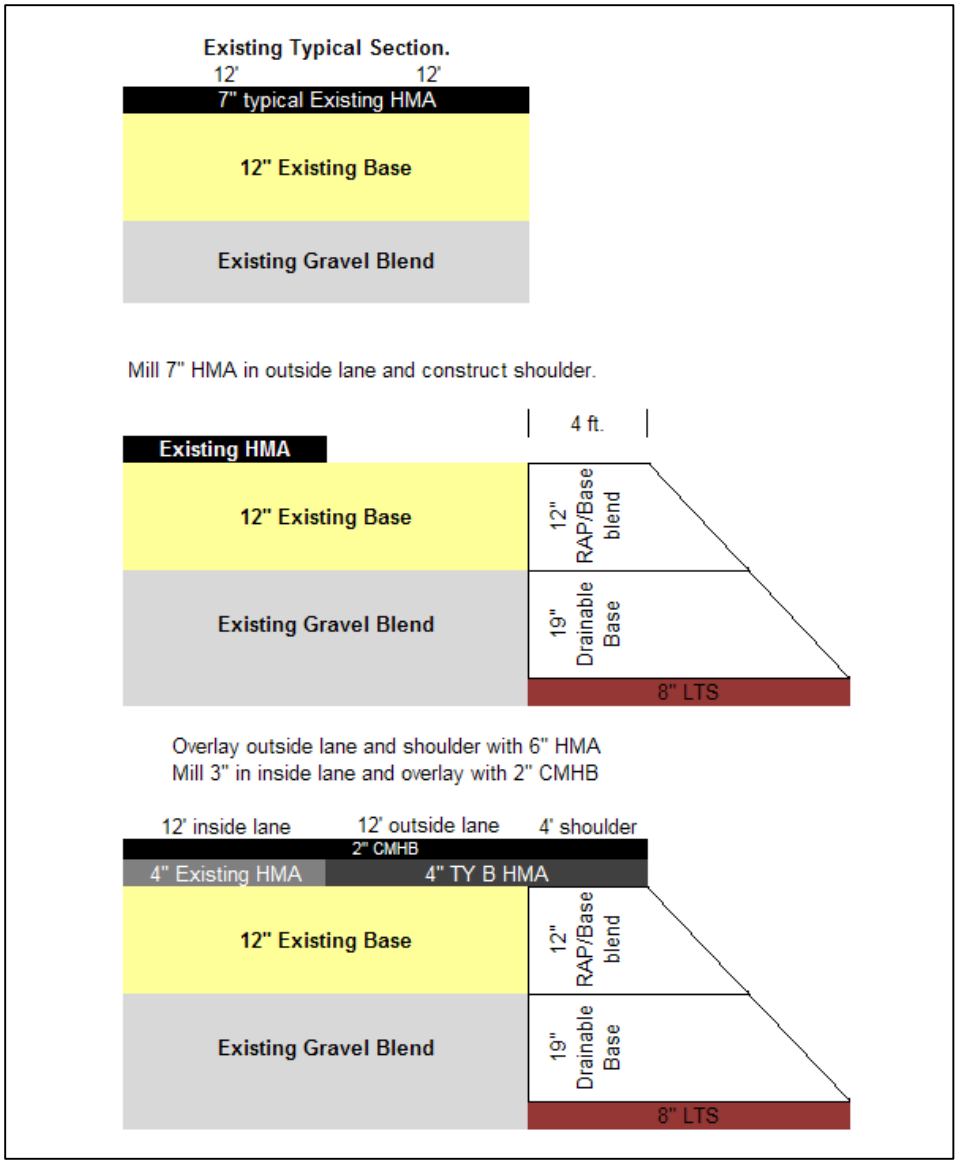

Figure A.14: Recommendations for SH-21 at 13500 to 15200 feet from Southern Project (Texas Transportation Institute, 2010)

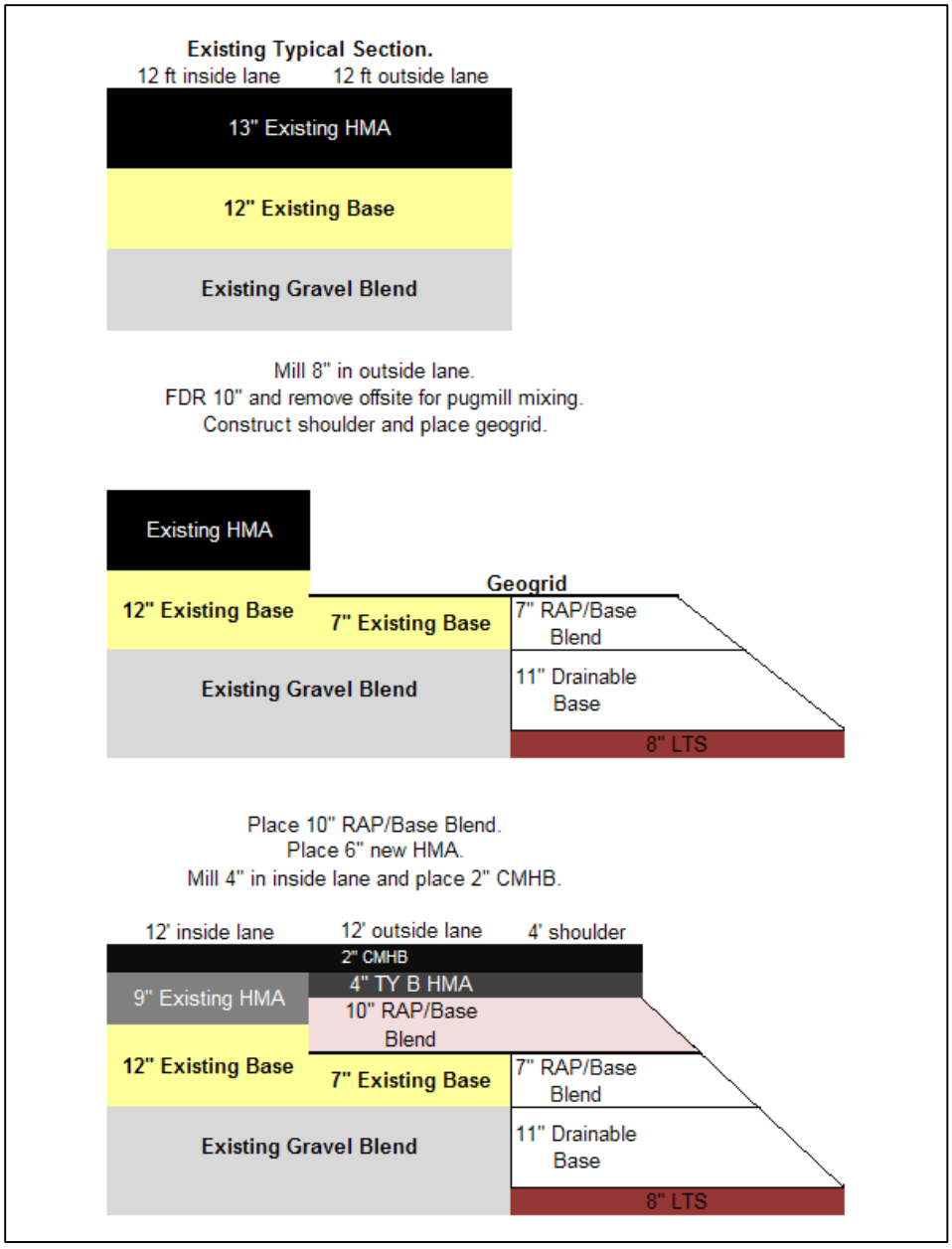

Figure A.15: Recommendations for areas of SH-21 where there are Class 1, 2, and 3 distresses (Texas Transportation Institute, 2010)

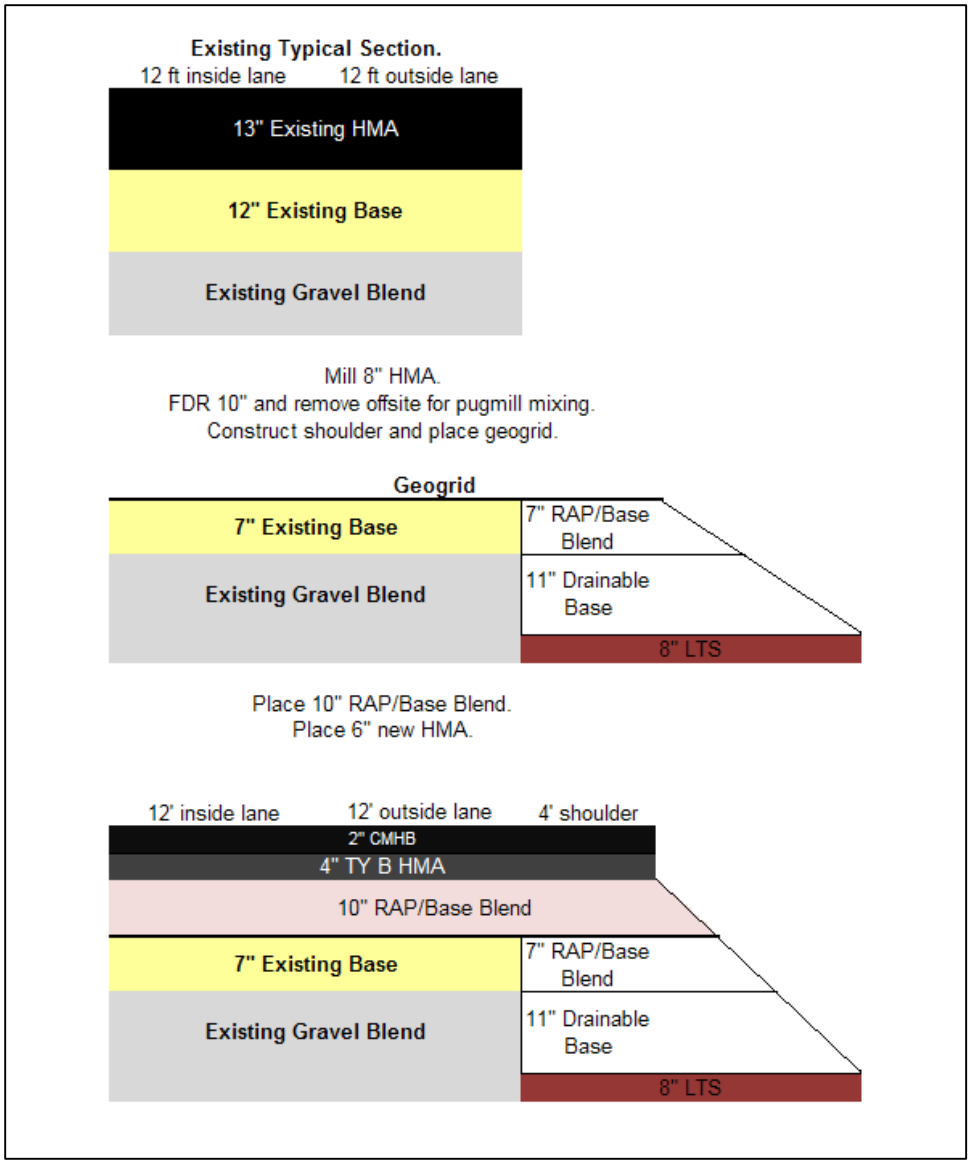

Figure A.16: Recommendations for SH-21 where there are Class 4 distresses (Texas Transportation Institute, 2010)

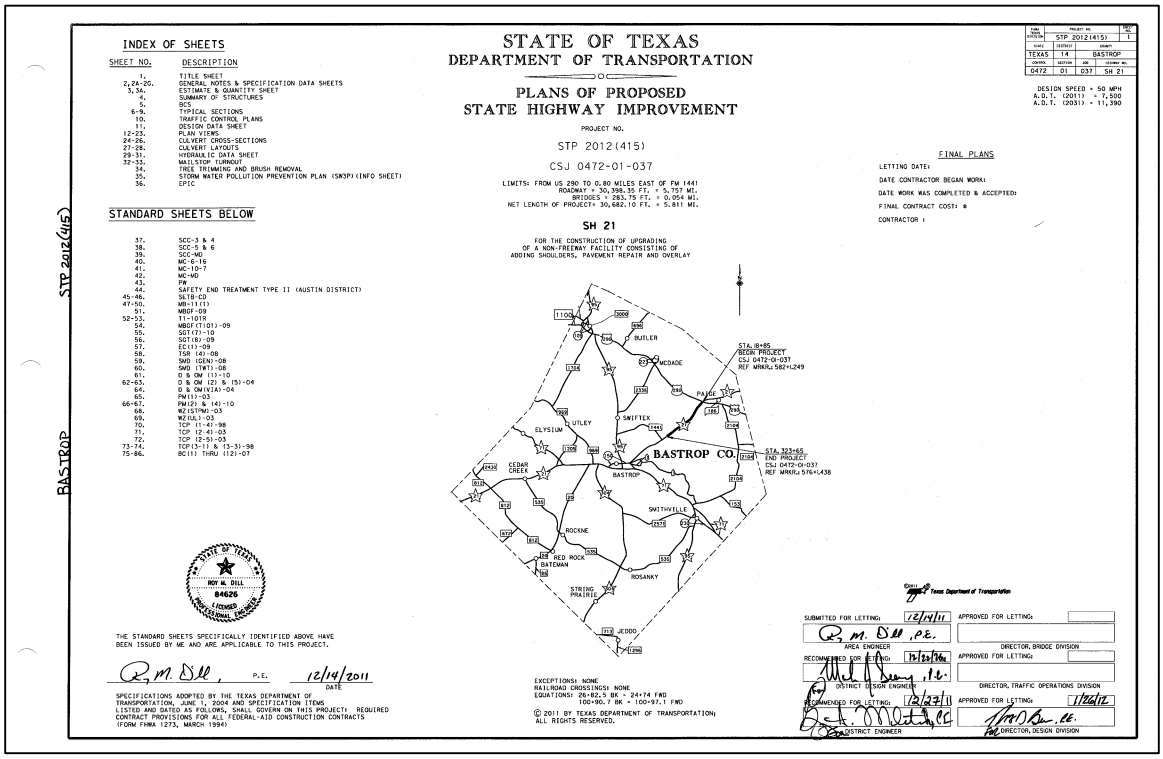

Figure A.17: TxDOT cover for design plans for SH-21 from Sta 23+00 to 323+65

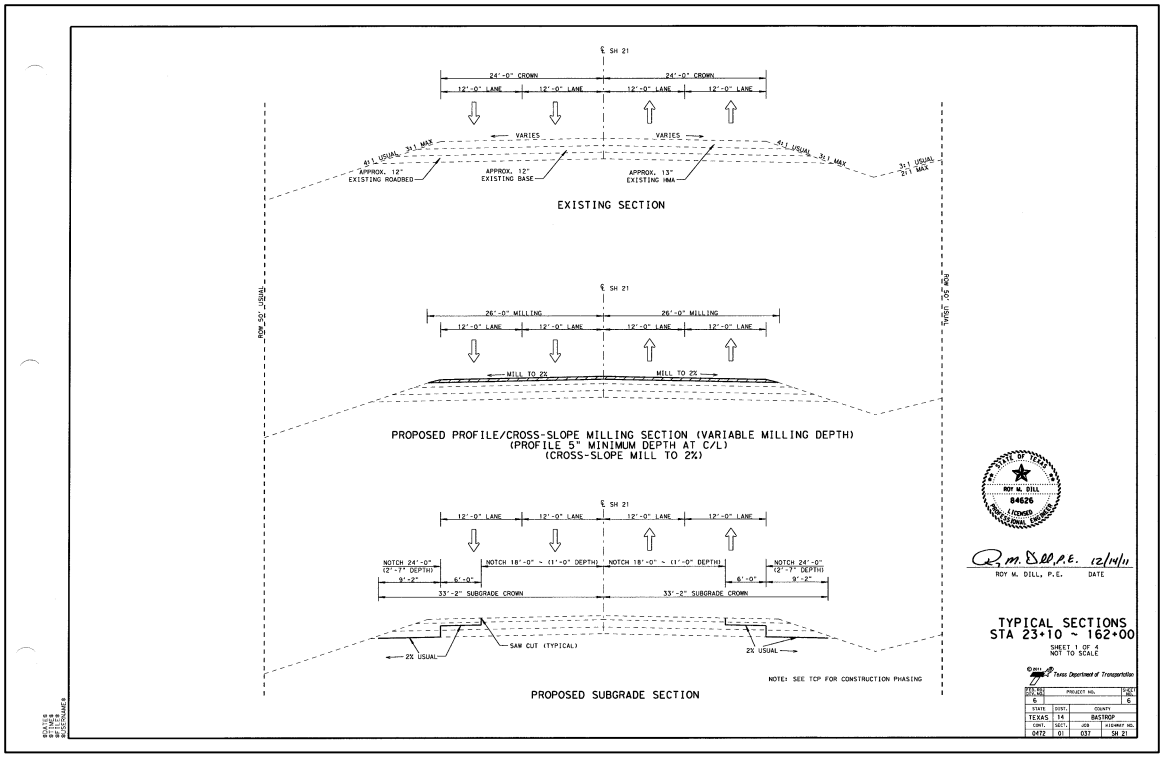

Figure A.18: Final Design plans for SH-21 from Sta 23+00 to 162+00 (A)

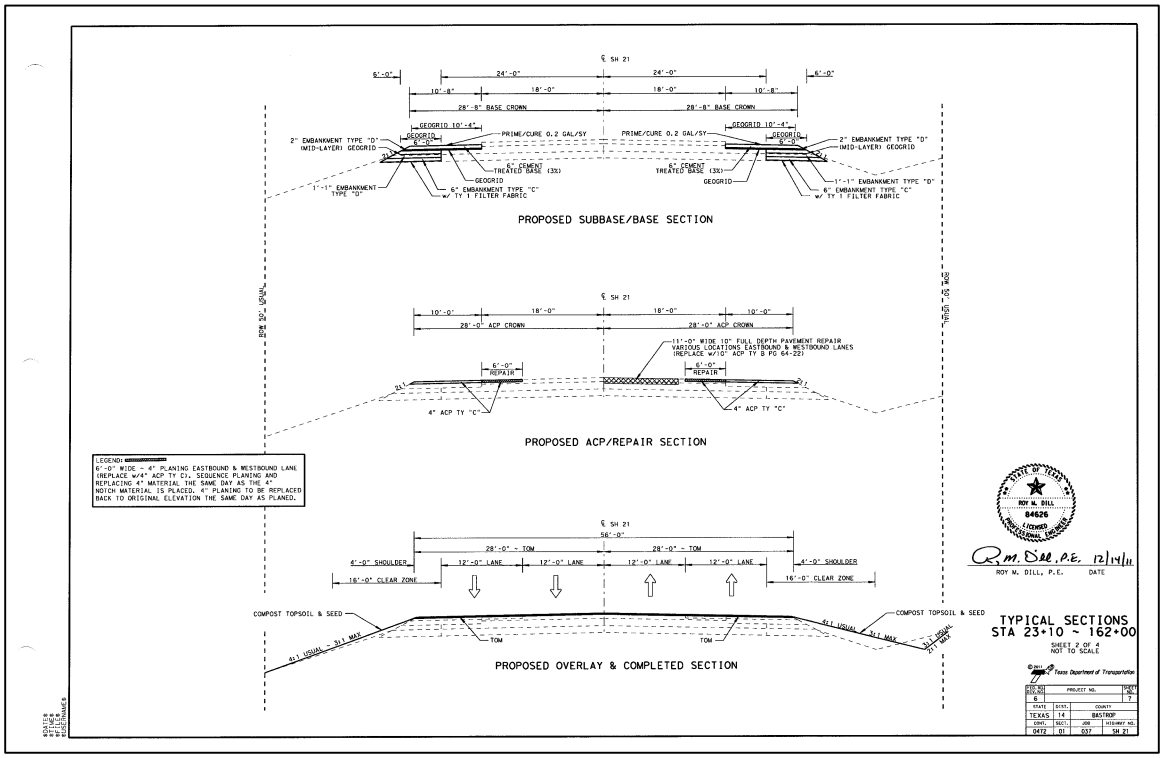

Figure A.19: Final Design plans for SH-21 from Sta 23+00 to 162+00 (B)

Appendix B: Results from Visual Condition Surveys

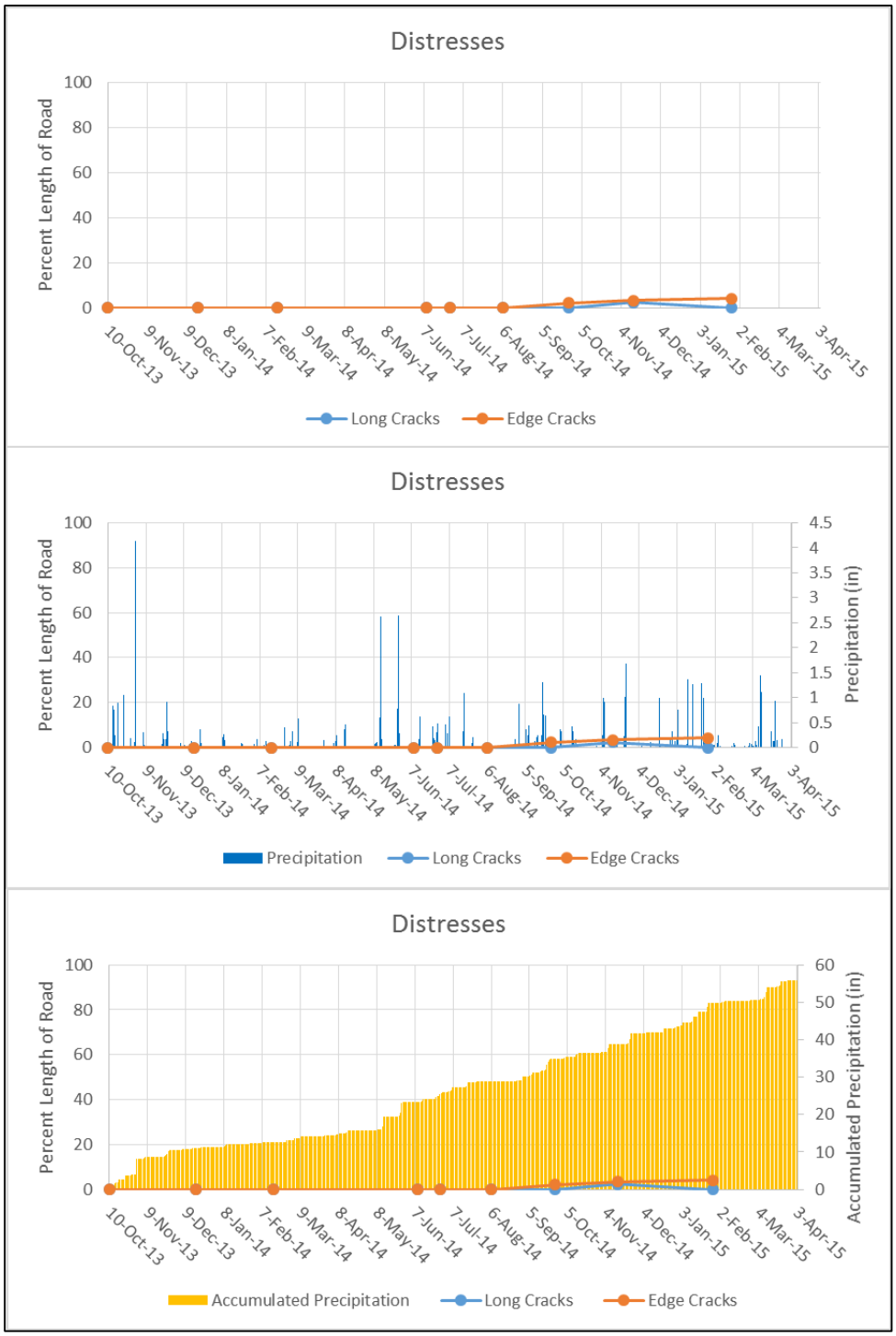

Figure B.1: Summary of distresses in Section 1

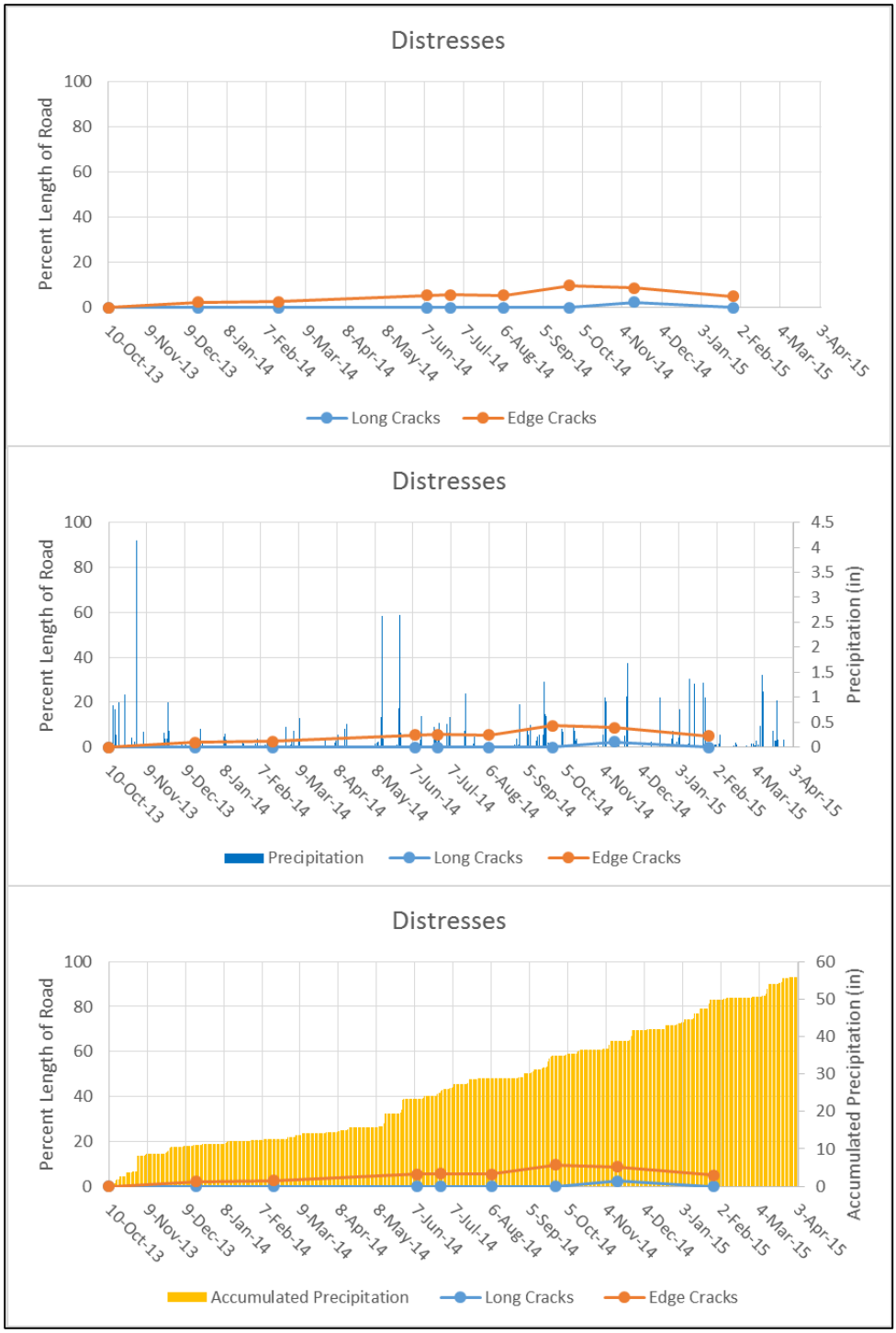

Figure B.2: Summary of distresses in Section 2

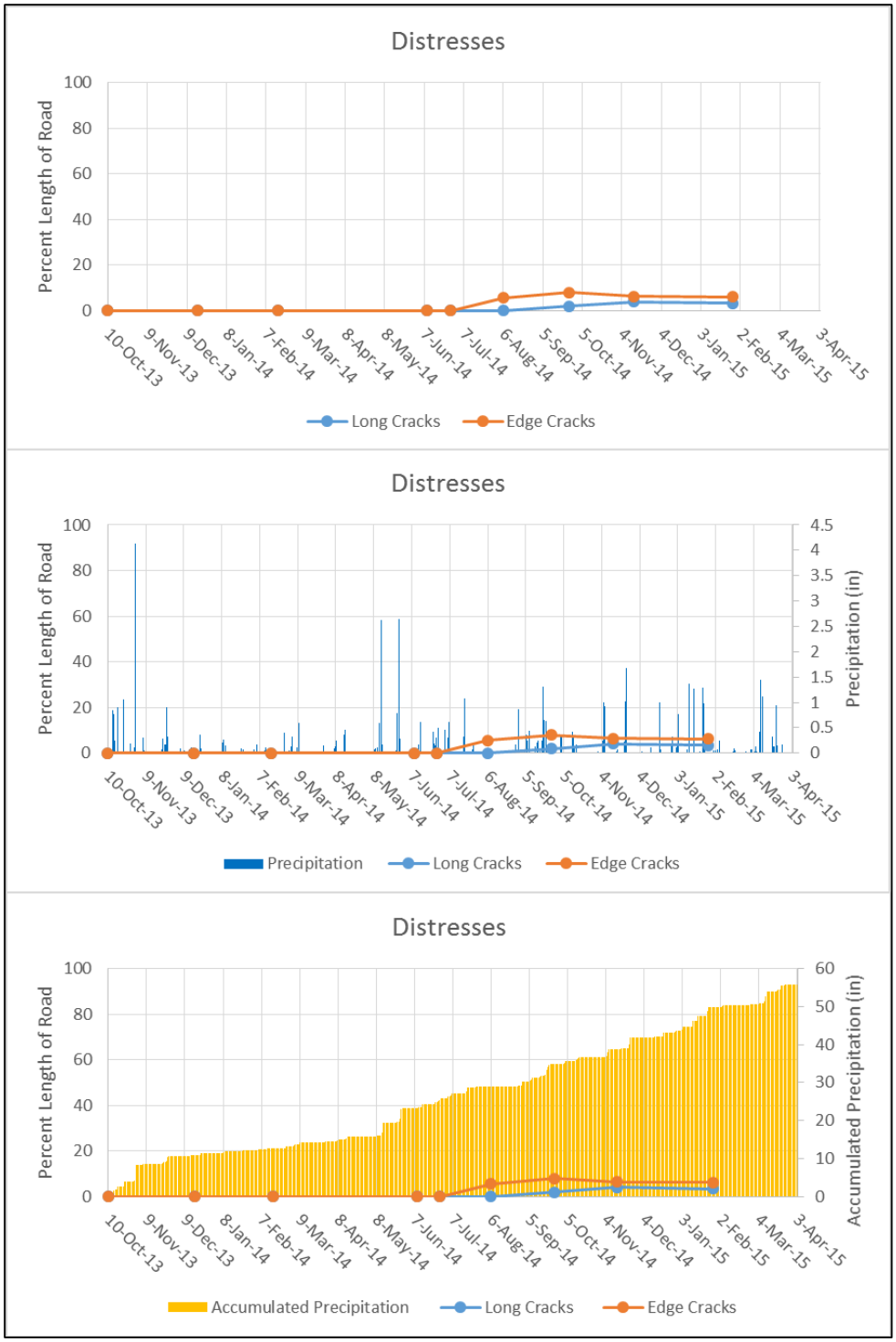

Figure B.3: Summary of distresses in Section 3

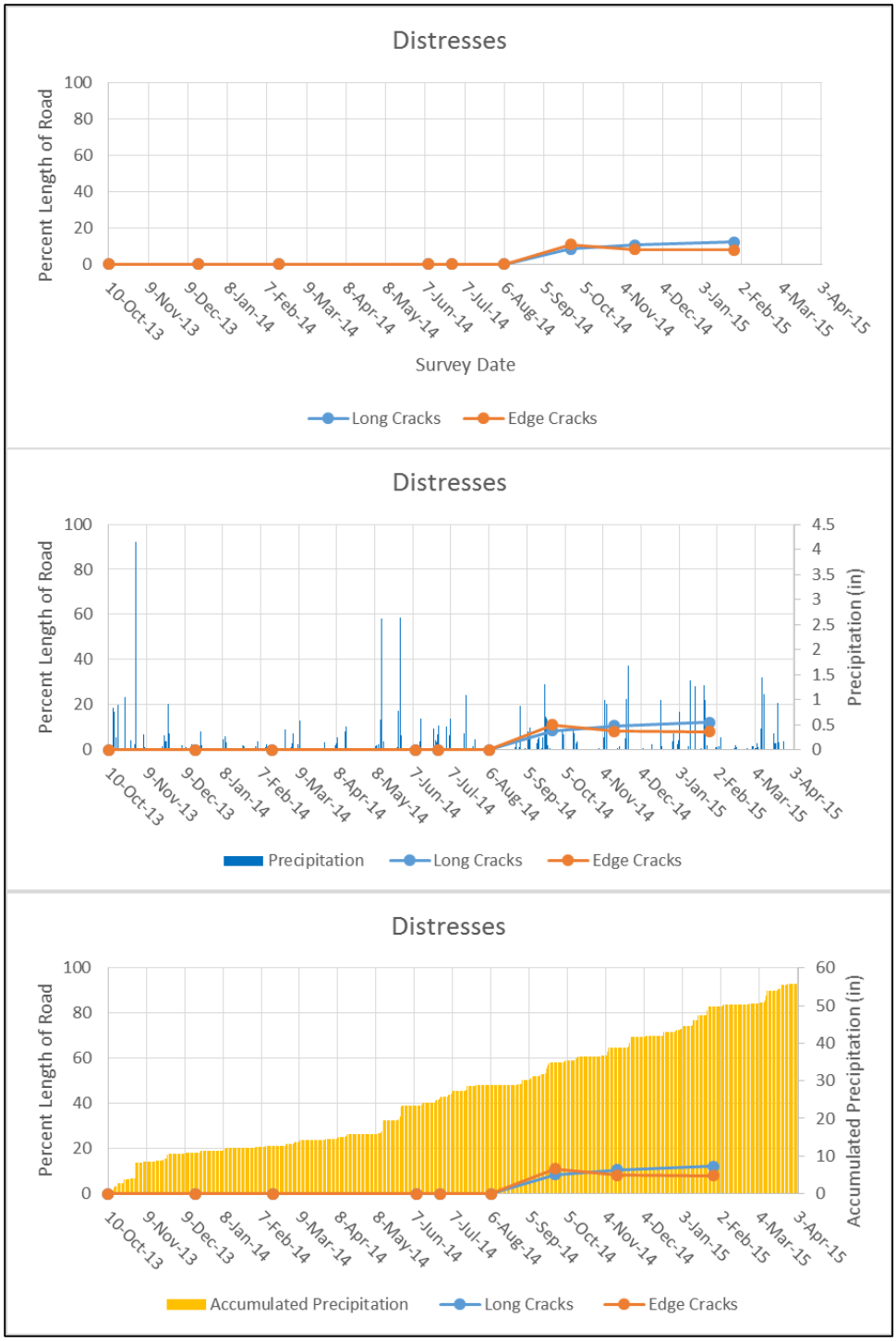

Figure B.4: Summary of distresses in Section 4

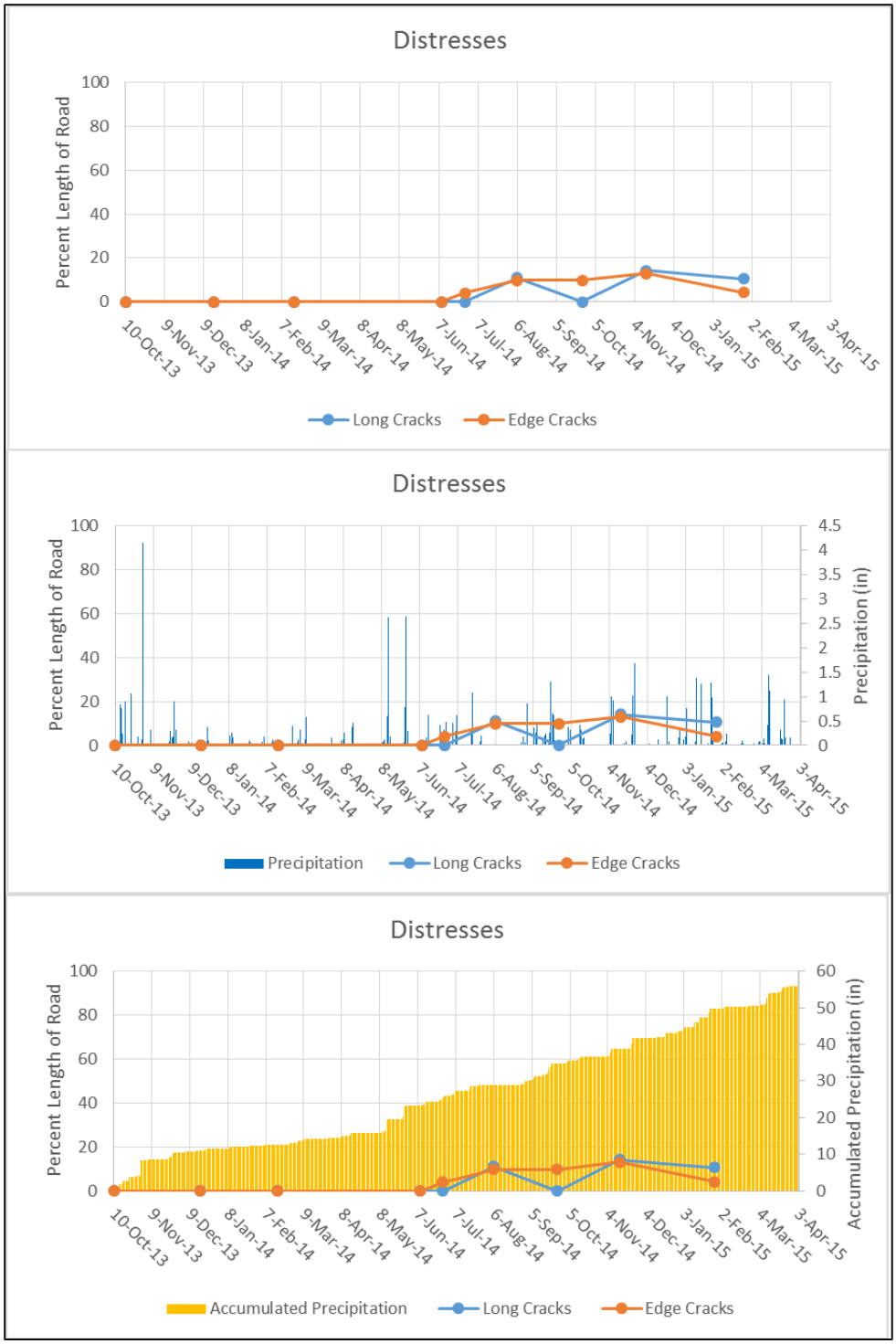

Figure B.5: Summary of distresses in Section 5

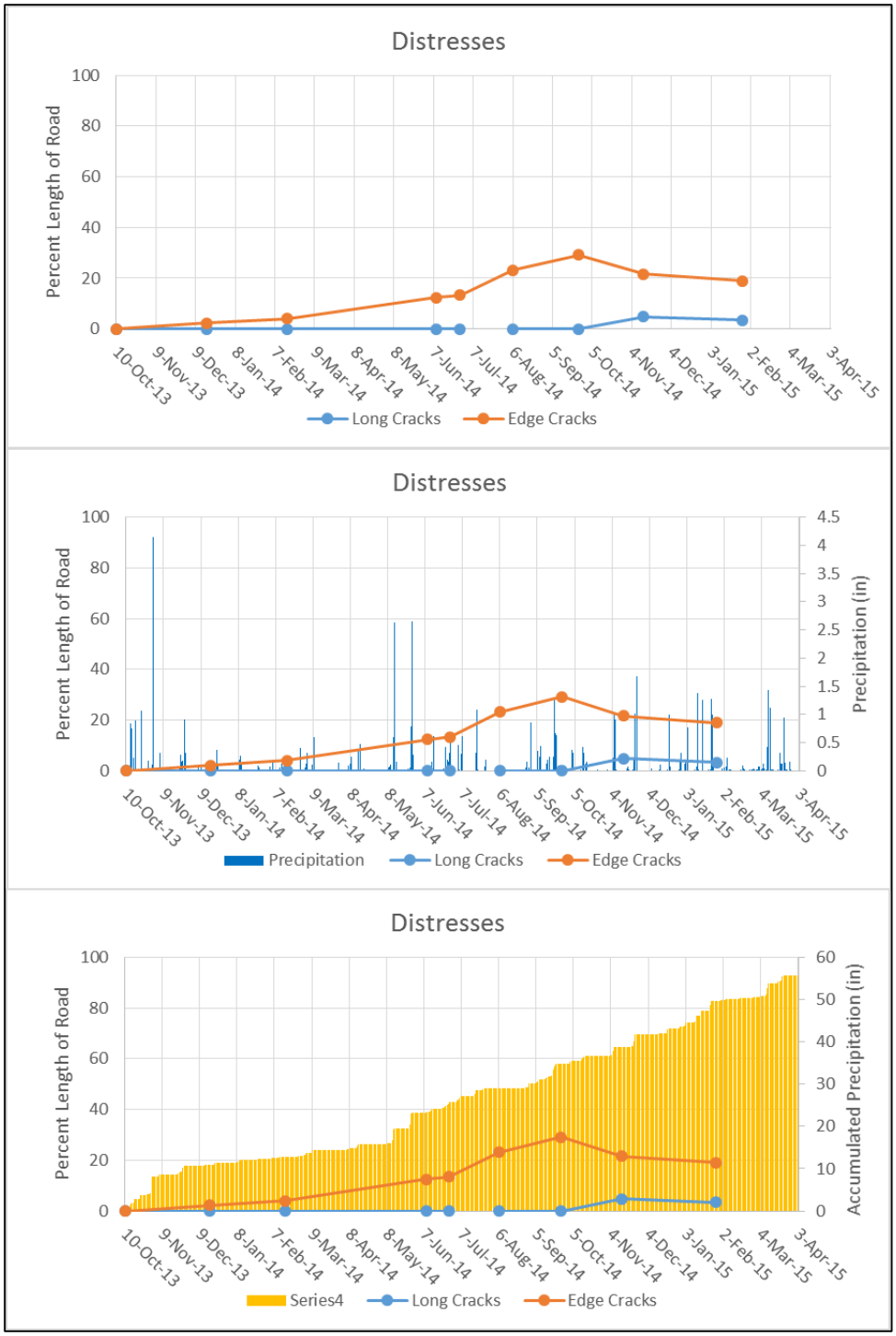

Figure B.6: Summary of distresses in Section 6

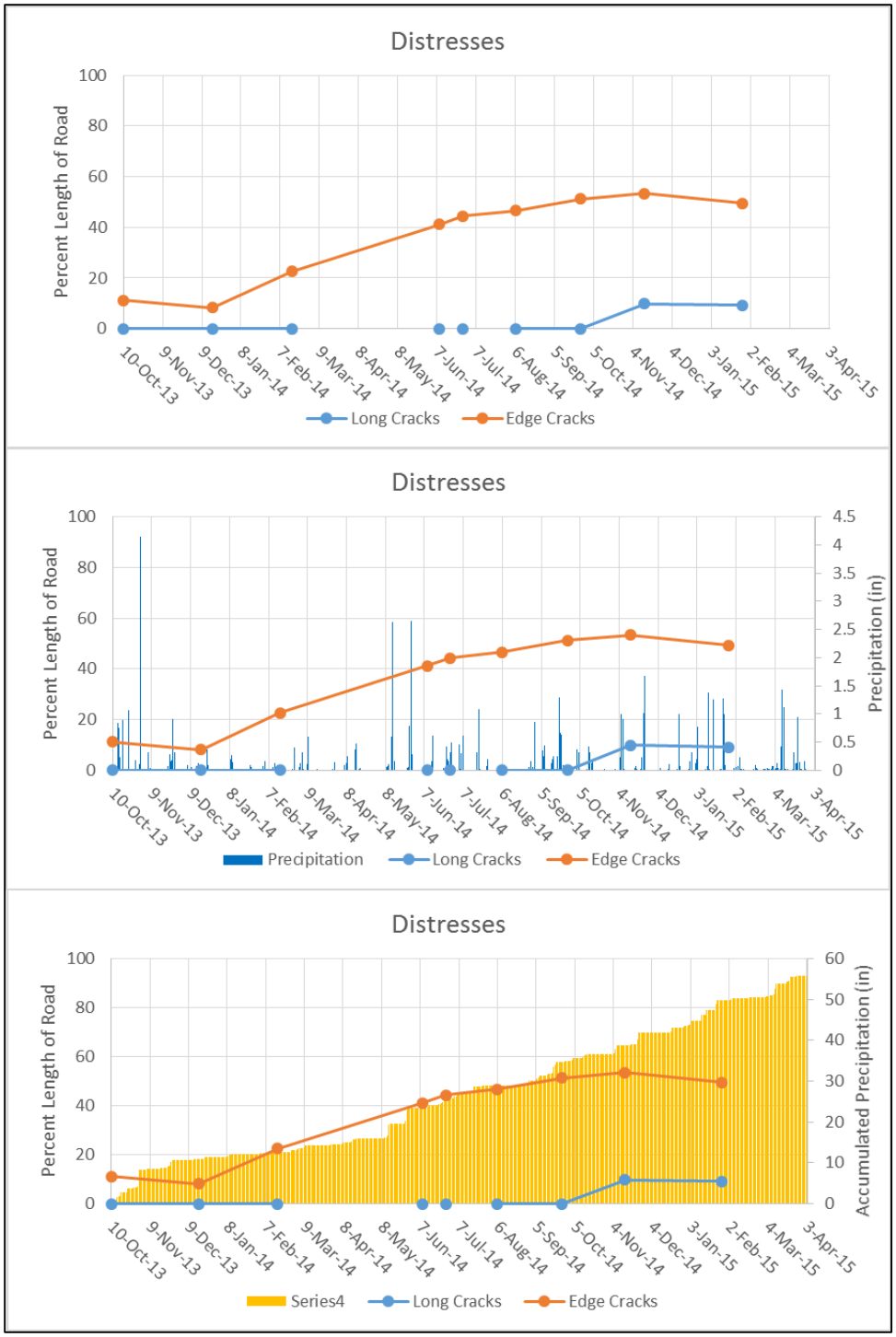

Figure B.7: Summary of distresses in Section 7

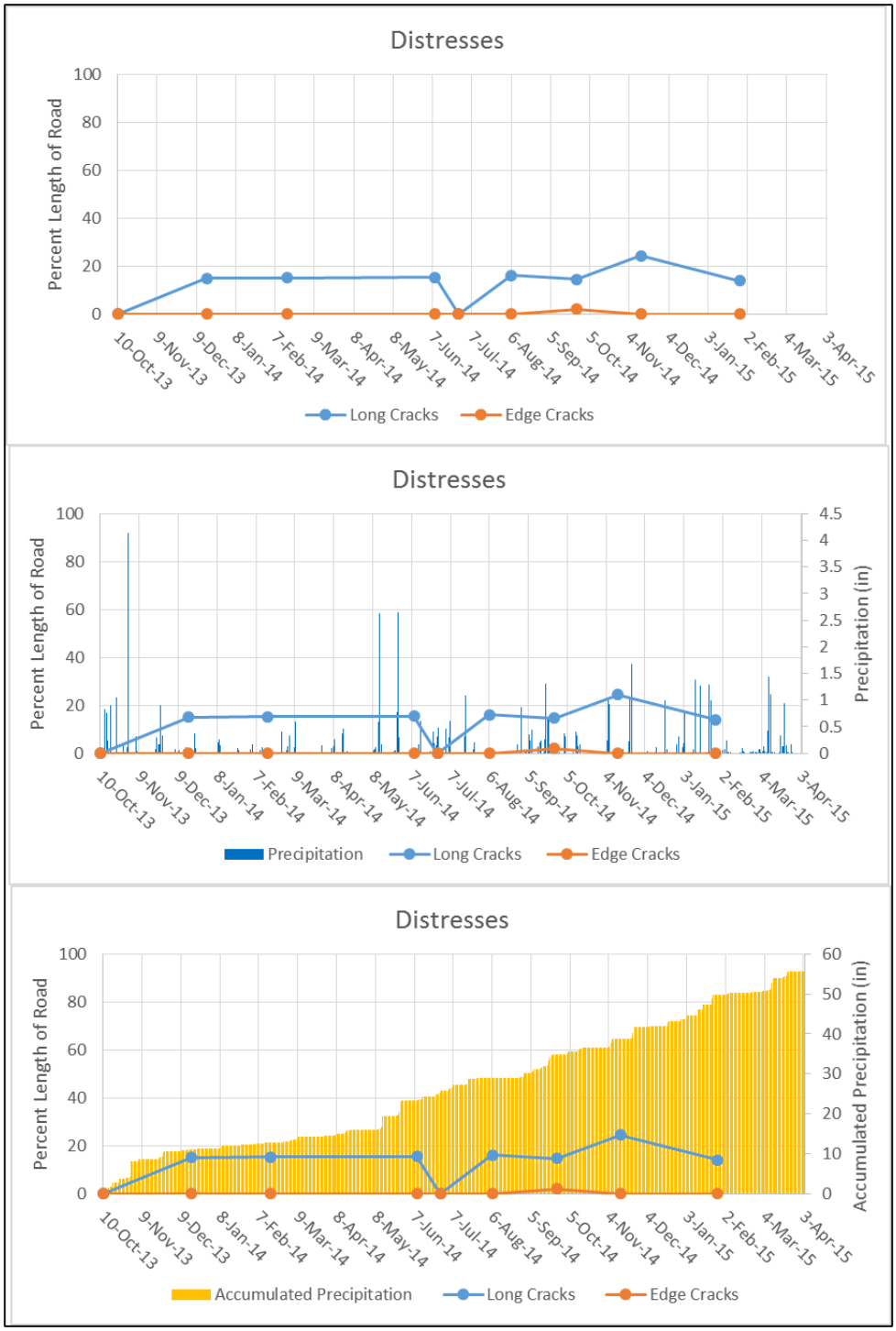

Figure B.8: Summary of distresses in Section 8

References

ARA, Inc., ERE Division. (2000, June). Appendix DD-1: Resilient Modulus as function of soil moisture-Summary of Predictive Models. *Guide for Mechanistic-Empirical Design of New and Rehabilitated Pavement Structures*. National Cooperative Highway Research Programe.

Azevedo, M. a. (2013). Capillary barrier dissipation by new wicking geotextile. *Advances in Unsaturated Soils*, 559-565.

Barnes, V. (1981). *Geologic Atlas of Texas, Austin Sheet, digitilized from Barnes 1981 map: Texas Water Development Board, Scale 1:250,00.*

Christopher, B. R. (2006). *Geotechnical Aspects of Pavements.* FHWA.

Cobos, D. a. (2015, March 1). Retrieved from Decagon Devices, Inc.: http://www.decagon.com/education/correcting-temperature-sensitivity-of-ech2o-soil-moisture-sensors-13394-02-an/

Decagon Devices, Inc. (2015). *EC-5 Soil Moisture Sensor, Operator's Manual.* Pullman, WA: Decagon Devices, Inc.

Decagon Devices, Inc. (Version 7). *ECH2O-TE/EC-TM Probe Operator's Manual.* Pullman, WA: Decagon Devices, Inc.

Decagon Devices, Inc. (Version 8). *Em50/Em50R/Em50G User's Manual.* Pullman, WA: Decagon Devices, Inc.

Hare, J. A. (1990). *Airport Pavement Drainage.* Washington, D.C.: U.S. Department of Transportation.

Henry, K. S. (2015, 10 February). Retrieved from http://www.google.com/url?sa=t&rct=j&q=&esrc=s&source=web&cd=9&ved=0CEYQFjAI&url=http%3A%2F%2Fibrarian.net%2Fnavon%2Fpaper%2FGeocomposite_capillary_barrier_drain_for_unsatura.pdf%3Fpaperid%3D4926254&ei=ZEsSVYnIH8mngwTI4oLwAg&usg=AFQjCNEVR4PgLi-JXSFJn4B80m

Jones, L. D. (2012). Chapter C5-EXPANSIVE SOILS. *ICE manuals*.

Lebeau, M. a.-M. (2009). Pavement subsurface drainage: importance of appropiate subbase materials. *Canadian Geotech Journal*, 987-1000.

Olive, W. C. (1989). Swelling Clays Map of the Conterminous United States. *Miscellaneous Investigations Series Map I-1940*. Department of the Interior, U.S. Geological Survey.

Rokade, S. A. (2012). DRAINAGE AND FLEXIBLE PAVEMENT PERFORMANCE. *International Journal of Engineering Science and Technology*, 1308-1311.

Stormont, J. a. (2001). *Improving Pavement Sub-surface Drainage Systems by Considering Unsaturated Water Flow.* Albuquerque, NM.

Tencate Mirafi. (2010). *Case History: Frost Heave/Subgrade Stabilization, Dalton Highway, AK.* Dalton Highway, AK: TenCate Mirafi.

Tencate Mirafi. (2010). *Mirafi HP570.* Tencate Mirafi.

Tencate Mirafi. (2011). *Mirafi H2Ri.* Tencate Mirafi.

Tencate Mirafi. (2011). *Mirafi H2Ri Woven Geosynthetic for Soil Stabilization and Base Reinforcement Applications where differential settlement occurs due to heaving in the subgrade soils.* Pendergrass, GA: Tencate Geosynthetics North America.

Tencate Mirafi. (2012). *Case History: Subgrade Stabilization, St. Louis County, MO.* St. Louis County, MO: TenCate Mirafi.

Tencate Mirafi. (2012). *Case Study: Roadway Drainage and Subgrade Stabilization, Corono, CA.* Corona. CA: Tencate Mirafi.

Tencate Mirafi. (2013). *Case History: Subgrade Stabilization, Jefferson County, WI.* Jefferson County, WI: Tencate Mirafi.

Tencate Mirafi. (2013). *Mirafi RS580i.* Tencate Geosynthetics Americas.

Tencate Mirafi. (2014, April 30). *Mirafi 140NC.* Pendergrass, GA: Tencate Geosynthetics Americas. Retrieved from Tencate: http://www.tencate.com/amer/geosynthetics/products/geotextiles/TenCate-Mirafi-N-Series/default.aspx

Tencate Mirafi. (2015, March 9). *Tencate Mirafi H2Ri.* Retrieved from Tencate: http://www.tencate.com/amer/geosynthetics/products/geotextiles/tencate-mirafi-h2ri/default.aspx

Texas Department of Transportation. (2010). *Pavement Management Information System, Rater's Manual.* College Station, TX: Texas Department of Transportation.

Texas Transportation Institute. (2010). *Pavement Design Report: SH 21 from US 290 to ~ 2.85 miles West.* College Station, TX: Texas Transportation Institute.

Zhang, X. P. (2014). Use of Wicking Fabric to Help Prevent Frost Boils in Alaskan Pavements. *Journal of Materials in Civil Engineering*, 728-740.

Zhang, X., & Belmont, N. (2011). Use of Wicking Fabric to Help Prevent Differential Settlements in Expansive Soil Embankments. *Geo-Frontiers*, 3915-3924.

Zhang, X., & Belmont, N. (2011). Use of Wicking Fabric to Help Prevent Differential Settlements in Expansive Soil Embankments. *Geo-Frontiers*, 3915-3924.

Zornberg, J. a. (2009). Reinforcement of pavements over expansive clay subgrades. *Proceedings of the 17th International Conference on Soil Mechanics and Geotechnical Engineering*, (pp. 765-768).

Zornberg, J. G., Roodi, H., & Azevedo, M. (August 2013). *Rehabilitation of State Highway 21 Using Four Different Types of TenCate Mirafi Geotextile Products, Report No. 1.* Austin, TX.